1989

Post-compression and superimposed trusses utilized in bridge rehabilitation

Samuel Milton Planck
Iowa State University

Post-compression and superimposed trusses utilized in bridge rehabilitation

by

Samuel Milton Planck

A Thesis Submitted to the

Graduate Faculty in Partial Fulfillment of the

Requirements for the Degree of

MASTER OF SCIENCE

Department: Civil and Construction Engineering

Major: Structural Engineering

Approved:

_____

_____
In Charge of Major Work

_____
For the Major Department

_____
For the Graduate College

Iowa State University
Ames, Iowa

1989

TABLE OF CONTENTS

LIST OF TABLES

LIST OF FIGURES

1. INTRODUCTION

1.1. General Background

Nearly half of the approximately 600,000 highway bridges in the United States were built before 1940. The majority of those bridges were designed for lower traffic volumes, smaller vehicles, slower speeds, and lighter loads than they experience today. In addition, maintenance has not been adequate on many of these older bridges. According to the Federal Highway Administration (FHWA), almost 40% of the nation's highway bridges are classified as deficient and thus in need of rehabilitation or replacement.

The deficiency in some of these bridges is their inability to carry current, legal live loads. Rather than posting these bridges for reduced loads or replacing them, strengthening has been found to be a cost-effective alternative in many cases.

Many different methods exist for increasing the live load-carrying capacity of various types of bridges. One series of research projects, sponsored by the Iowa Department of Transportation (Iowa DOT), examined the concept of strengthening steel-beam simple-span bridges by external post-tensioning; the research covered the feasibility phase through the implementation and design methodology phases. Results of these projects verified that strengthening of the simple-span bridges by post-tensioning is a viable, economical strengthening technique.

As a result of the success in strengthening simple-span bridges by post-tensioning, a laboratory investigation, Iowa DOT project HR-287 [7], was undertaken to examine the feasibility of strengthening continuous composite steel-beam and concrete-deck bridges by post-tensioning. This research program indicated that the strengthening of continuous composite bridges by post-tensioning is also feasible. Longitudinal as well as transverse distribution of post-tensioning must be considered if only exterior or only interior stringers are post-tensioned. Laboratory testing of a 1/3-scale model bridge constructed for this project and finite-element analysis showed that post-tensioning of positive moment regions with straight tendons was more effective than post-tensioning negative moment regions with straight tendons. It was also determined that changes in the tension in tendons may either be beneficial or detrimental when live loads are applied to strengthened bridges and thus must be carefully considered in design.

Results of Iowa DOT project HR-287 have shown that by post-tensioning the positive moment regions of continuous bridges, stress reduction can also be obtained in the negative moment regions. However, in certain instances, additional stress reduction is required in the negative moment region. Because post-tensioning tendons in negative moment regions would need to be placed above the neutral axis located near the top flange, post-tensioning would require removal of a portion of the bridge deck. Since this action is usually undesirable

(extra cost, closure of bridge, etc.), an alternate method of reducing stress in the negative moment regions of continuous, composite bridges is needed.

As a result of work on the National Cooperative Highway Research Program NCHRP-12-28(4) [21] project, several concepts for strengthening bridges were conceived; some concepts are applicable to strengthening the negative moment regions of continuous spans. This report describes the investigation of two strengthening schemes for use in the negative moment regions of continuous spans.

1.2. Objectives

From the seven strengthening schemes (shown in Fig. 1.1) conceived for use in negative moment regions of continuous beams, two were selected for additional investigation in this study. Therefore, the primary objective of this study was to determine the feasibility of strengthening the negative moment region of composite bridges by two new methods:

1. Post-compression of stringers
2. Superimposed truss within stringers.

To evaluate the feasibility of these strengthening techniques, the more detailed objectives of this study were as follows:

1. Determine the best design for applying and maintaining post-compression in negative moment regions of composite bridges.
2. Determine the effectiveness of post-compression in reducing flexural stress in the negative moment region.

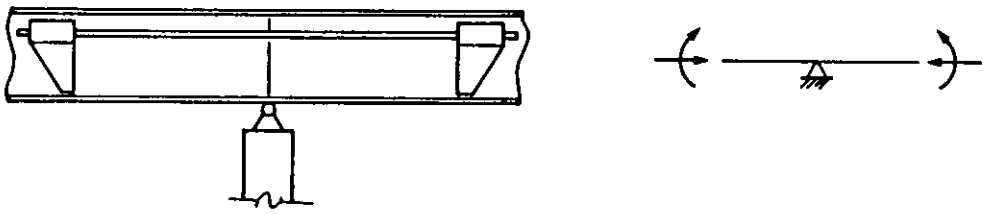

a. POST-TENSIONING AND APPLIED MOMENT

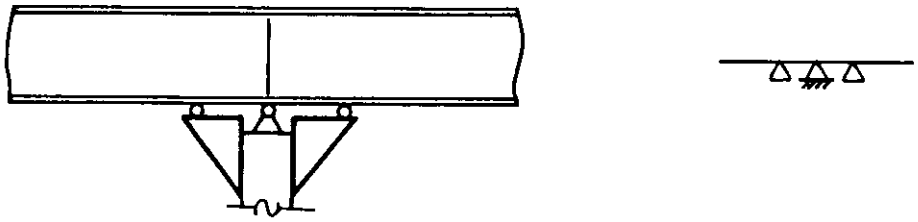

b. INCREASE NUMBER OF SUPPORTS

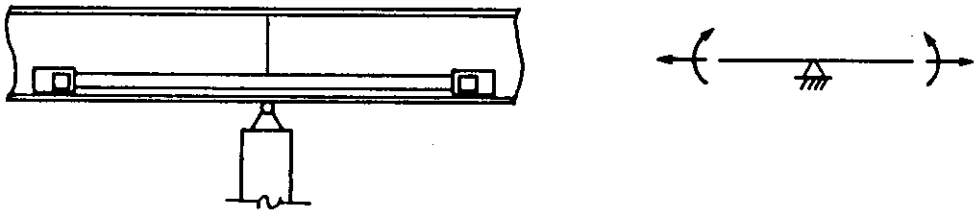

c. POST-COMPRESSION WITH JACKING BRACKETS

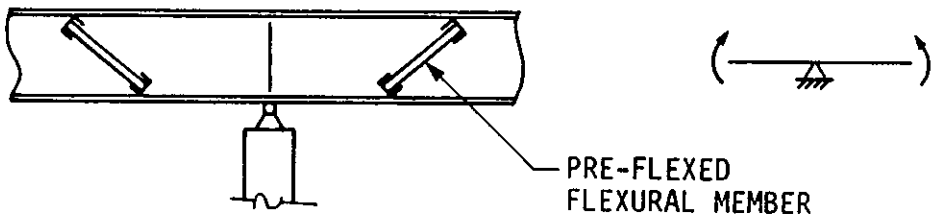

d. APPLIED MOMENT

Fig. 1.1. Negative moment strengthening schemes and force diagrams

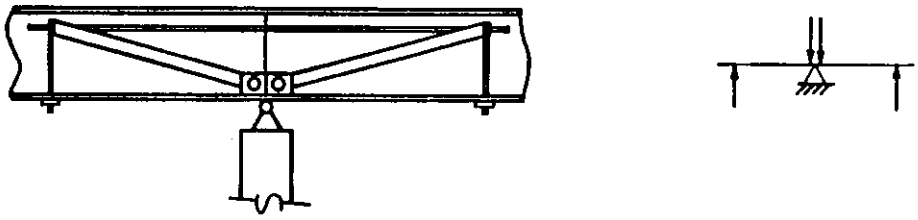

e. SUPERIMPOSED TRUSS

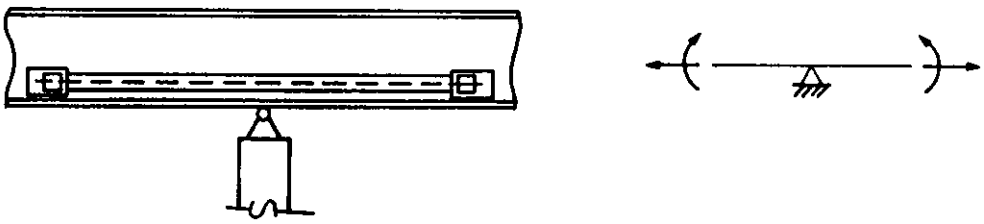

f. PRETENSIONED POST-COMPRESSION TUBE

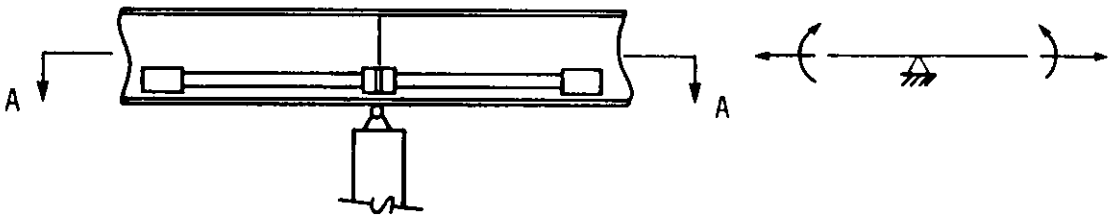

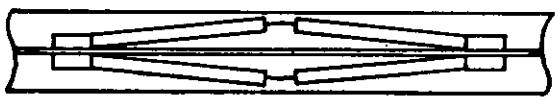

SECTION A-A

g. POST-COMPRESSION SCISSOR TUBE

Fig. 1.1. Continued

3. Determine the best configuration and design for a superimposed truss.
4. Determine the effectiveness of the superimposed truss in reducing flexural stress in the negative moment regions.

These objectives were pursued through reviewing available engineering literature, testing a full-scale mockup of a composite bridge beam in the Iowa State University (ISU) Structural Engineering Research Laboratory, conducting a finite-element analysis of the laboratory bridge mockup with each of the previously described strengthening schemes in place, and conducting a finite-element analysis of the one-third scale laboratory bridge model strengthened with superimposed trusses.

1.3. Research Program

The research program consisted of the distinct parts as outlined above; however, a strong emphasis was placed on laboratory testing. As part of a previous research project (Iowa DOT project HR-287) [3], plans for standard continuous, composite bridges were obtained from the Iowa DOT Office of Bridge Design. From the various sets of plans provided, the V12 (1957) series of composite, three-span bridges was selected for additional review. This series of bridges was wide enough for two standard 12-ft traffic lanes; also a considerable number of these bridges were constructed in Iowa. Based upon these plans, a full-size mockup was constructed representing the negative moment region of a typical bridge stringer above an interior support. The

mockup consisted of a W24 x 76 beam on which a composite concrete deck was cast (see Ref. [3]).

Post-compression (ST2.1) and the superimposed trusses (ST2.2 and ST2.3) were tested on this mockup as part of this investigation. Post-compression tests consisted of a series of vertical load cycles applied to the mockup with varying magnitudes of post-compression force initially applied to the compression members. Two variations of the superimposed trusses were developed and also tested on the full-scale mockup previously described.

Tests similar to those conducted for post-compression were performed with the superimposed trusses in place so a comparison of the three strengthening schemes could be made. During all tests, deflection of the full-scale mockup as well as strains in both the mockup and the strengthening system were monitored.

The full-scale mockup was also analyzed with SAP IV [1], a finite-element program. Each of the three strengthening techniques was analyzed with the finite-element program for the operating level of loads tested in the laboratory.

In order to determine distribution effects of the superimposed truss in a three-span continuous composite bridge, a finite element analysis was also performed on a one-third scale model bridge Ref. [3]. Three possible arrangements for placing the superimposed trusses on a three-span bridge were examined as well as three different lengths of trusses.

The results from the various parts of the research program are summarized in this report. The literature review for the project is given in Section 1.4. Chapter 2 describes the full-scale mockup and the strengthening schemes developed. Chapter 3 covers the tests and test procedures used to evaluate the effectiveness of the strengthening systems. The results from the laboratory testing program and the finite-element analysis schemes are summarized in Chapter 4. Following the results are the summary and conclusions, which are presented in Chapter 5. In Chapter 6 recommendations for further research are presented.

1.4. Literature Review

The research completed in this project can be viewed as extensions of work in two separate areas: post compression and applied strengthening mechanisms.

Post-compressing of a structure is analogous to post-tensioning of a structure. With post-compression, however, the member being strengthened is subjected to axial tension rather than axial compression. Although strengthening of structures by post- tensioning is much more common, the engineering literature contains one example of strengthening an existing structure by attaching elements that were subsequently compressed.

Applied strengthening mechanisms are independent structures that, when added to an existing structure, provide redundancy to the original structure or impose forces and displacements on the original structure.

Strengthening mechanisms are independent, except for lateral stability (in some cases) of the original structure. Failure of either the original structure or the applied strengthening mechanism does not necessarily cause collapse of the entire structure. Several examples of applied strengthening mechanisms were found in the engineering literature.

1.4.1. Post-Compression

The use of slender compressed elements in concrete structures was suggested by Kurt Billig in the early 1950s [32]. In 1953, a West German patent was filed and, in 1956, a separate patent was filed in Austria each for the use of a post-compression system. As is often the case, neither patent resulted in immediate use of the system in construction.

Further work was done on post-compression by Dr. Hans Reiffenstuhl, an Austrian university professor, during the early 1970s. Dr. Reiffenstuhl developed a method of applying post-compression in concrete structures to cancel the axial effects associated with post-tensioning. By post-tensioning and post-compressing a member simultaneously the bending moment due to eccentric forces could be effectively doubled, while tension and compression axial forces would negate one another [18]. Dr. Reiffenstuhl developed the design methodology and construction details to overcome the problems of friction loss, buckling and anchorage inherent with post-compression.

Dr. Reiffenstuhl applied this system in 1977 for the design of a 245 ft concrete, single box girder bridge in Austria. Due to the use of post-tensioning and post-compression the bridge was constructed with a span/depth ratio of 30.4, significantly larger than a typical bridge of that span.

Dr. Reiffenstuhl also employed the post-compression technique in the rehabilitation of an existing structure [18]. In 1979 the system was used to strengthen a prestressed concrete folded-plate roof spanning 121 ft. The building was an athletic complex built in 1972. In order to maintain the original design of the roof, and allow continued use of the facility during strengthening, 1 3/8 in.-diameter post-compressed bars were added to the exterior of each plate in the roof. The strengthening allowed addition of roof insulation and replacement of the deteriorated roofing.

1.4.2. Applied strengthening mechanisms

Strengthening of a railway bridge in Ostrava, Czechoslovakia was accomplished with an applied strengthening mechanism prior to 1964 [6]. The 67-ft single span bridge consisted of two steel-plate girders which supported a deck structure. For each of the two plate girders, a strengthening mechanism was constructed. The mechanism was a closed loop similar in shape to a bar joist, built with a steel tee, top and bottom, spaced by steel plate stiffeners. The steel tees provided additional compression and tension flange material for the existing girders.

In order to remove dead load stress from the existing girders, the entire bridge was jacked upward from cribbing placed underneath at approximately the outer quarter points. A strengthening mechanism was then attached to the outside of each existing plate girder. To provide lateral stability to the mechanisms, the new plate stiffeners for each mechanism were anchored to the existing girder stiffeners. The bridge was then lowered downward with each of the girders strengthened by the addition of the attached mechanisms. In addition to a strengthened section, redundancy was also provided in the top and bottom flanges because either an existing flange or a new attached flange could fail without causing collapse of a girder.

In 1968 Kandall proposed strengthening existing structures by means of prestressing and the addition of independent compression members [9]. Kandall discussed the advantages and disadvantages of adding cover plates, of adding prestressing tendons, and of adding prestressing tendons with associated compression members. He concluded that prestressing with the compression members was the best of the three options.

Kandall found that prestressing tendons could be used in both the positive and negative moment regions of existing structures to reverse dead-and live load moments. He also found, however, that the axial compression associated with post-tensioning could outweigh the benefits from the applied moments. To overcome the problem, Kandall proposed the use of a "free" compression member spanning between the post-

tension anchorages. With the compression member in place, the tendon mechanism exerts only upward forces on the existing structure. Thus, the mechanism reverses applied load effects without generating undesireable axial forces.

Prior to 1969, a wrought-iron truss bridge in Switzerland was strengthened with a mechanism similar to that proposed by Kandall [15]. Each of the bridge's two 157-ft truss spans was strengthened with the addition of post-tensioning tendons and independent compression members. The tendons and saddles were located to provide upward forces to each truss at the quarter points. The compression members (which also served as the bridge guardrail) carried the axial force associated with the post-tensioning.

In the United States, Kim, Brungraber, and Yadlosky have proposed and used applied strengthening mechanisms in through-truss bridges [10]. Steel through-truss bridges often lack redundancy, thus the failure of a single member or joint could cause collapse of the entire bridge. Steel through-truss bridges also have many members and connections that are subject to corrosion and fracture.

To provide redundancy and strengthen this type of bridge, Kim, Brungraber, and Yadlosky developed an arch that is constructed within a truss. The superimposed arch is stressed against the existing truss, however, it is independent except for lateral stability.

2. DESCRIPTION OF TEST SPECIMENS

This chapter outlines the physical details of the full-scale mockup, the post-compression strengthening system (ST2.1), and the superimposed truss strengthening system (ST2.2 and ST2.3).

2.1. Full-Scale Mockup of the Negative Moment Region

The full-scale mockup of the negative moment region was initially fabricated to test negative moment region post-tensioning schemes. The theoretical development and fabrication of the mockup are reported in detail in the final report for Iowa DOT Project HR-287 [3] and thus will only be briefly discussed in this report. This full-scale model of the negative moment region in a stringer of a continuous bridge will henceforth simply be referred to as the mockup.

The mockup was designed to simulate the negative moment region of the V12 (1957) series of bridges as shown in Fig. 2.1. General dimensions of the mockup are given in Fig. 2.2, whereas photographs of the mockup are given in Fig. 2.3.

A W24 x 76 beam 30 ft long, which is the size on an interior stringer in a 150 ft V12 (1957) series bridge, was provided by the Iowa DOT for use in the mockup. AASHTO effective-width requirements for an interior stringer in this type of bridge required a concrete slab 6 ft 3 in. wide (see Fig. 2.2). Also shown in these figures is the slab thickness of 6.5 in., which is the specified average thickness of V12 (1957) bridge decks.

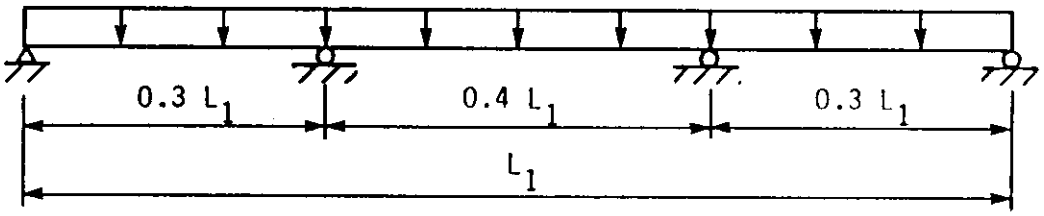

a. SPANS FOR V12 (1957) BRIDGE SERIES

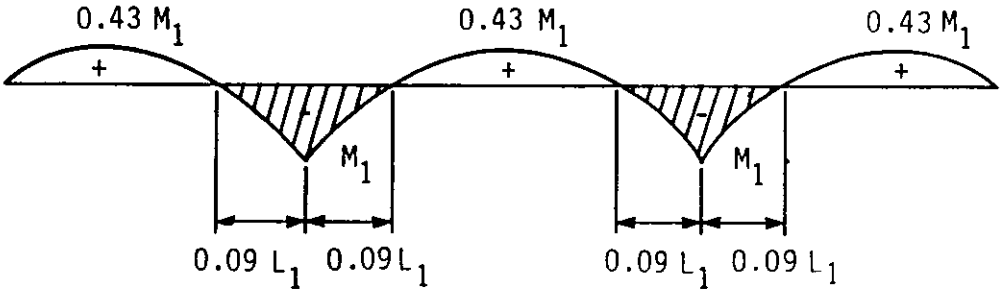

b. MOMENT DIAGRAM FOR V12 (1957) BRIDGES WITH UNIFORM LOAD

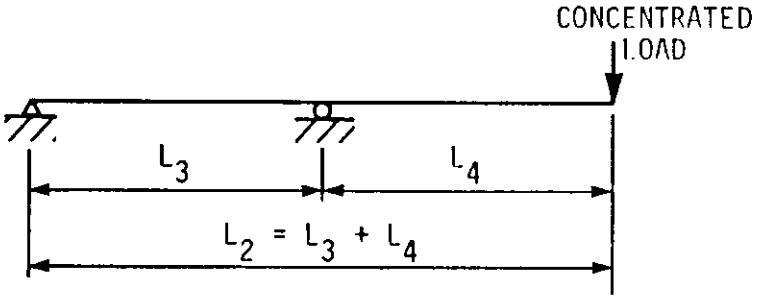

c. MOCKUP SPANS

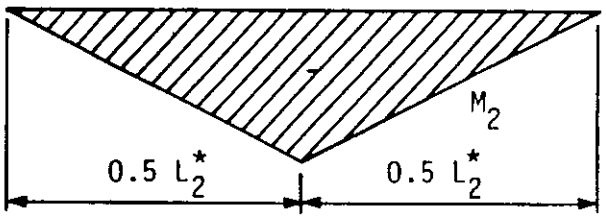

*ASSUMING $L_3 = L_4$

d. MOMENT DIAGRAM FOR MOCKUP

Fig. 2.1. Correlation between full-scale mockup and prototype

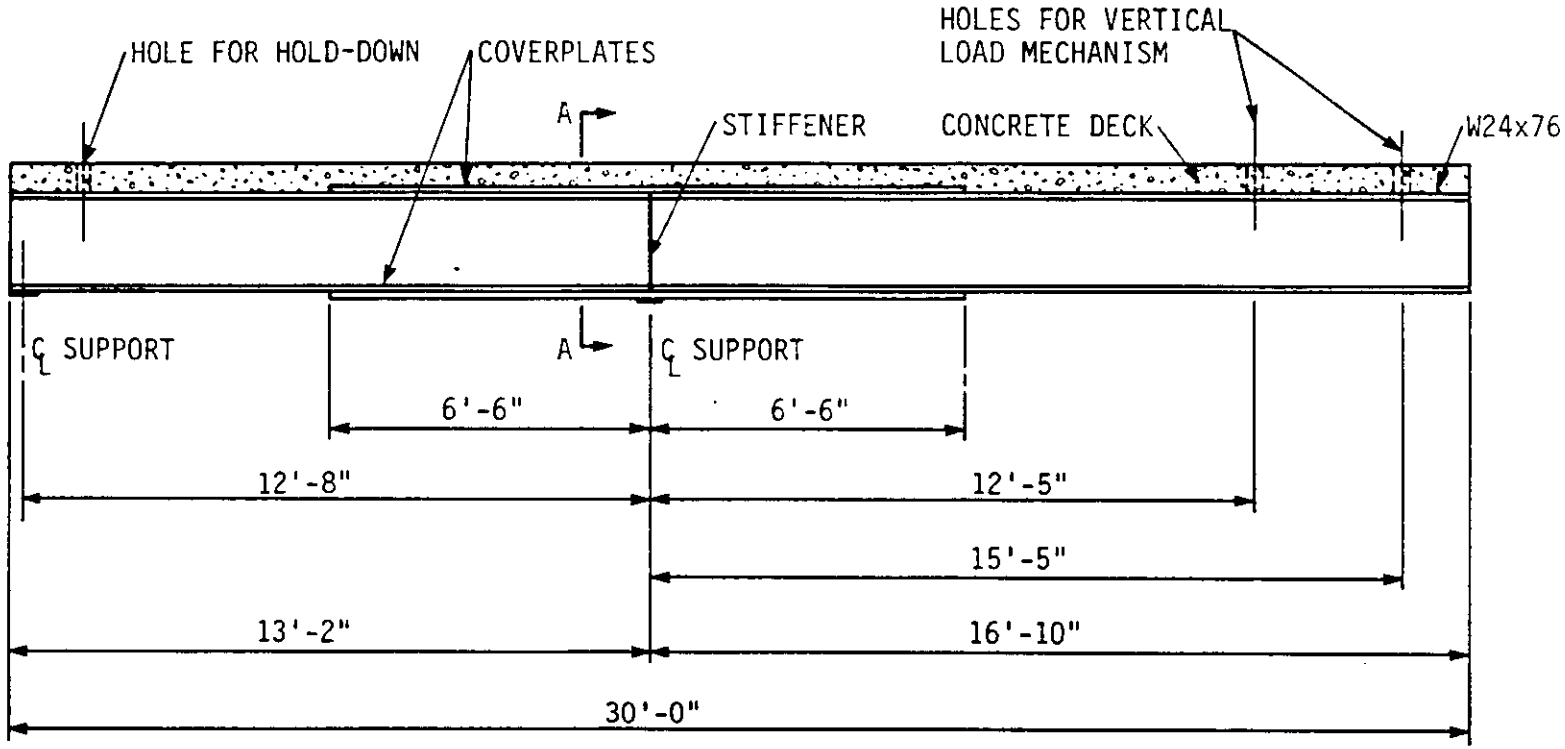

a. ELEVATION

Fig. 2.2. Full-scale mockup

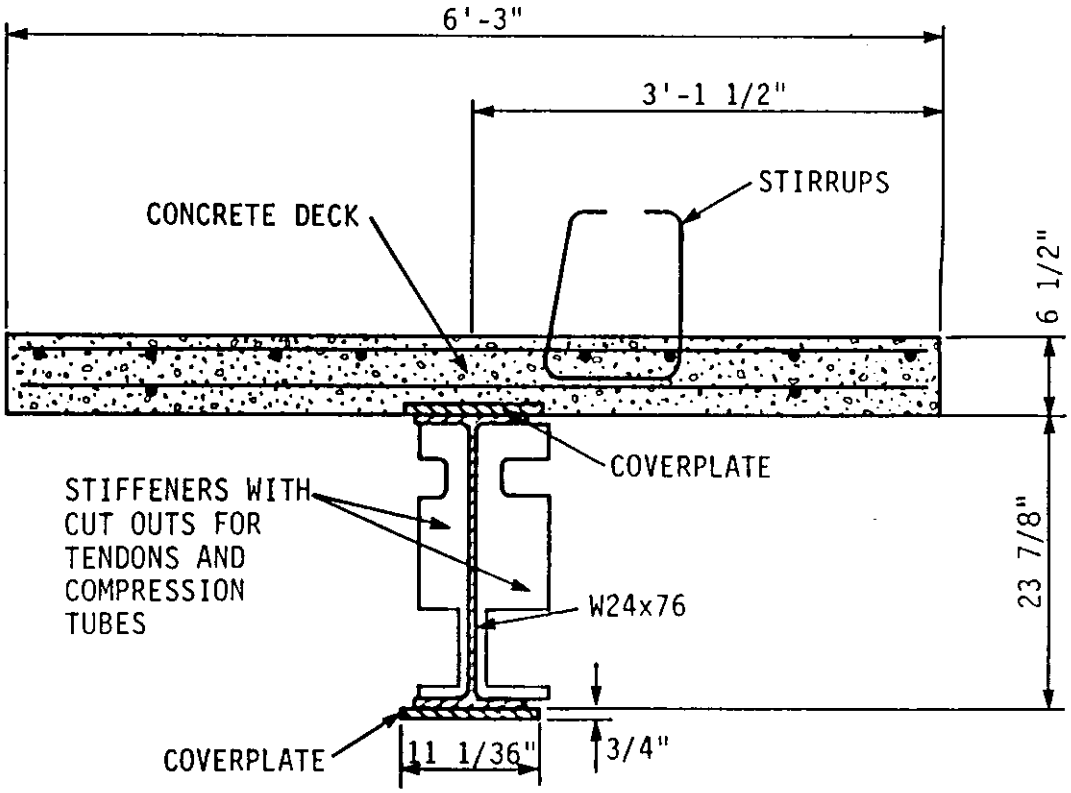

b. CROSS-SECTION A-A

Fig. 2.2. Continued

Figure 2.3b shows the 2 ft x 2 ft blockouts that were left in the deck from the original post-tension testing. Since the blockouts were not required in the strengthening procedures investigated in this study, appropriate reinforcing and concrete were placed in the blockouts, thus essentially eliminating them when the mockup was subjected to loads causing deck compression.

While preparing the mockup for the installation of the post-compression strengthening scheme, a considerable number of cracks were found in the concrete deck. In Fig. 4.28 of Ref. [3] the final crack patterns due to initial vertical load tests are documented. The additional cracks found in the deck at the initiation of this investigation (which was approximately eight months after the cracks shown in Fig. 4.28 of Ref. [3] were noted) were attributed to negative moment bending during loading of the mockup and to the age of the mockup. As a result of this cracking, additional loss of composite action and increased flexibility in the mockup were expected.

2.2. Post-Compression Strengthening Technique (ST2.1)

ST2.1 was designed to produce positive moment bending in the negative moment region of the mockup as shown in Figs. 2.4a,b. The moment diagram in Fig. 2.4b is exactly the same as if the moment were applied by post-tensioning the negative moment regions. To create the positive moment bending, a tension force below the beam's neutral axis was applied to the mockup within the negative moment region. The tension was to be applied by post-compressing a member located in this

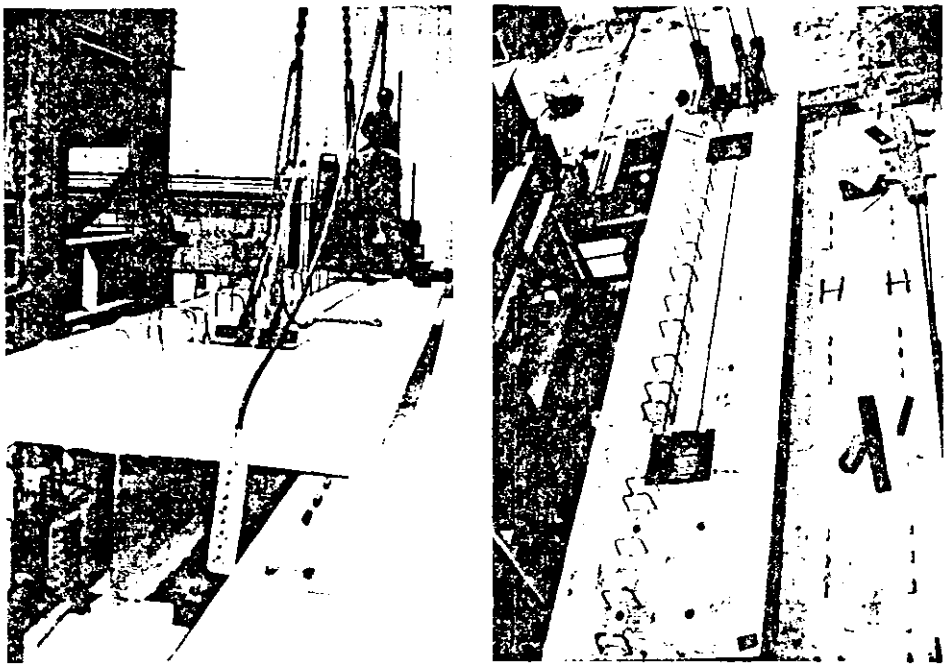

a. INSTALLATION OF HOLD-DOWN b. DECK BLOCKOUTS AND CABLE GROOVES

Fig. 2.3. Photographs of mockup

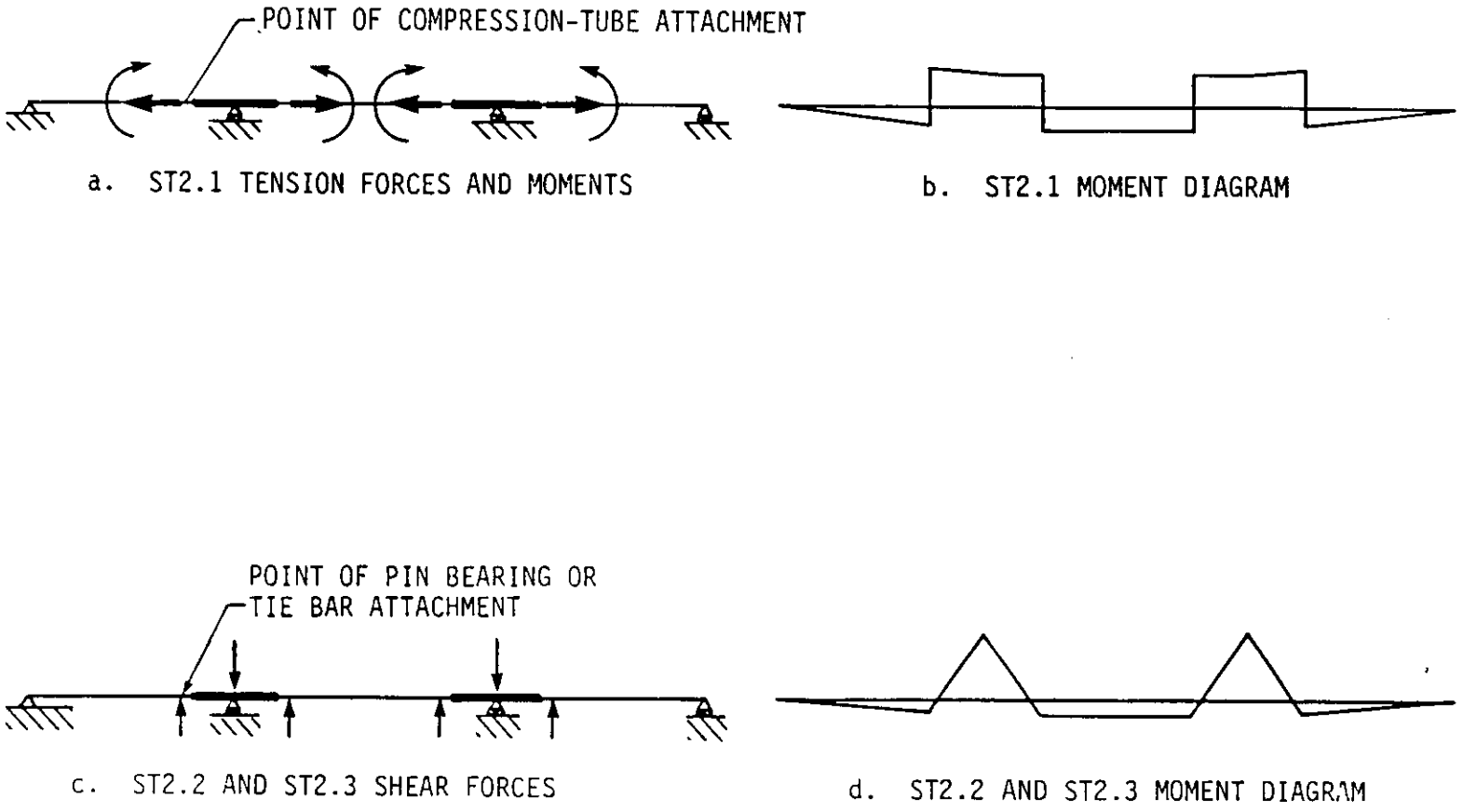

Fig. 2.4. Forces and moments applied to three-span beam by post-compression and truss-strengthening schemes

region. The compressive force required to reduce the service load stresses in the mockup the desired degree was calculated to be approximately 200 kips. Thus, the need for 100 kips of compression on each side of the web of the mockup was the controlling factor in the design of ST2.1.

Potential buckling of the required compression members introduced problems that obviously are not encountered with post-tensioned systems. (In post-tensioned systems, tendons will not buckle; however, post-tensioned portions of the structure when compressed are subject to buckling.) A method for locking the compression into the compression members also had to be designed. The locking mechanism required great precision since the 100 kip forces would create only small deformations in the compressive members. Thus, small seating losses would cause large decreases in the compressive force in the compression members.

The final design for ST2.1 is shown in Figs. 2.5 and 2.6. The system consists of two brackets and one compression tube mounted on each side of the web of the mockup. One bracket was designed to transfer the required load to the compression member. Since this bracket was involved in loading, it was designated the live bracket (see Fig. 2.5c). The bracket at the opposite end of the compressive member was not used for loading and thus was designated the dead bracket (see Fig. 2.5b).

Matching brackets were bolted together through the web of the mockup; twelve 7/8-in.-diameter A325 bolts were used in double shear

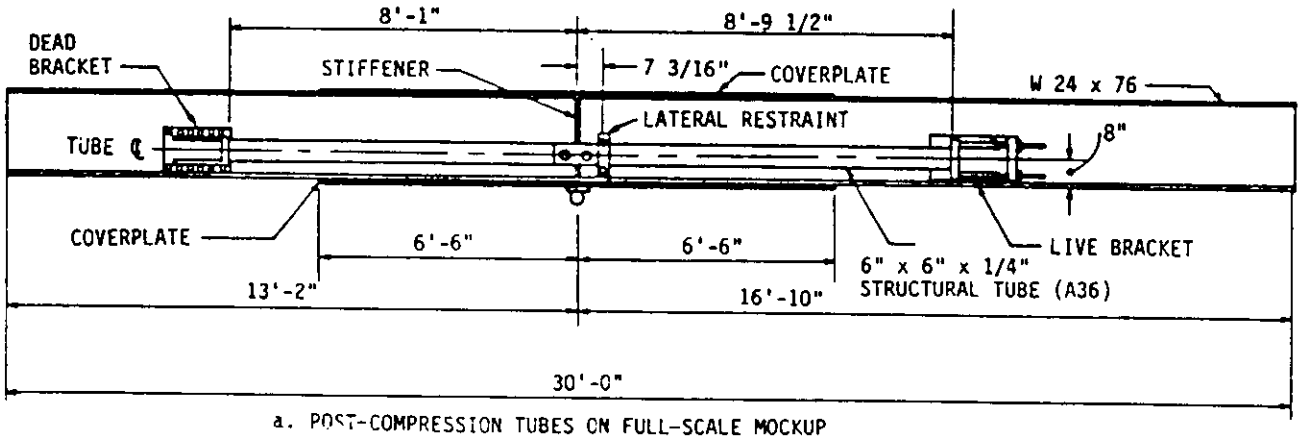

a. POST-COMPRESSION TUBES ON FULL-SCALE MOCKUP

Fig. 2.5. Post-compression strengthening technique (ST2.1)

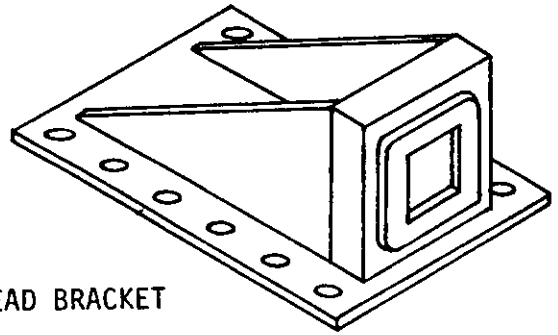

b. DEAD BRACKET

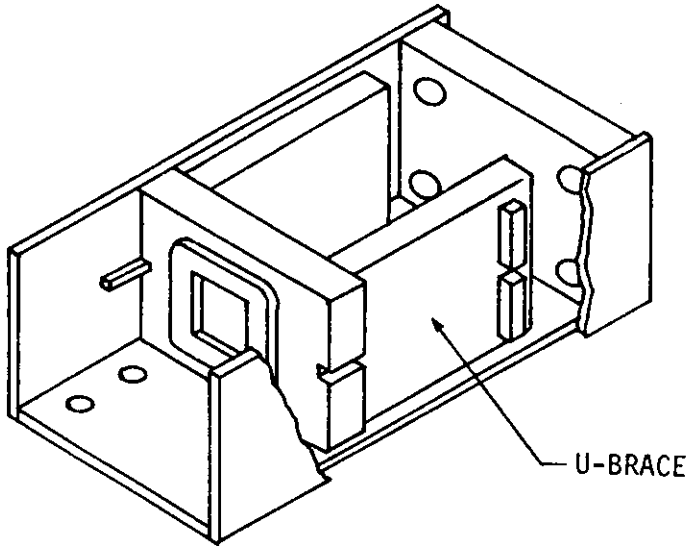

c. LIVE BRACKET

Fig. 2.5. continued

for each connection. Each bracket was designed to resist a load of 216 kips, which was approximately twice the design load.

2.2.1. Live bracket

The live bracket (shown in Figs. 2.5c, 2.6a, and 2.7a) was designed to accommodate a 60-ton hydraulic cylinder and to transfer the compressive force in the structural tubes to the beam web. The centerline of the live brackets was 9 ft-1 in. from the stiffener on the mockup and 8 in. above the bottom surface of the lower flange. General dimensions for the live bracket are given in Fig. 2.6a.

The transfer of the compressive force to the structural tubes was accomplished with a sliding cartridge called a U-brace (shown in Figs. 2.6a and 2.7a). The U-brace, which housed the hydraulic cylinder, was capable of sliding within the live bracket as compression was applied. The U-brace with the 60-ton hydraulic cylinder in place is shown in Fig. 2.7a. To lock a compression force in the compression tube, four 1-in.-diameter high strength threaded rods were tightened against the back of the U-brace. Each threaded rod transferred the compressive force through a nut to a 2-in.-thick bearing plate at the rear of the live bracket. Once the threaded rods were tightened against the U-brace, the hydraulic pressure was released and the hydraulic cylinder removed.

To lock the force into the compression tubes permanently, steel plates would be fit into the space previously occupied by the hydraulic cylinder. The threaded rods would then be loosened until the

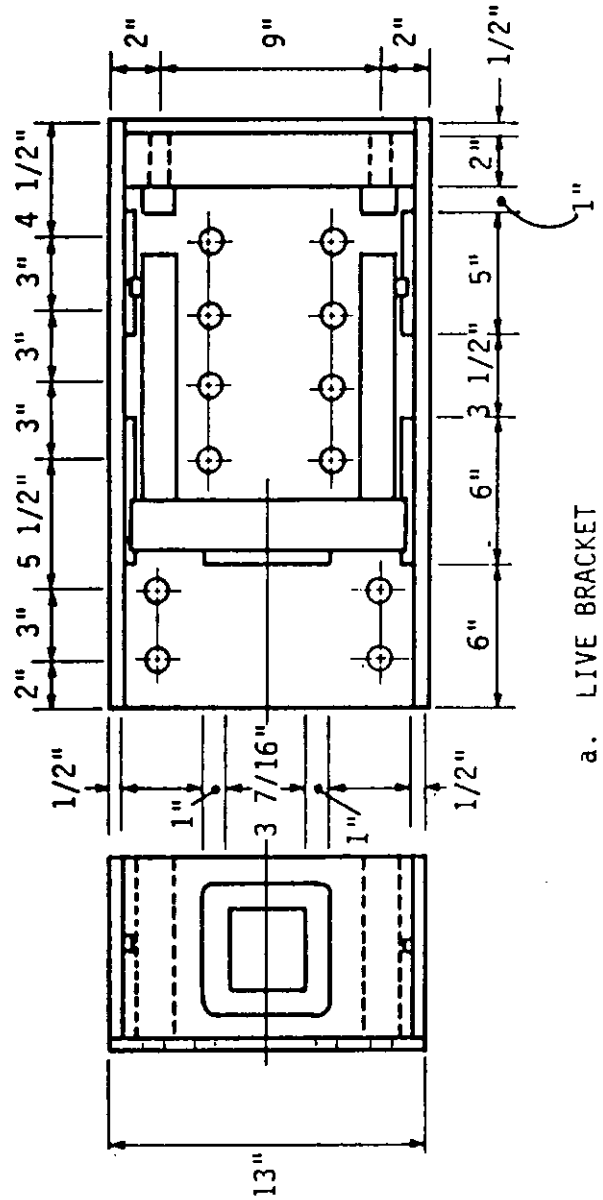

a. LIVE BRACKET

Fig. 2.6. ST2.1 brackets

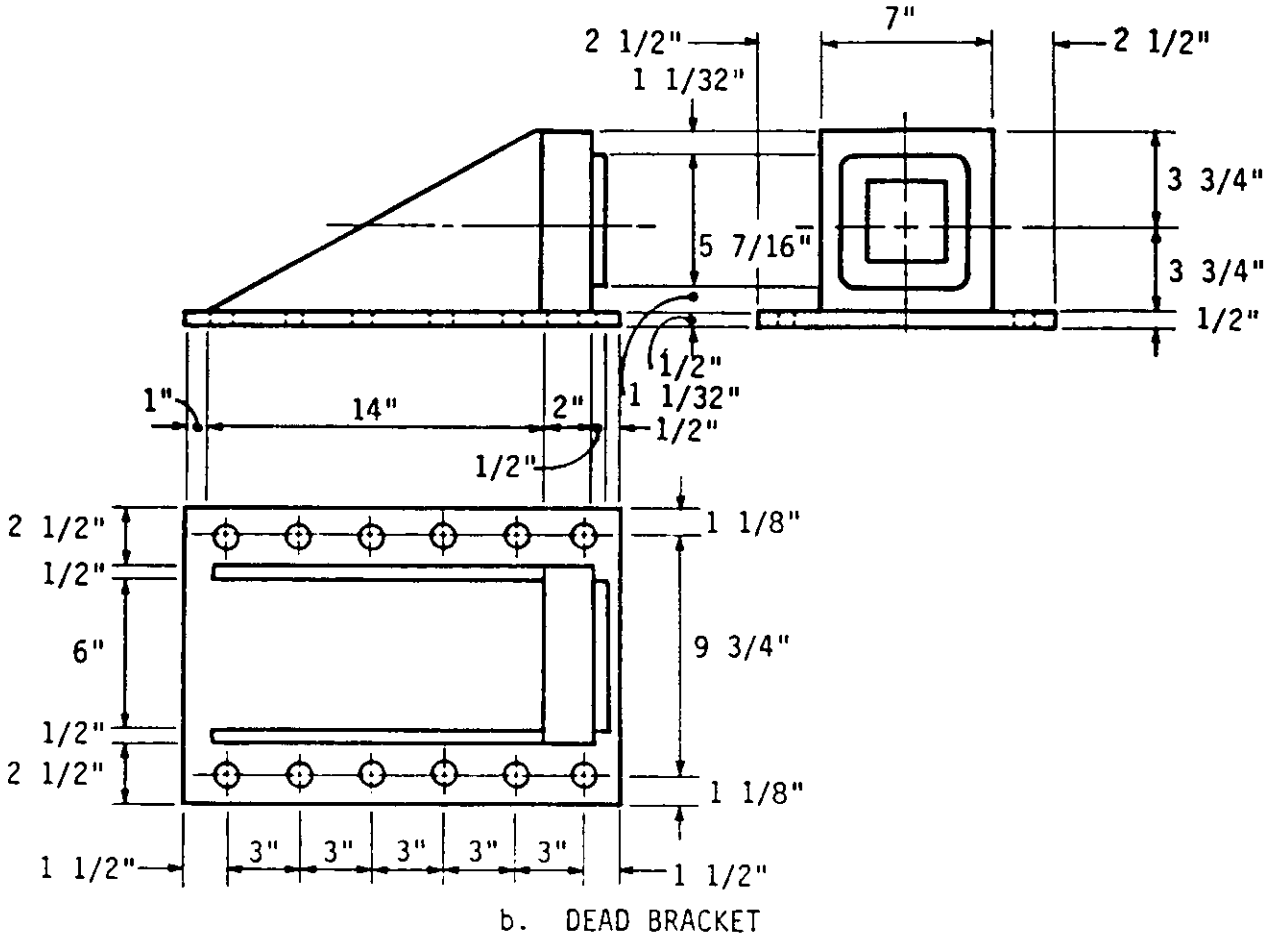

b. DEAD BRACKET

Fig. 2.6. continued

compressive force was carried by the steel plates. To prevent lateral movement of the U-brace within the live bracket, a series of restraints were designed to control any movement other than along the line of force. These restraints, which appear as slots in the U-brace, can be seen in Fig. 2.5c.

The front surface of the U-brace was the bearing plate for the compression tubes. To approximate a pinned connection, the compression tubes fit over 1/2-in.-thick plates, which were welded to the bearing surfaces. The plates that held the compression tubes in place are shown on the front surface of each bracket, in Figs. 2.5c and 2.6a.

2.2.2. Dead brackets

The dead brackets (shown in Figs. 2.5b, 2.6b, and 2.7b) were designed to resist the loads applied by the compression tubes and to transfer the force to the mockup. General dimensions for the dead brackets are given in Fig. 2.6b. The centerline of the dead brackets was located 8 ft 9 in. from the mockup stiffener and 8 in. above the bottom surface of the lower flange. As with the live bracket, the compression tube was not rigidly attached to the dead bracket. A 1/2-in.-thick plate was welded to the dead-bracket bearing plate. The compression tube fit snugly around the restraint, thus simulating a pinned connection similar to that on the live bracket. Two triangular 1/2-in.-thick plates held the bearing plate in place. Figure 2.7b shows one of the dead brackets on the mockup with the compression tube in place.

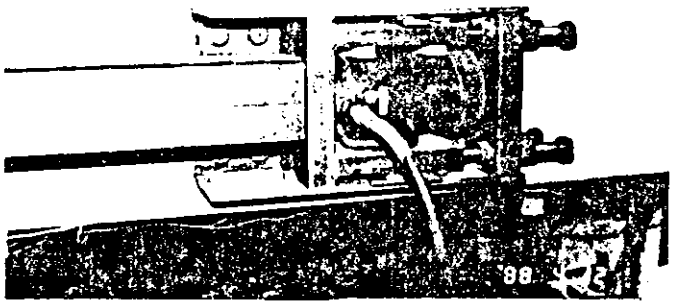

a. LIVE BRACKET AND COMPRESSION TUBE WITH 60-TON HYDRAULIC CYLINDER IN PLACE

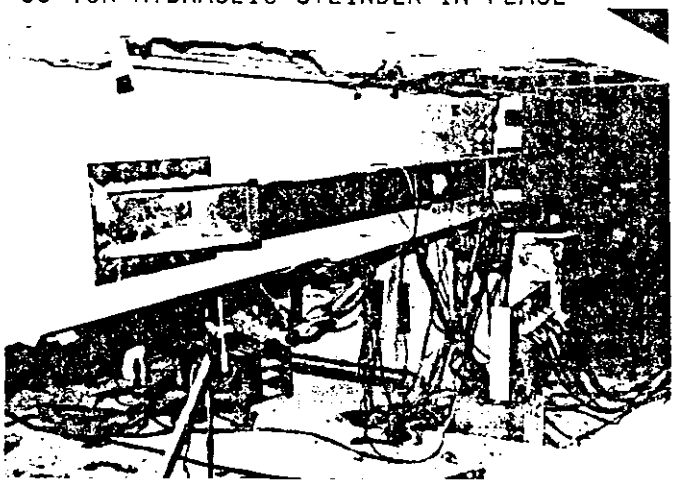

b. DEAD BRACKET WITH COMPRESSION TUBE

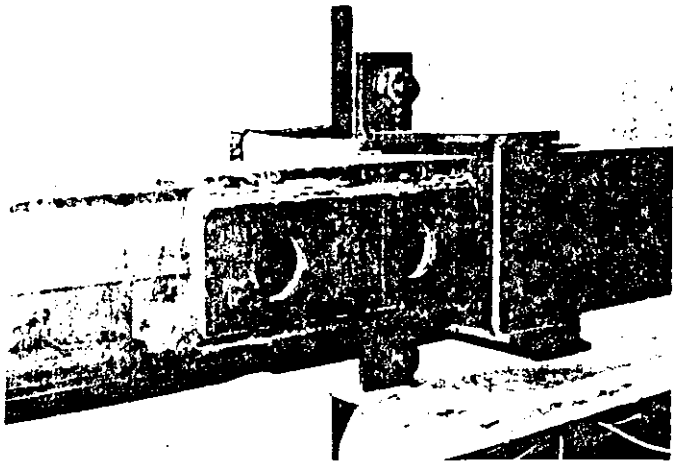

c. COMPRESSION-TUBE LATERAL RESTRAINT

Fig. 2.7. Photographs of ST2.1 on full-scale mockup

2.2.3. Compression tubes

The compression members were designed to resist approximately 120 kips each. This design value was based on a 100-kip design load plus an expected increase in load due to vertical loading of the mockup. The total length of the members between the brackets was 16 ft-5 1/2 in. To increase the buckling strength of the compressive tubes, lateral restraint was located near the center of the members, resulting in a maximum unbraced length of 8 ft-9 1/2 in. Only symmetric sections were considered because of the potential for bending about either axis. Based on the design requirements, 6 in. x 6 in. x 1/4 in. A500 (46 ksi) structural tubes were selected for the compression members.

Two lateral restraint schemes were evaluated during preliminary tests of ST2.1. The first scheme is shown in Fig. 2.8a. This scheme consisted of two bolts connecting the tubes together through the web of the mockup. Steel pipes 1 1/4 in. in diameter enclosed the bolts. The pipes enabled the connection to be tightened without pulling the compression tubes together toward the mockup web. The pipes maintained the correct distance between the compression tube on each side of the web. Two slots were cut in the web of the mockup beam so that the mockup did not prevent movement of the tubes when they were compressed. Nuts were tightened against the inside of each tube as shown in Fig. 2.8a to restrain the tubes from movements away from the web of the mockup. Two holes were cut in the outside face of each compression tube for access to the connection. Stiffeners added to the tubes at

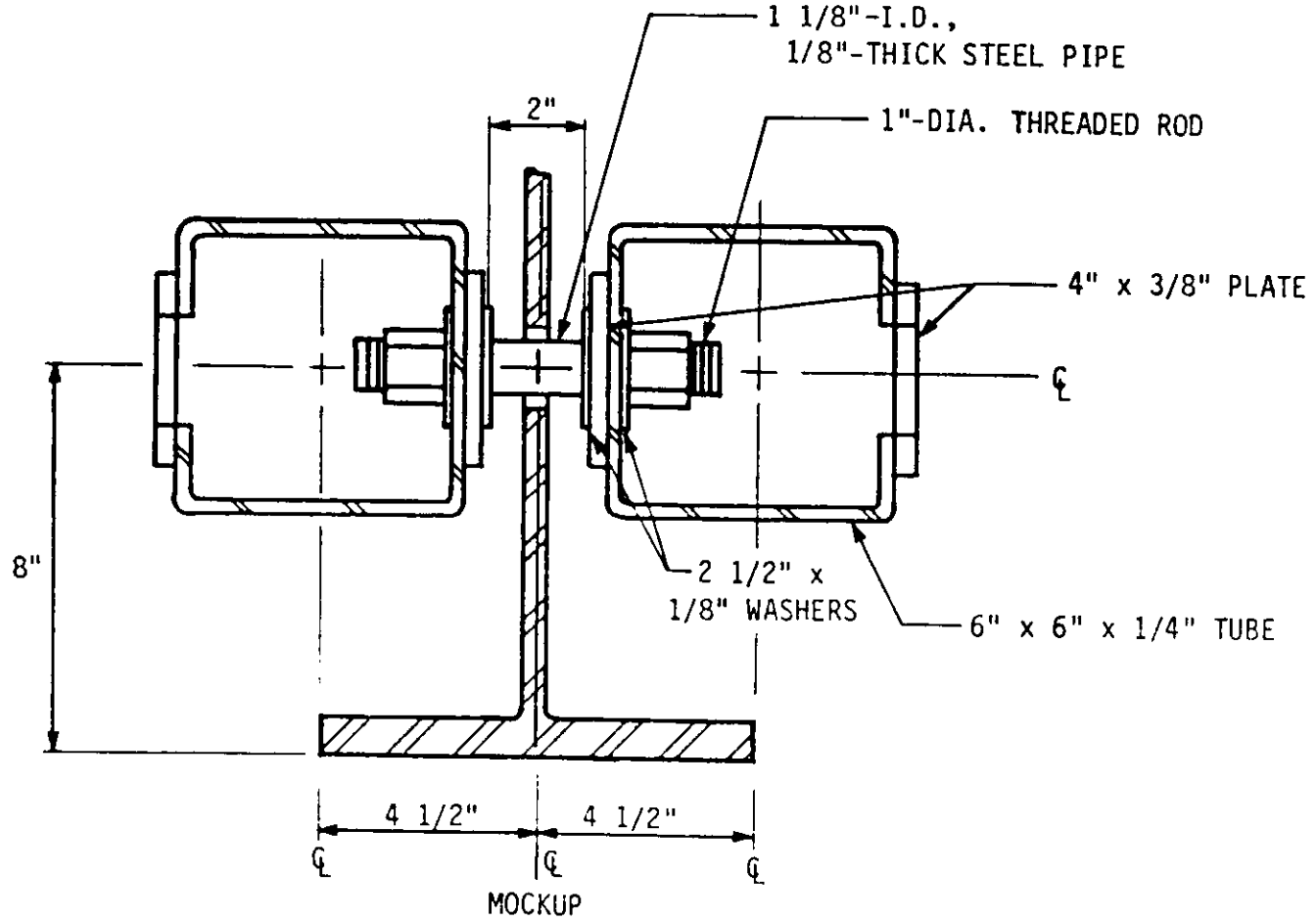

a. INTERNAL LATERAL RESTRAINTS

Fig. 2.8. Compression-tube lateral restraints

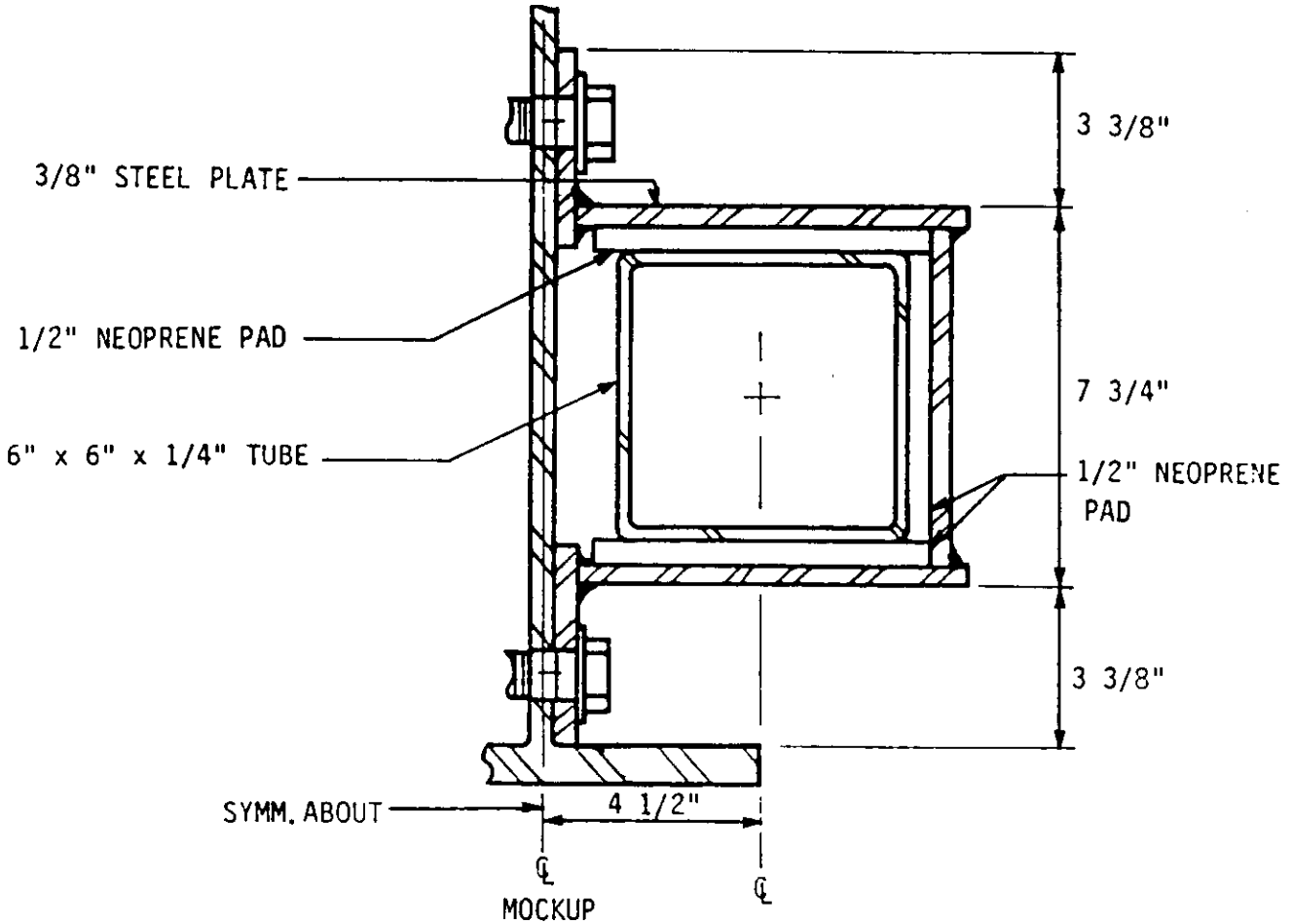

b. INDEPENDENT LATERAL RESTRAINT

Fig. 2.8. continued

this section, to replace the material removed when the holes were drilled, can be seen in Figs. 2.7c and 2.8a.

During preliminary testing, this restraint system did not perform as desired. The compression tubes did not respond in proportion to the loading. Since the tubes were connected, bending in one tube resulted in bending in the other tube. The restraining system that connected the compression tubes together actually increased the bending stresses in the tubes.

The second type of lateral restraining system investigated was a strap that confined the compression tube and was bolted to the web of the beam. The strap, shown in Figs. 2.7c and 2.8b was offset from the beam stiffener by 7 3/16 in. By providing independent restraint to each tube, researchers reduced flexural stresses in the tubes to acceptable levels.

2.3. Superimposed Truss Strengthening Techniques (ST2.2, ST2.3)

The superimposed truss was designed with two configurations for applying the required upward strengthening load to the mockup. Although each design had unique end conditions, identical tendons and compression struts were used by both ST2.2 and ST2.3.

ST2.2 and ST2.3 were also designed to produce positive moment bending in the negative moment region of the mockup. Tensioning the truss created upward forces on the mockup at 9 ft 1 in. on either side of the stiffener. Loading the truss was accomplished by tensioning the 1 1/4-in.-diameter Dywidag thread bar shown in Figs. 2.9a and 2.11a.

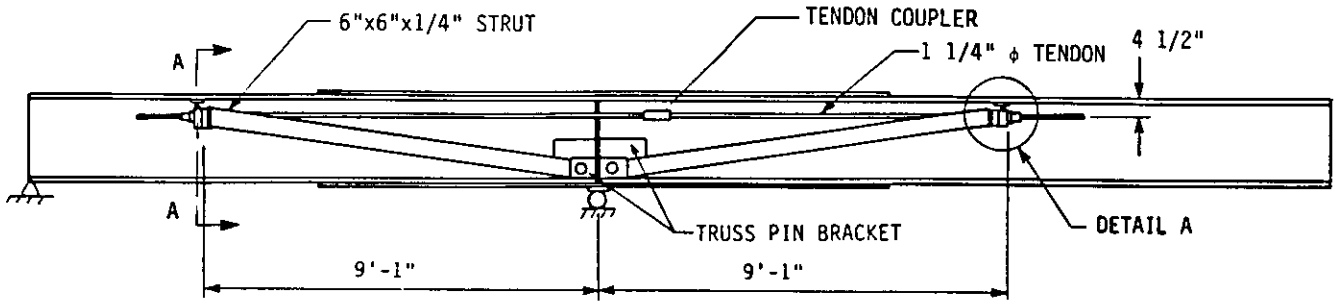

a. ST2.2 ON FULL-SCALE MOCKUP

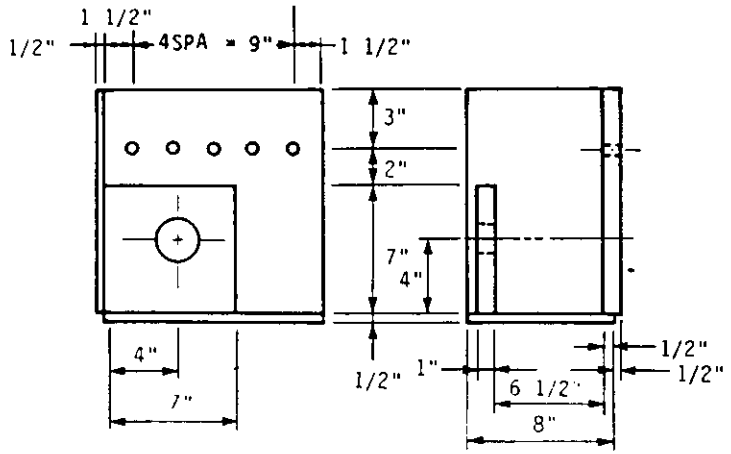

b. PIN BRACKET

Fig. 2.9. Superimposed truss-strengthening technique (ST2.2)

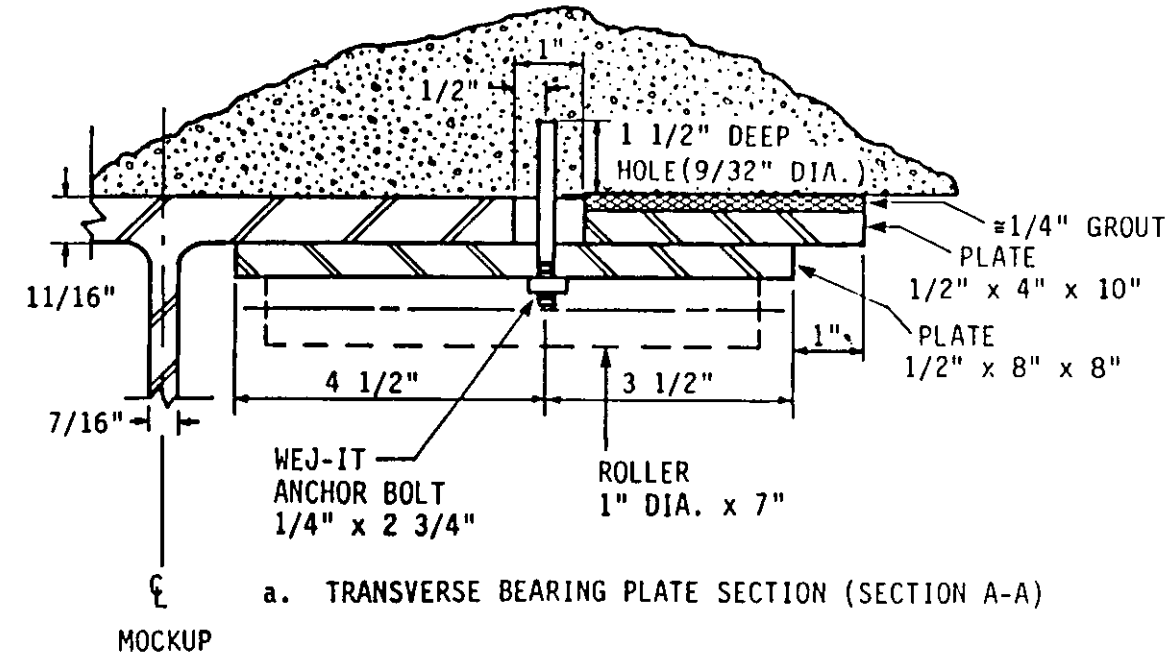

a. TRANSVERSE BEARING PLATE SECTION (SECTION A-A)

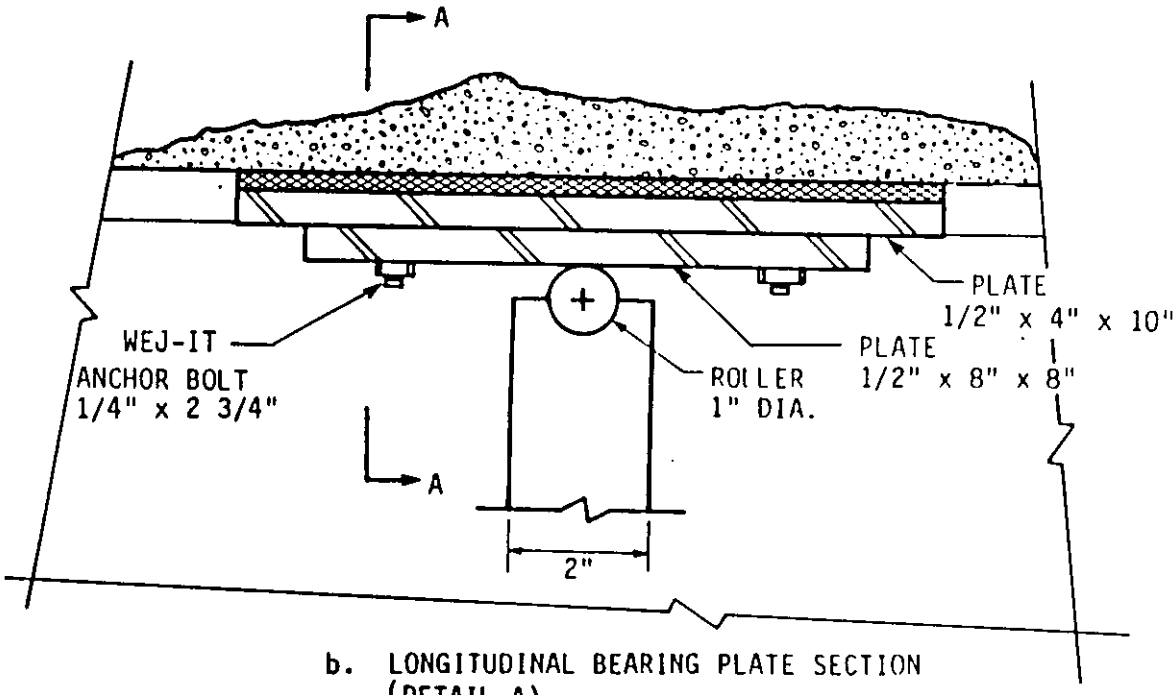

b. LONGITUDINAL BEARING PLATE SECTION (DETAIL A)

Fig. 2.10. ST2.2 bearing plate assembly

The trusses on each side of the beam web were tensioned simultaneously from the same end of each truss. The force schematic and moment diagram for ST2.2 and ST2.3 are shown in Figs. 2.4c,d. The upward force required to reduce the service load stresses in the mockup to the desired degree was calculated to be approximately 25 kips. Since one truss was located on each side of the web of the mockup, approximately 12.5 kips of upward force were required at each end of the truss. As shown in Figs. 2.9a and 2.11a, the compression members were inclined at an angle of 7° to longitudinal axis of the mockup. To obtain the desired upward force, the researchers used basic truss analysis to determine that each compression tube and tension member would have to support forces of 102 kips and 100 kips, respectively.

2.3.1. Pin bracket

The pin bracket (see Fig. 2.9b) for the truss acted as a true pin-ended condition for the compression struts as a 2 1/2-in.- diameter pin passed through the webs of the compression struts and into the bracket on each side of the beam. Figure 2.12a shows two pin brackets with compression struts bolted to the mockup. Since the brackets reacted against each other (horizontal) and into the bottom flange (vertical), the connection to the mockup had to resist lateral forces only. Five 7/8-in.-diameter A325 bolts, also shown in Fig. 2.12a, connected the two brackets through the web and thus prevented lateral movement.

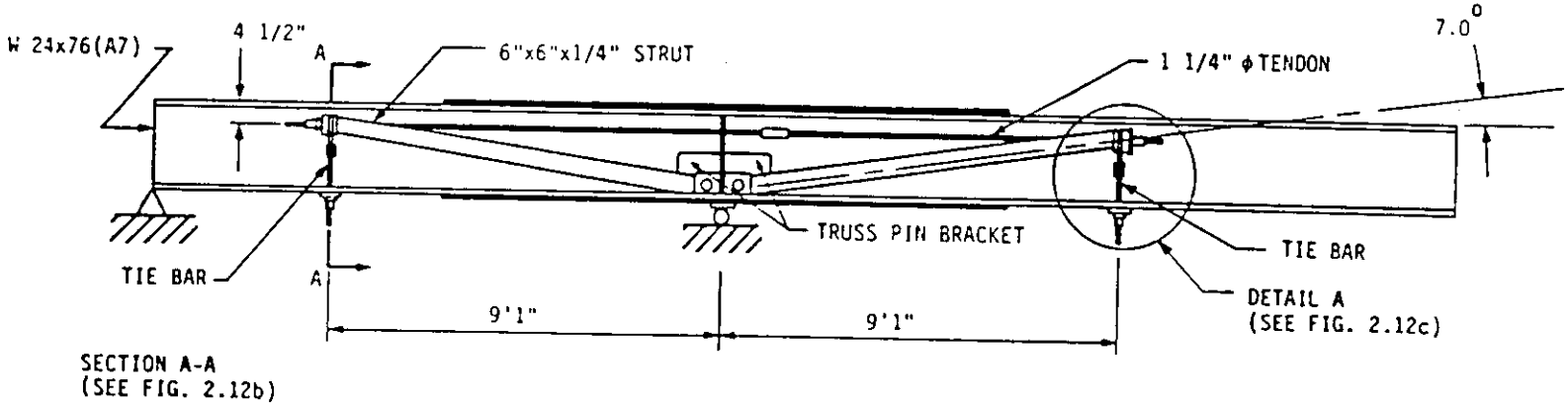

a. ST2.3 ON FULL-SCALE MOCKUP

Fig. 2.11. Superimposed truss-strengthening technique (ST2.3)

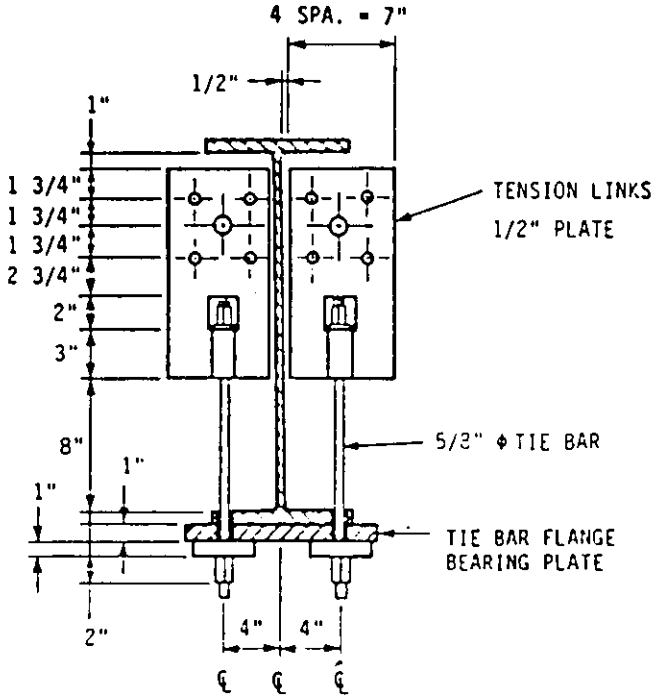

b. SECTION A-A

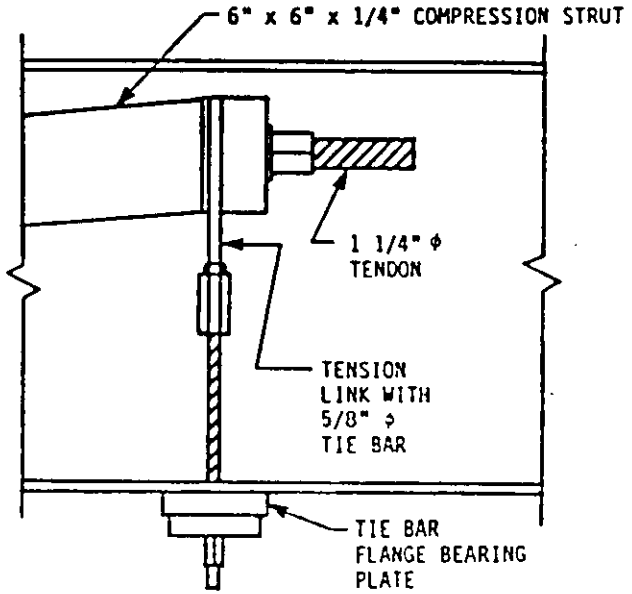

c. DETAIL A

Fig. 2.11. continued

2.3.2. Compression struts

Based on the required load, researchers selected 6 in. x 6 in. x 1/4 in. A500 (46 ksi) structural tubes as compression struts for ST2.2 and ST2.3. The tubes had to be significantly modified for use in the trusses. At the pin bracket end, stiffeners were added to two sides of each tube. The stiffeners shown in Fig. 2.13a were necessary for distributing the compressive load to the bearing pin. Bearing plates, shown in Fig. 2.13b, were welded on the jacking end of each strut. The plates were at a 7° angle to create a vertical surface when the truss was in place. The bearing plate also had four pins that allowed attachment of the two types of end conditions. A 1 3/4-in.-diameter hole at the center of the bearing plate allowed the 1 1/4-in.-diameter tendon to pass through the end of the truss (see Figs. 2.9a and 2.11a). The tubes were also modified in order for the 1 1/4-in.-diameter tendons to pass through the top surface of each tube, as shown in Figs. 2.10a and 2.12a. An 18-in.-long, 2-in.-wide slot was cut in the tubes and stiffened with two 30-in. x 1 1/4-in. x 1/2-in. steel plates welded along each side of the slot. The stiffeners were necessary to replace the steel removed from the tube for the slot.

Lateral restraints, which are shown in Figs. 2.12b and c, were bolted to the beam web near the end of each compression strut. Although no out-of-plane forces would normally be expected in the truss system, the restraints were added as a safety precaution. They were essential when the mockup with ST2.3 in place was tested to failure.

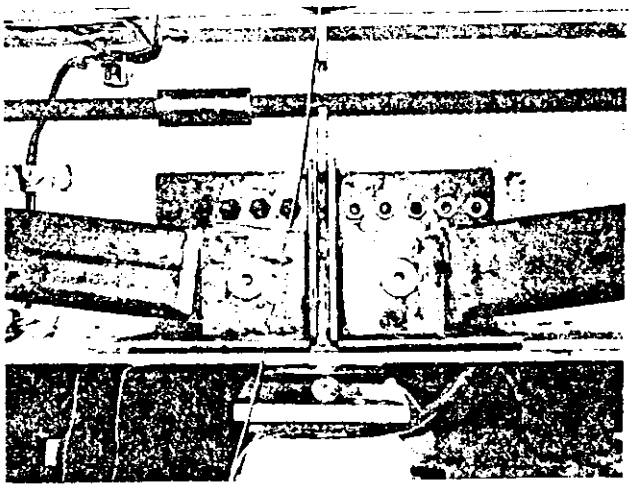

a. PIN BRACKETS

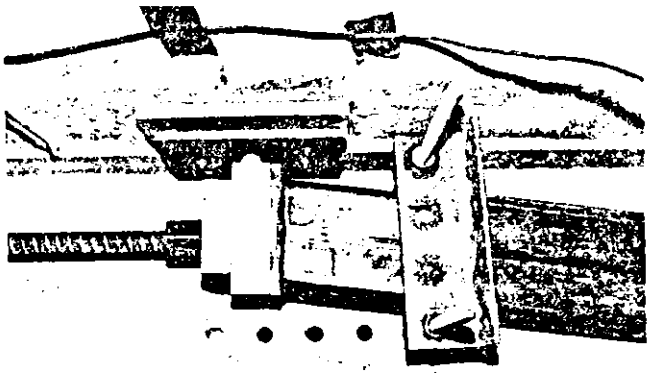

b. ST2.2 END CONDITION

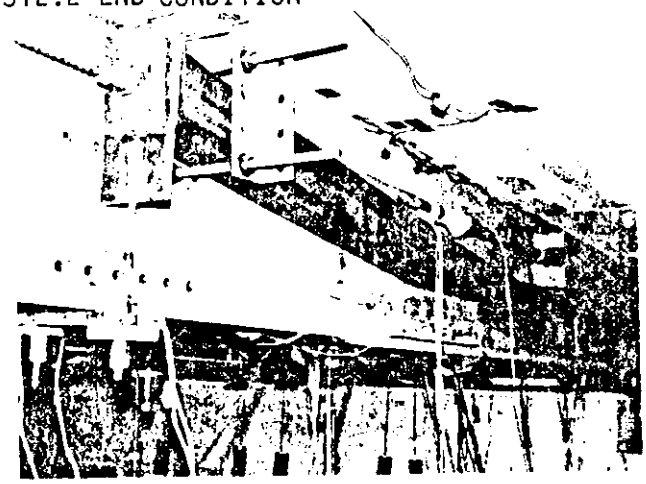

c. ST2.3 END CONDITION

Fig. 2.12. Photographs of ST2.2 and ST2.3 on full-scale mockup

2.3.3. End conditions

As previously noted, two different schemes were investigated for applying the vertical strengthening force to the mockup. The first scheme involved the truss bearing up against the bottom of the deck (ST2.2), while the second scheme connected the truss to the bottom flange of the beam (ST2.3).

2.3.3.1. ST2.2 For applying the upward force to the lower surface of the top flange of the mockup, a 7-in. x 7-in. x 2-in. plate with a bearing roller was attached to the compression struts (see Figs. 2.9a, 2.10, and 2.12b). A bearing plate was anchor-bolted to the bottom of the deck of the mockup as shown in Fig. 2.10. Approximately half the area of the bearing plate was on the bottom of the concrete deck, and half was on the bottom of the upper beam flange. As the 1 1/4-in.-diameter tendon was tensioned, the ends of the compression struts deflected upward into contact with the bearing plate on the lower surface of the mockup.

2.3.3.2. ST2.3 In ST2.3 the vertical component of force in the truss, which produced the positive moment, was resisted by the lower flange of the beam. Tension links consisting of four 5/8-in. 150-grade, Dywidag threadbars (see Figs. 2.11 and 2.12c) connected the end of each compression strut to the bottom flange of the mockup. The strap shown in Figs. 2.11b,c distributed the vertical force across the bottom flange of the mockup. When the 1 1/4-in.-diameter tendon was

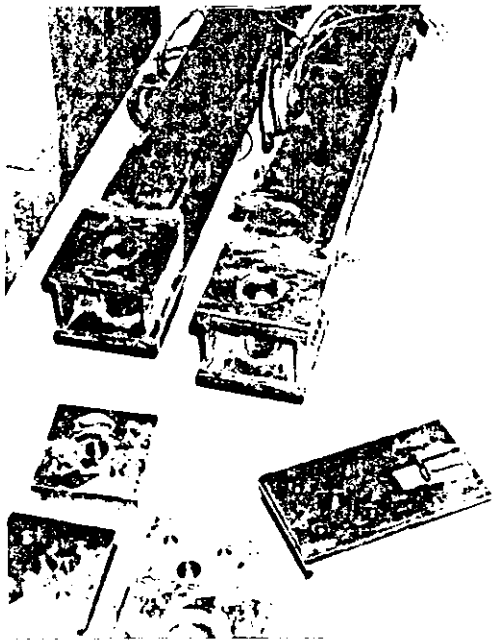

a. COMPRESSION STRUT PIN BRACKET END

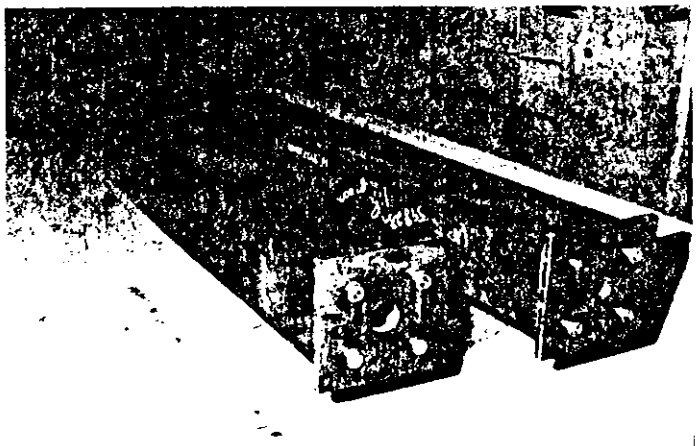

b. COMPRESSION STRUT BEARING PLATE END.

Fig. 2.13. Photographs of ST2.2 and ST2.3 compression struts

tensioned, the tension links reacted against the bottom flange of the mockup truss producing positive moment.

3. TESTS AND TEST PROCEDURES

This chapter outlines the details of the instrumentation and testing of the full-scale mockup and the strengthening systems. Locations of instrumentation for measuring strain and displacement will be given for the mockup and each of the strengthening schemes. A detailed description of the tests performed on the unstrengthened mockup, as well as on the mockup with each strengthening scheme in place will also be given. Discussion and analysis of results obtained will be presented in Chapter 4.

3.1. Vertical Load Mechanism

The vertical loading mechanism used to create the negative moment is shown in Fig. 3.1. This figure indicates that the left and right "inflection points" were located 12 ft. 8 in. and 12 ft. 5 in., respectively, from the "interior support". The left inflection point hold down was preloaded with a 75-kip clamping force to hold the beam on the support when loading was applied to the free end of the beam. As previously noted, Fig. 2.1 illustrates how this loading mechanism simulated negative moment regions of a prototype bridge.

The load cell shown in Fig. 3.1 measured the force of one of the two hollow-core hydraulic cylinders used. Since the cylinders were in parallel, the load cell read one-half the total vertical load. This loading mechanism produced the desired negative moment between the two inflection points of approximately 534 ft-kips when a 43-k vertical load was applied at the load point (i.e., the right inflection point).

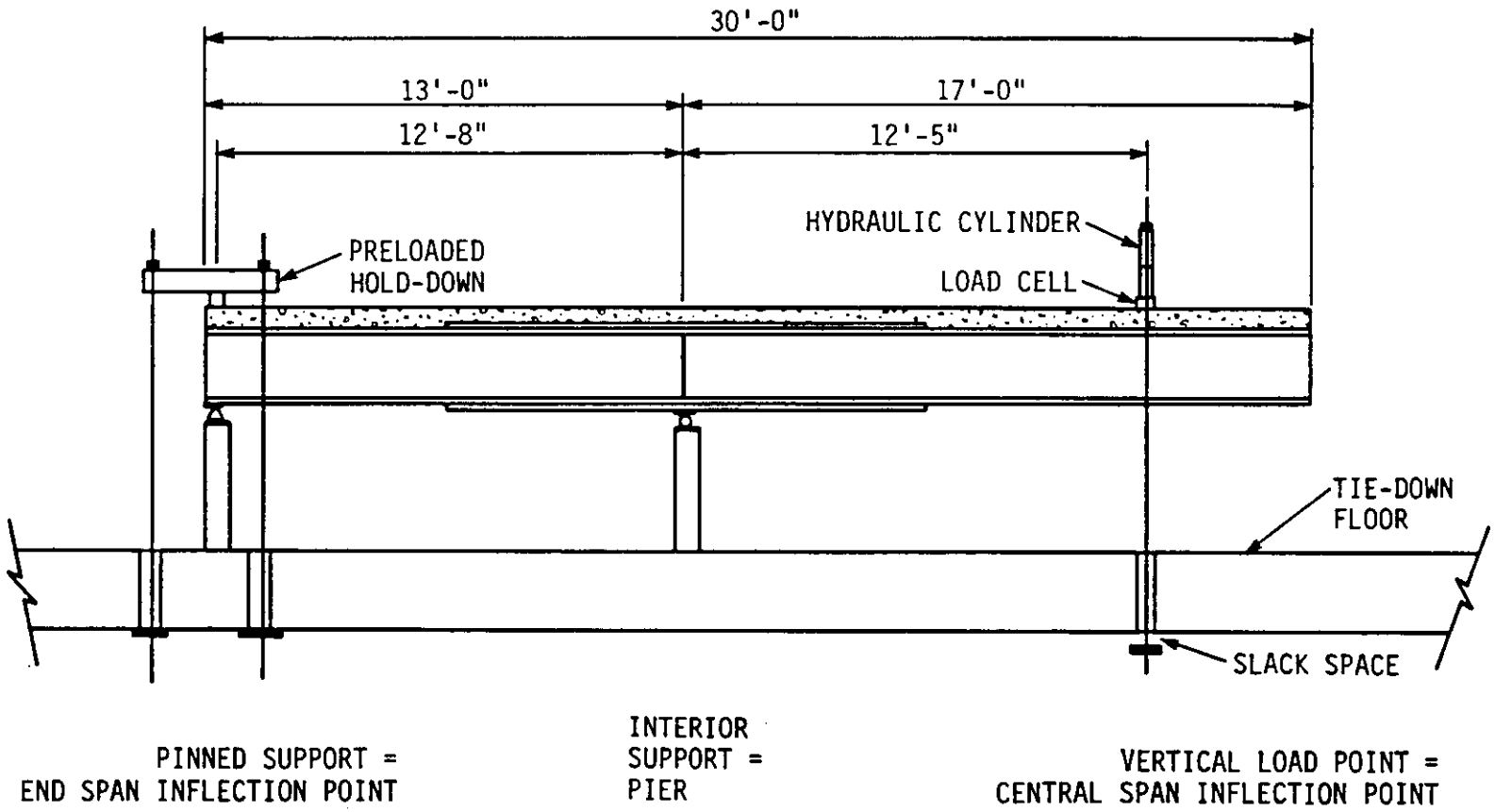

Fig. 3.1. Vertical loading mechanism for full-scale mockup

3.2. Instrumentation

The instrumentation for all tests consisted of electrical-resistance strain gages (strain gages), direct current displacement transducers (DCDTs), and a load cell. Strain gages were temperature compensated and were attached to the specimens with recommended surface preparation and adhesive. Three-wire leads were used to minimize the effect of long lead wires and temperature changes. All strain gages were waterproofed with a minimum of two layers of protective coatings. Strain gages and DCDTs on the mockup and strengthening systems were read and recorded with a computerized data acquisition system (DAS). Each strain gage was bonded with its axis parallel to the axis of the beam, tube, or tendon.

3.2.1. Mockup instrumentation

The locations of strain gages used on the beam and cover plates are shown in Fig. 3.2. Strain gages were offset from the support centerline because of the sole plate. They were also offset from the cover plate cutoff points to avoid the high stress gradients at these locations. A total of 28 strain gages were placed on the beam and cover plates. At each of the numbered sections in Fig. 3.2, there were four strain gages on the beam: two on the top surface of the top beam flange and two on the bottom surface of the bottom beam flange. Figure 3.3 shows the position of the DCDTs used for measuring the vertical displacements. Although not shown in Fig. 3.3, a dial gage was located at the loaded end of the mockup to detect any lateral movement.

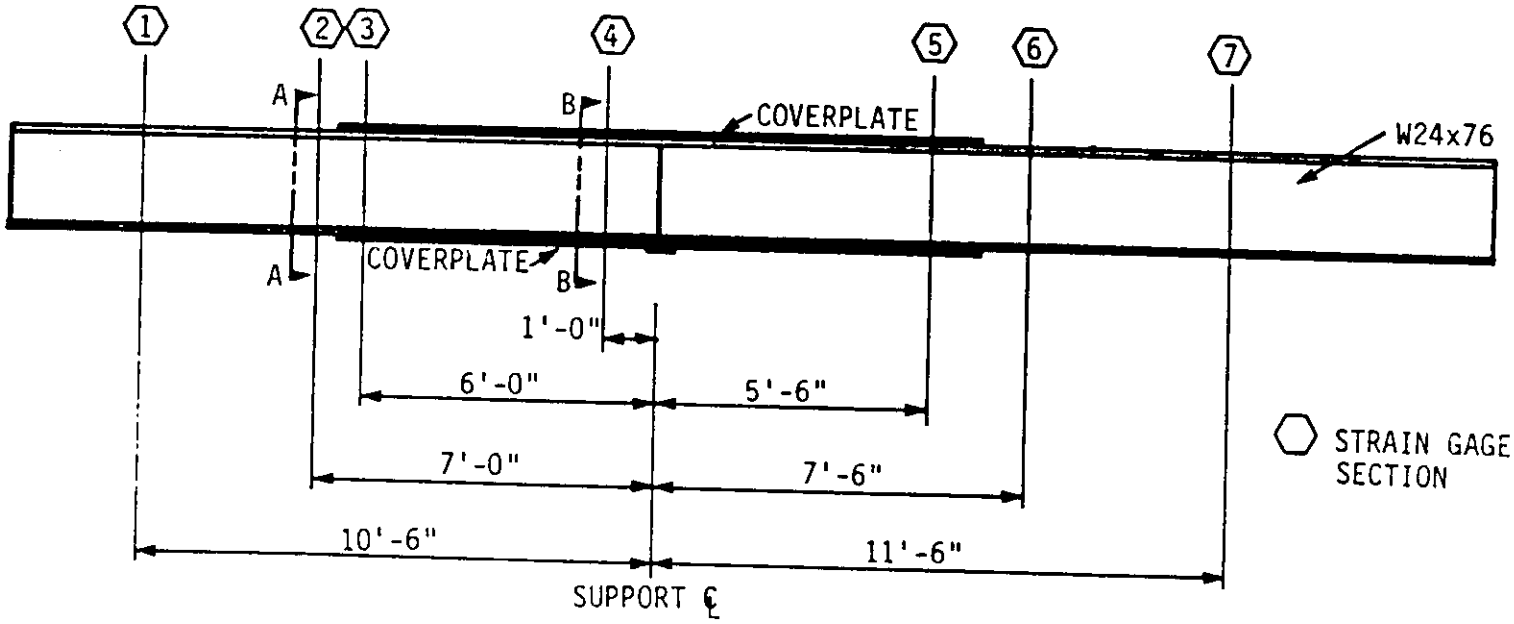

a. LAYOUT

Fig. 3.2. Strain gage locations for full-scale mockup

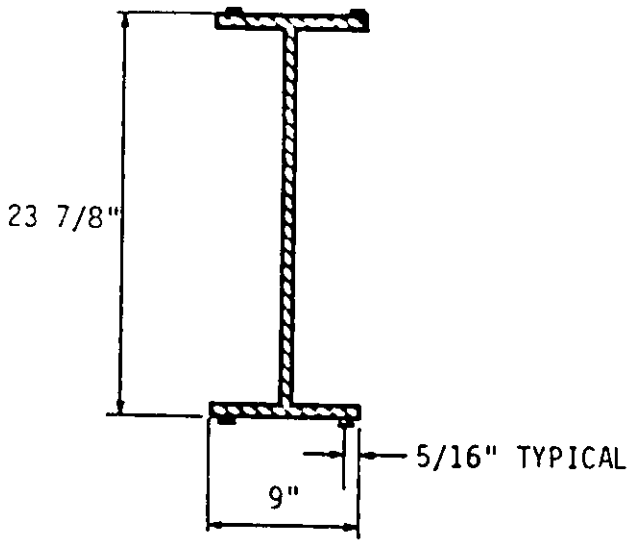

b. SECTION A-A

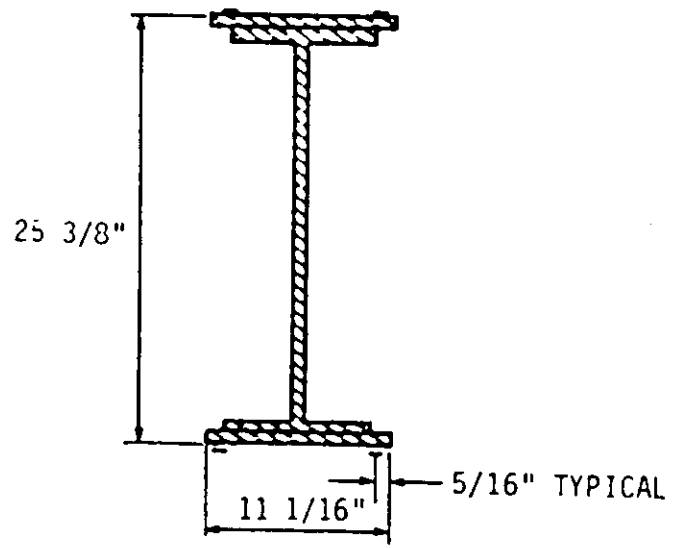

c. SECTION B-B

Fig. 3.2. continued

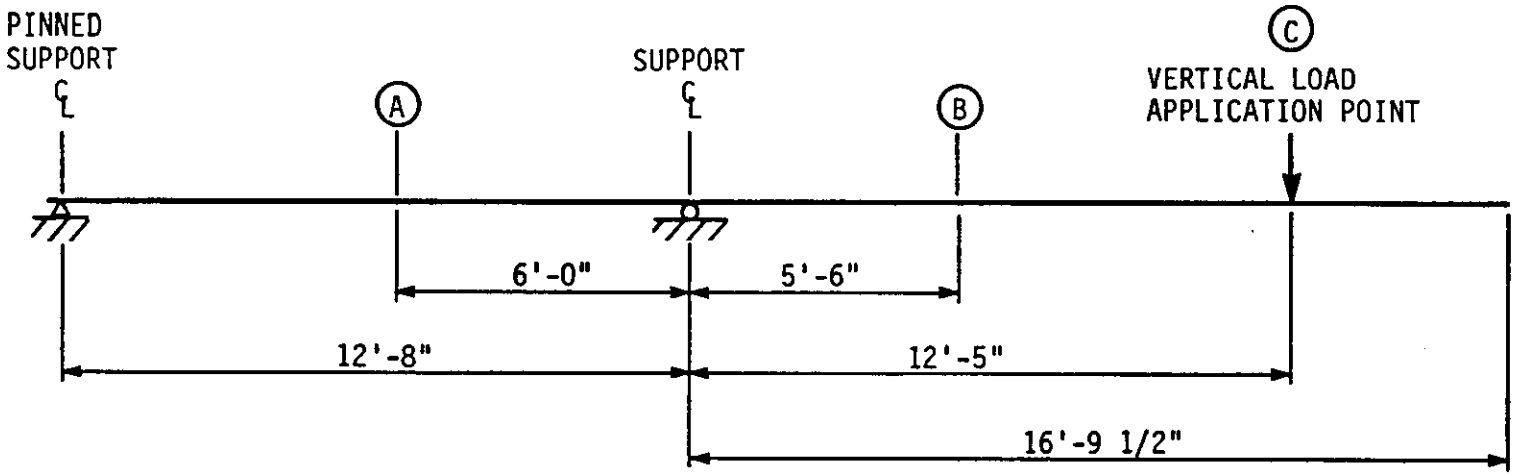

Fig. 3.3. Vertical displacement measurement (DCDT) locations on full-scale mockup

3.2.2. ST2.1 Instrumentation

Strain gage locations on the post-compression tubes are shown in Fig. 3.4. A total of 30 strain gages were placed on the post-compression tubes. Strain gages were located at a section approximately midway between the lateral restraint and each end of the tubes. If any bending took place in the tubes, it would be a maximum at these locations and thus easy to detect. An additional section located 1 ft from the lateral restraint on one tube was instrumented with strain gages to determine the effectiveness of the lateral restraint in reducing bending.

At each section, six strain gages were arranged around the tube as shown in Fig. 3.4b,c. Two strain gages were located on the top surface of the tubes to straddle the weld seam, which ran along the centerline. Locating the strain gages as shown in Fig. 3.4c avoided stress concentrations at the seam and the corners of the tubes. Strain gages on the bottom surface of the tubes were placed similarly, for consistent data. The arrangement of six strain gages at each instrumented section made it possible to determine accurately the bending and axial force at each section.

3.2.3. ST2.2 and ST2.3 Instrumentation

Instrumentation used on the superimposed truss is illustrated in Fig. 3.5. A total of 38 strain gages were used on ST2.2. Strain gages on the compression struts were similar to those on the post-compression

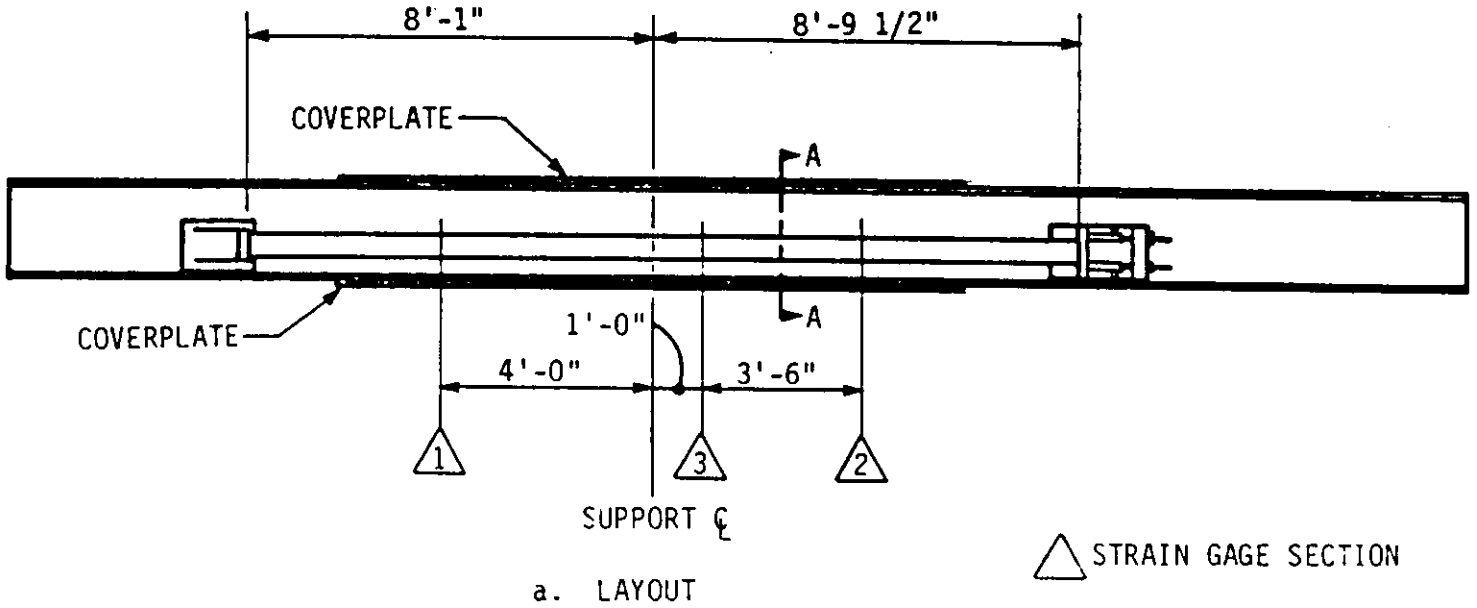

a. LAYOUT

Fig. 3.4. ST2.1 strain gage locations

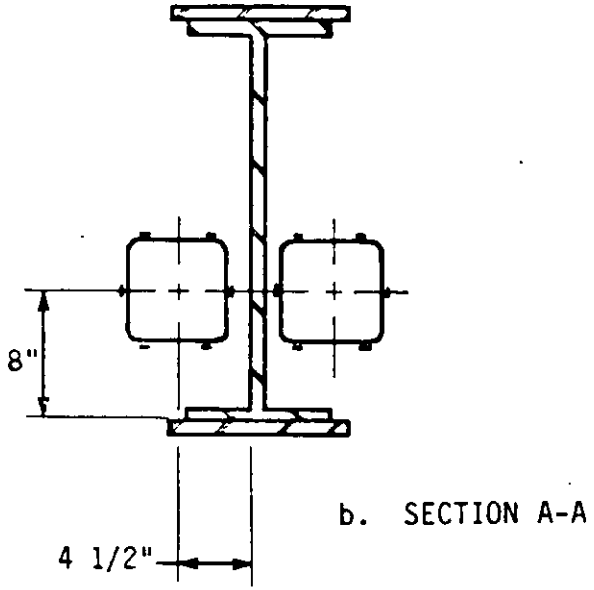

b. SECTION A-A

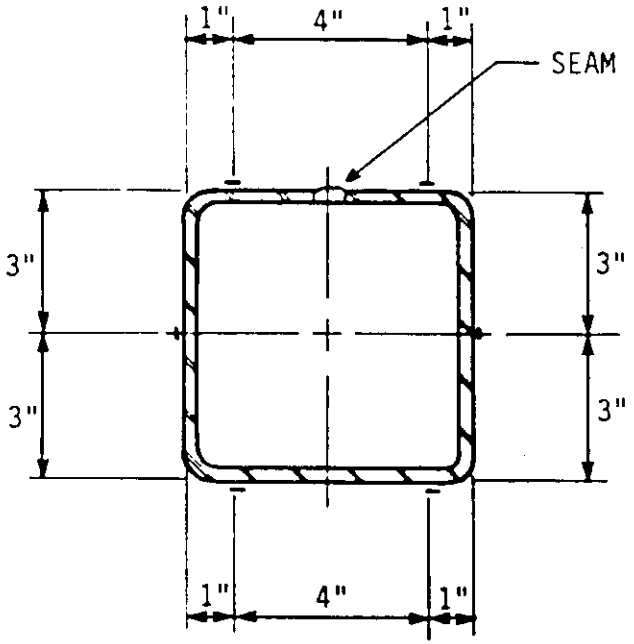

c. COMPRESSION-TUBE STRAIN GAGE LOCATIONS

Fig. 3.4. continued

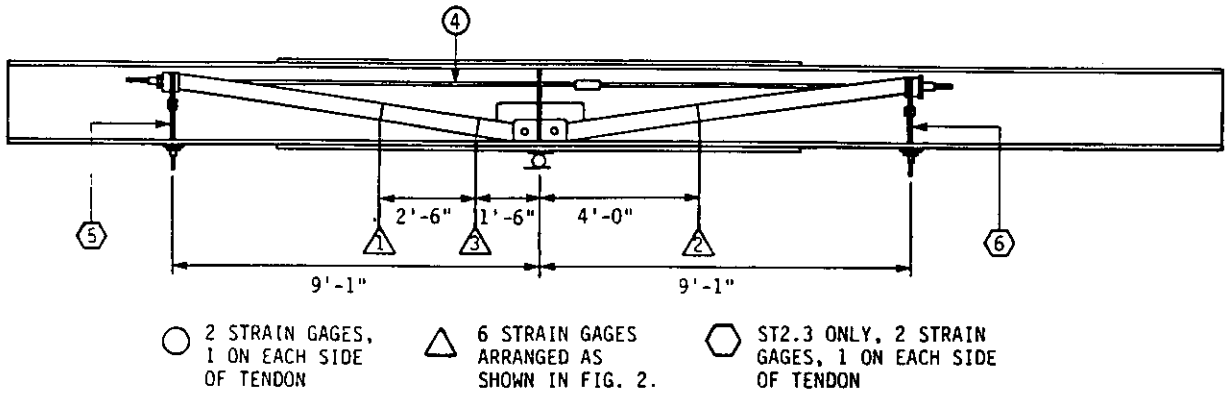

a. LAYOUT

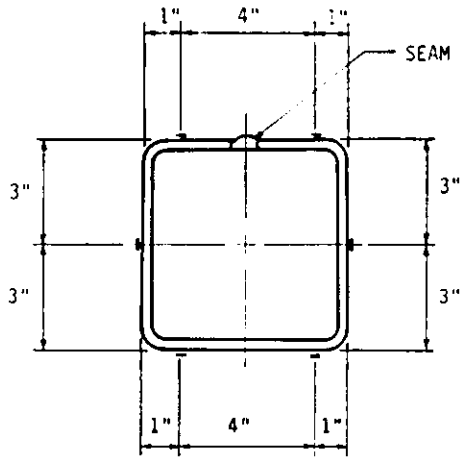

b. COMPRESSION-STRUT STRAIN GAGE LOCATIONS.

Fig. 3.5. ST2.2 and ST2.3 strain gage locations

tubes described in Section 3.2.2. Sections of six strain gages were located at the midpoint of each strut. An additional section of strain gages was located 1 ft 6 in. from the pin bracket on one tube to determine the amount of bending near the bracket. Two strain gages were located on each of the 1 1/4-in.-diameter tendons to determine the tension being applied to the truss. These strain gages were located symmetrically on each side of a tendon to compensate for the effects of bending. For ST2.3, an additional eight strain gages were used. Two strain gages were placed on each tiebar (see Fig. 3.5) to measure the vertical force applied to the lower flange of the beam. As with the 1 1/4-in.-diameter tendons, strain gages were located on opposite sides of the tie bars to compensate for the effects of bending.

3.3. Preliminary Vertical-Load Tests

As noted in Ref. [3], initial tests on the mockup were performed prior to the post-tensioned strengthening tests. These tests included an initial cracking test, a post-cracking test, and a strengthened beam test. Descriptions and results of these tests can be found in Section 4.2 of the final report for HR-287 [3].

Unstrengthened mockup tests were also run prior to ST2.1, ST2.2, or ST2.3. Although one of the strengthening systems was in place at the time of the tests, it was not structurally attached to the mockup. These tests established a reference for the unstrengthened mockup. A

summary of all the tests performed on the mockup is presented in Table 3.1.

For the given tests, Table 3.1 lists the strengthening technique in place, the maximum design strengthening load in the compression tubes (ST2.1) or tendons (ST2.2, ST2.3), the maximum nominal vertical load applied to the mockup, and the amount of partial vertical load (if any) applied to the mockup before the strengthening systems were stressed.

For each of the strengthening schemes, a nominal strengthening force was established. This force was the amount of compression in the tubes (ST2.1) or tension in the tendons (ST2.2, ST2.3) determined to produce the desired change in stress in the mockup. For ST2.1 this was 60-kips compression per tube. For ST2.2 and ST2.3, the nominal strengthening force was 100-kips tension per tendon. For the majority of tests performed on the mockup, the strengthening schemes were loaded to these levels. However, in order to determine the behavior of the mockup with each strengthening scheme in place, tests were also performed with strengthening loads both above and below the nominal design values. For ST2.1, compression loads of 40 and 75 kips per tube were also investigated. For ST2.2 and ST2.3, tension forces of 50 and 130 kips per tendon were examined.

A maximum applied vertical load of 43 kips was initially chosen for the mockup to limit stress in the steel beam and cover plates to 18 ksi compression or tension under various test conditions. For the test

Table 3.1. Tests on the full-scale mockup.

Test	Strengthening Technique	Maximum Strengthening Load (kips)	Maximum Vertical Load (kips)	Partial Vertical Load (kips)
1	--	0	43	0
2	ST2.1	60/tube	0	0
3	ST2.1	40/tube	43	0
4	ST2.1	60/tube	43	0
5	ST2.1	75/tube	43	0
6	ST2.1	60/tube	43	20
7	ST2.2	100/tendon	0	0
8	ST2.2	50/tendon	85	0
9	ST2.2	100/tendon	85	0
10	ST2.2	130/tendon	85	0
11	ST2.2	100/tendon	85	40
12	ST2.3	100/tendon	0	0
13	ST2.3	50/tendon	85	0
14	ST2.3	100/tendon	85	0
15	ST2.3	130/tendon	85	0
16	ST2.3	100/tendon	85	40
17	ST2.3	130/tendon	120	0

of the mockup with ST2.2 and ST2.3, this value was increased to approximately 85 kips of vertical load applied in order to investigate the behavior of the mockup and strengthening scheme at higher stress levels.

3.4. ST2.1 Tests

Tests 2 through 6 in Table 3.1 were performed to evaluate the strengthening effects of ST2.1 in place. These tests examined how the mockup responded to various levels of post-compression force in the tubes throughout a vertical load cycle. Strengthening was also done while a partial vertical load was present (Test 6) to simulate the replacement of a portion of the bridge deck. In an actual bridge, there would be stresses in the stringers even when the deck was removed due to a significant portion of the dead load still being present. Test 2 examined the behavior of the mockup with post- compression alone. The test was also conducted to determine the amount of lockoff (seating) loss in the post-compression arrangement. Initially, the tubes were compressed to 60 kips each. Data were recorded by the DAS at 5-kip increments during compression. At 60 kips, the sliding U-braces were locked in place and the jacking pressure was released. At this point a reading was taken to determine the loss in compression force due to lockoff.

Tests 3, 4, and 5 evaluated the combination of vertical loading plus compressive strengthening loads. Three compressive forces were investigated: 40 kips, 60 kips, and 75 kips per tube. To begin these

tests, the tubes were compressed to the desired load, with data taken every 10 kips. The U-braces were locked in place and the hydraulic pressure was released. A reading at this point determined the actual compressive force in each tube. A vertical load cycle was then applied to a maximum of 43 kips with data recorded using the DAS at 5-kip intervals. The vertical load was then decreased to zero with data taken every 10 kips.

As previously noted, Test 6 simulated the replacement of a portion of a bridge deck. During Test 6, the tubes were compressed while a partial vertical load was present. After the initial readings were taken, a vertical load of 20 kips, approximately half the peak load, was applied with data recorded every 5 kips. The U-braces were then compressed to 60 kips each with data recorded every 5 kips. The tubes were then locked in place and the hydraulic pressure released. Readings were again taken at this point to determine the actual compressive force in each tube. The vertical load was next increased to 43 kips and data were recorded every 5 kips. The vertical load was then removed and reapplied (simulating the replacement of the bridge deck) with data recorded at the same 5-kip increments.

3.5. ST2.2 and ST2.3 Tests

Tests 7 through 11 for ST2.2 and Tests 12 through 16 for ST2.3 were similar to Tests 2 through 6 for ST2.1. Vertical loads on the mockup with ST2.2 or ST2.3 in place, however, were increased to twice that used when ST2.1 was mounted on the mockup (i.e., approximately 85

kips). By using a vertical load of 85 kips, researchers could examine higher stress levels in preparation for the ultimate load test. Test 17, the ultimate load test, was performed with ST2.3 in place on the mockup.

Tests 7 and 12 (similar to Test 2) determined the behavior of the mockup with ST2.2 or ST2.3 alone. During these tests, the truss tendons were tensioned to 100 kips each with data recorded by the DAS every 5 kips.

Tests 8, 9, and 10 (similar to Tests 3, 4, and 5) evaluated the effects of a vertical load on the mockup with ST2.2 and ST2.3. Tensions of 50 kips, 100 kips, and 130 kips per tendon were investigated. To begin these tests, the tendons were tensioned to the desired load with data taken at 10-kip increments. The truss tendons were then locked in place and the hydraulic pressure was released. Data were then taken to determine the actual tension in each of the truss tendons. The vertical load was then applied to a maximum of approximately 85 kips with data being recorded at 10-kip intervals. The vertical load was removed and data taken every 10 kips.

Tests 11 and 16 were similar to Test 6 with ST2.1 in place in that a partial vertical load and vertical load cycle were used to simulate the replacement of a portion of a bridge deck. In Tests 11 and 16, however, the partial vertical load on the mockup was 40 kips and the maximum vertical load was 85 kips. In Test 17, the mockup with ST2.3 in place was tested to failure. After an initial reading, the tendons

in each truss were tensioned to 130 kips each. The tendons were locked off and data were taken after the hydraulic pressure was released. Vertical load was then applied to the mockup until failure occurred. Data were recorded at 20-kip intervals of vertical load throughout the test.

4. ANALYSIS AND TEST RESULTS

This section presents both the data obtained from tests of the mockup and the analysis of the finite-element model. To illustrate the effectiveness of the strengthening systems on the mockup, two types of data were recorded and are presented: deflections of the vertical load point and strain distributions at the critical sections, 4 and 5. Section 4 is at the support; Section 5 is within the cover-plated region 5 ft 6 in. from the support (see Fig. 3.2).

Data unique to the behavior of each strengthening scheme will also be presented in the appropriate section. For ST2.1, data relating to the change in force and bending of the compression tubes due to vertical load will be presented. For ST2.2 and ST2.3 the effects of vertical load on the force in the tendons and compression struts will be presented. Also for ST2.3 the change in force in the tie bars resulting from vertical loading will be presented.

4.1. Preliminary Vertical-Load Tests

Initial cracking and performance tests of the mockup were performed prior to the post-tensioned tests of HR-287. The results of these tests are presented in Section 4.2 of Ref. [3]. Test 1 of the present investigation (listed in Table 3.1) established the deflection and strain characteristics of the unstrengthened mockup. At a vertical load of 43 kips, the deflection at the load point was 0.735 in. downward. This value is approximately 20% larger than the

unstrengthened beam deflection of 0.603 in. reported in HR-287 (Ref. [3]). This suggests that the testing program of HR-287 caused additional cracking in the deck of the mockup, thus making the mockup more flexible. (Tests were performed on the mockup after the initial unstrengthened tests (see Table 43 of Ref. [3]).) Another reason for this increase in deflection could be that more of the friction bond between deck and beam was broken as a result of the testing program of HR-287.

The finite-element analysis of the mockup predicted a downward deflection of 0.531 in. for a 43-kip load. This indicated that the finite-element model was stiffer than the mockup under negative moment bending. However, it should be noted that although the finite-element model accounted for connector stiffness, it did not account for cracks in the concrete deck.

In Fig. 4.1a the theoretical and experimental average top and bottom strains at Section 4 of the mockup with 43-kips vertical load are illustrated. The solid line on the diagram represents strains predicted by the finite-element analysis for a vertical load of 43 kips, while the two data points are experimental strains recorded when the mockup was subjected to the same vertical loading. As may be noted, the bottom flange theoretical and experimental compression strains are in good agreement. However, the experimental tension strain on the top flange is approximately twice the theoretical strain. One explanation for this variation is that the deck of the mockup was

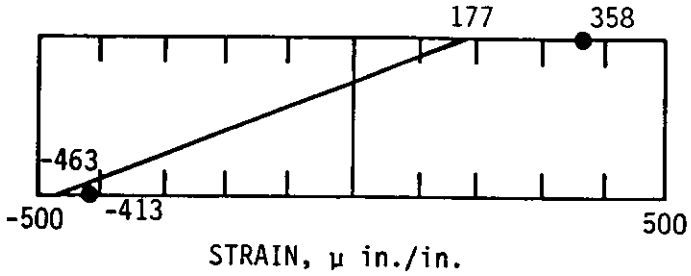

— THEORETICAL
● EXPERIMENTAL

a. 43k, VERT.

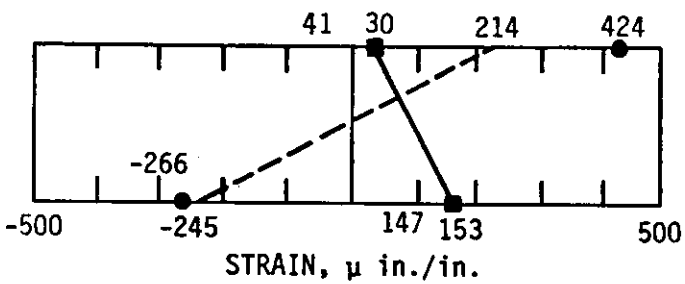

— 60k/TUBE-- THEORETICAL
■ 60k/TUBE-- EXPERIMENTAL
— 60k/TUBE, 43k VERT. --THEORETICAL
● 60k/TUBE, 43k VERT. --EXPERIMENTAL

b. ST2.1

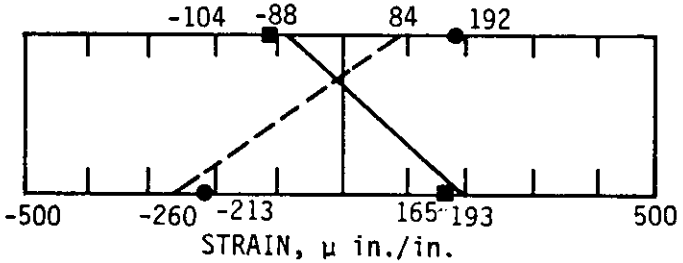

— 100k/TENDON-- THEORETICAL
■ 100k/TENDON-- EXPERIMENTAL
— 100k/TENDON, 43k VERT.-- THEORETICAL
● 100k/TENDON, 43k VERT.-- EXPERIMENTAL

c. ST2.2

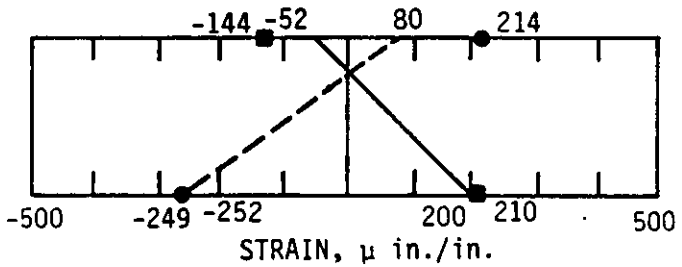

— 100k/TENDON-- THEORETICAL
■ 100k/TENDON-- EXPERIMENTAL
— 100k/TENDON, 43k VERT.-- THEORETICAL
● 100k/TENDON, 43k VERT.-- EXPERIMENTAL

d. ST2.3

Fig. 4.1. Experimental and theoretical strains at Section 4 for nominal loads

much less effective in tension than the finite-element analysis predicted.

4.2. Finite-Element Analysis

A finite element analysis of the mockup was performed by Dr. Kenneth F. Dunker of Iowa State University [14]. The development and results of the analysis will be presented as an analytical comparison to the experimental data.

The finite element model was created to represent as many of the structural irregularities present in the mockup as possible. As previously noted, the filled-in blockouts created a variable stiffness in the mockup since they were only effective during positive moment bending. The presence of shear connectors and cover plates were also modeled to create the proper stiffness throughout the section.

The mockup was analyzed with SAP IV [1] finite element analysis, and was adapted from a finite element analysis conducted in 1985 [5]. As shown in Fig. 4.2, the finite element model was developed with half-symmetry with the plane of symmetry in the plane of the beam web. Development of the elements was based on the study in Ref. [5]. The concrete deck was modeled with 12 in. x 12 1/2 in., rectangular plate elements with the 12 in. side parallel with the beam. Triangular elements were used in some locations to model load points and blockouts where the basic element pattern could not be matched.

The steel beam was modeled with beam elements capable of bending and shear deflections. The concrete deck of the mockup was modeled

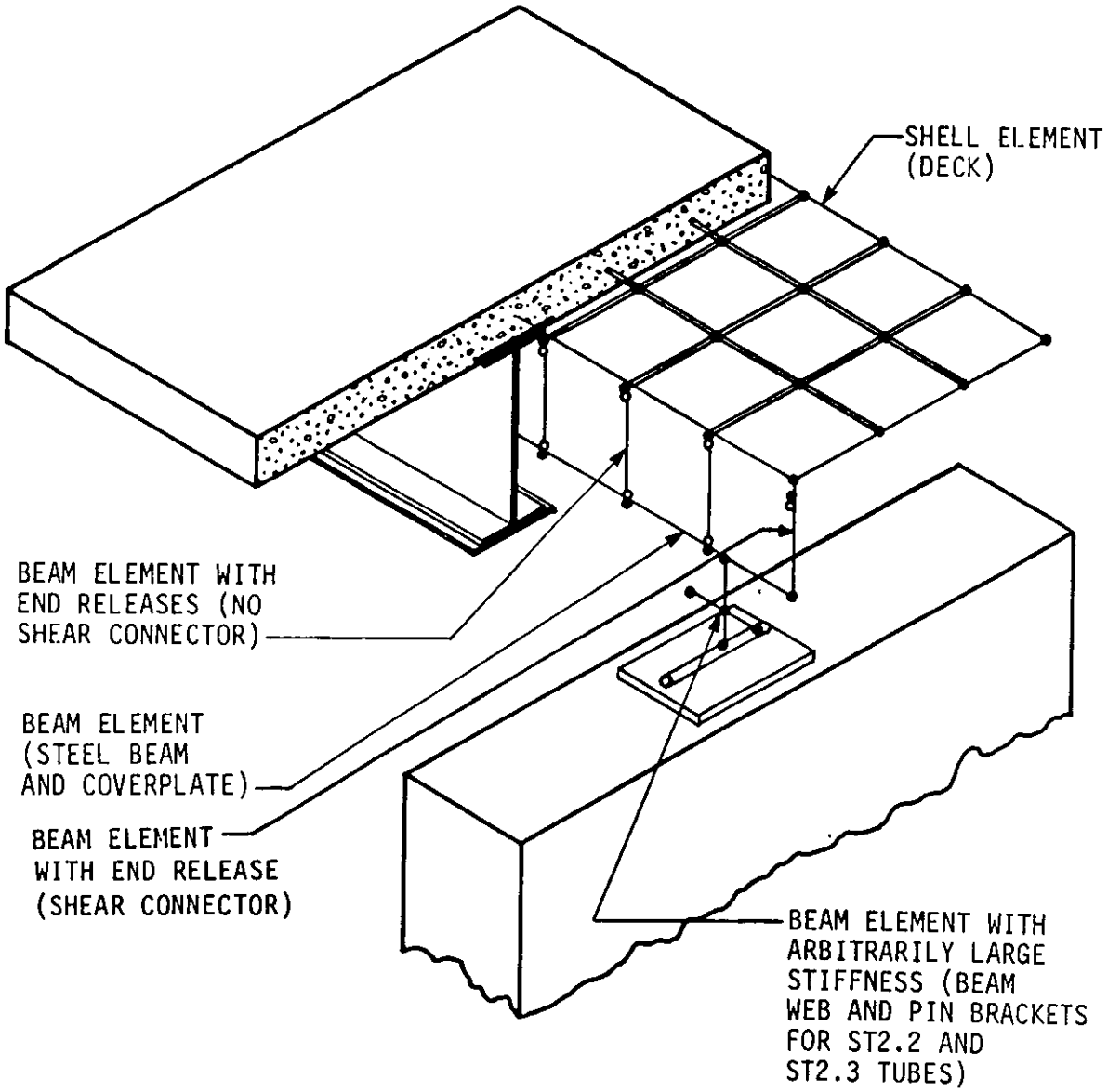

a. MODEL SCHEMATIC NEAR PIER SUPPORT

Fig. 4.2. Half-symmetry SAP IV finite-element model

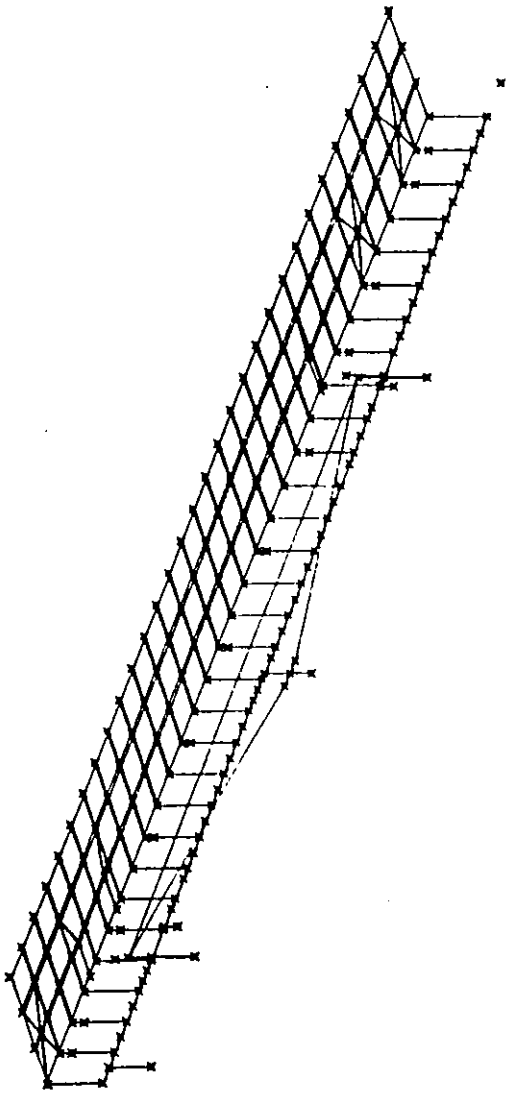

b. COMPLETE MODEL WITH ST2.3.

Fig. 4.2. Continued

with 6 1/2 in. thick elements without reinforcement. Connection of the beam to deck was made with shear connectors at eight locations and with vertical connection only at all other nodes.

From the results of experimental tests performed by Dedic (see Ref. [11]) compared with finite element analysis of the same structure in Ref. [5], it was known that the finite element results would indicate a stiffer section than occurred experimentally. This discrepancy is most likely due to cracks in the concrete decks and subsequent loss of composite action. The difference in the results, which is small during positive moment bending, increases as the deck is put under negative moment bending and the concrete is tensioned.

Strengthening schemes ST2.1, ST2.2 and ST2.3 were modeled with the appropriate elements corresponding to the tubes, tendons and connections in the respective strengthening schemes. Connection between the beam elements and strengthening elements were made with arbitrarily stiff beam elements. Figure 4.2b shows the complete half-symmetry finite-element model with ST2.3 in place.

4.3. Effects of ST2.1 on Mockup

In this section, the performance of ST2.1 when applied to the mockup will be presented. Shown in Fig. 4.3b is the effect of increasing the compression force in the compression tubes of ST2.1 on the deflection at the load point; note that no vertical load has been applied to the system at this time. An approximately linear relationship between the compressive forces in the compression tubes

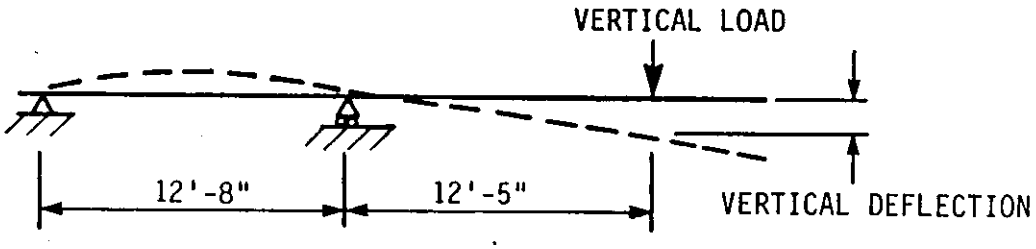

a. TEST SCHEMATIC

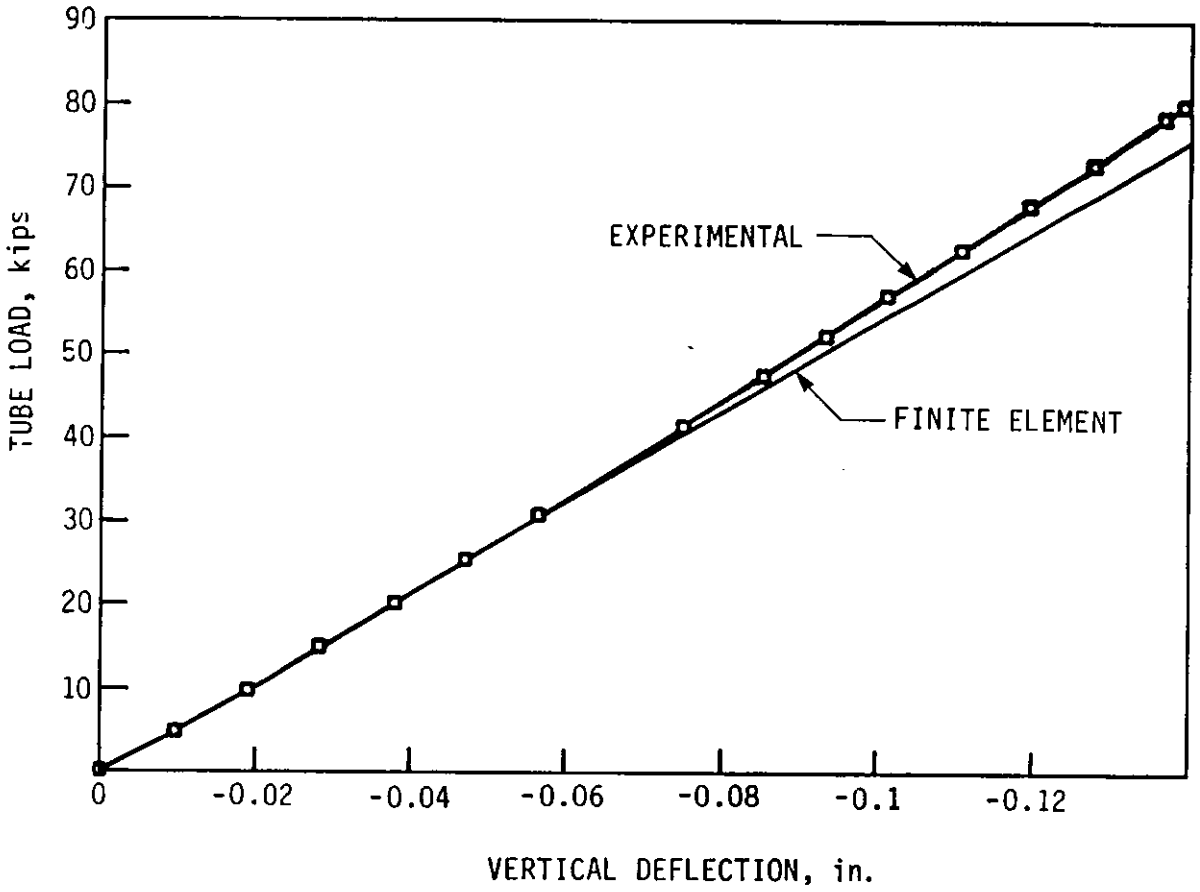

b. ST2.1 COMPRESSION-TUBE LOAD VS. DEFLECTION CURVE

Fig. 4.3. Test schematic and compression-tube load vs. deflection curve for ST2.1 on mockup

and the upward vertical deflection of the mockup is clearly shown. A maximum deflection of approximately 0.14 in. occurs at a load of 80-kips compression per tube. The solid line on the graph is the vertical deflection obtained from the finite-element analysis of ST2.1 applied to the mockup. For a given tube load, the finite-element model shows a larger deflection than was recorded experimentally for the mockup. Although the data are in good agreement, this indicates that while the section was undergoing positive bending, the mockup was slightly stiffer than the theoretical finite-element model with blockouts predicted.

Figure 4.4a illustrates the effects of vertical loading on the strengthened mockup. The graph plots vertical load versus deflection at the vertical load point for three different magnitudes of post-compression forces. Compressive forces of 40, 60, or 75 kips per tube were in place when the vertical load was applied.

The initial deflections due to post-compression are shown as negative (upward). The solid line is the deflection of the unstrengthened mockup with the same vertical loading. A review of the various curves in Fig. 4.4a indicated that the deflection at the load point decreased (i.e., deflected upward) with increasing post-compression force. The data in this figure also indicated that the deflection of the unstrengthened mockup was reduced by the amount of upward deflection due to post- compression. It was also apparent that the reduction in deflection due to ST2.1 remained essentially

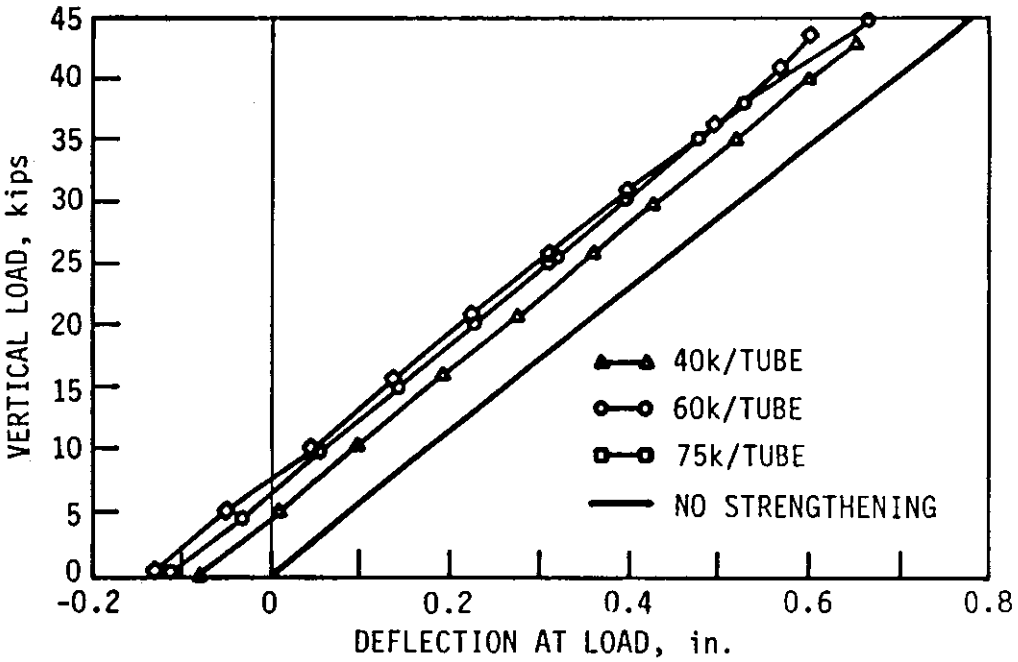

a. VERTICAL LOAD VS. DEFLECTION CURVES FOR THREE TUBE LOADS

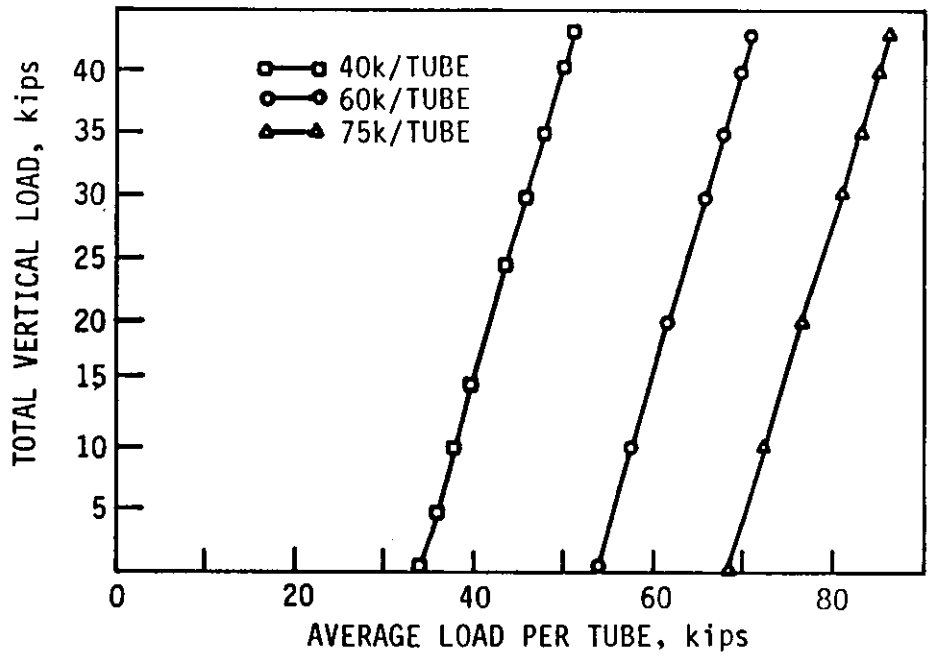

b. VERTICAL LOAD VS. AVERAGE TUBE LOAD FOR THREE TUBE LOADS

Fig. 4.4. Response of ST2.1 to vertical load

constant throughout the application of vertical loading. When researchers examined the data for the mockup with 60 kips per tube post-compression and 43 kips vertical load, the graph indicated that the deflection was reduced from 0.735 in. to 0.621 in., a 15.5% reduction. Because the slope of the various lines did not change noticeably, the compression tubes added no significant stiffness to the beam cross-section. The tubes thus behaved similarly to post-tensioning tendons, which also do not add significant stiffness.

Figure 4.1b illustrates a comparison of the experimental and theoretical strains for ST2.1 at Section 4 of the mockup. The solid line represents the theoretical strains predicted by the finite-element analysis of the mockup with 60 kips per tube post-compression applied by ST2.1. The experimental strains for the same post-compression force are represented by squares. These values indicated that positive moment bending of the section was occurring due to the post-compression being applied. The theoretical and experimental values are in very good agreement. The second set of data in Fig. 4.1b corresponds to 60 kips per tube post-compression and 43 kips of vertical load being applied to the mockup. For this condition, the theoretical strains are represented with a dashed line and the experimental strains are represented by dots. Experimental and theoretical bottom flange compressive strains for this loading were in good agreement, within 10%. The experimental tension strain on the top flange was again approximately twice the theoretical value. This supported the results

of the earlier comparison between experimental and theoretical results when the 43-kip load was acting alone. It indicated that during negative moment bending, the deck of the mockup was less effective in tension than the finite-element model predicted. This was most likely due to cracking in the deck, resulting in a reduction in the composite action of the mockup.

Figure 4.5 gives the strain distributions for the mockup at Sections 4 and 5. Parts a, b, and c of the figure represent strains at Section 4 for post-compression loads of 40, 60, and 75 kips per tube, respectively. Parts d, e, and f correspond to strains at Section 5 for the same loads. The heavy line in each graph represents the strains for an unstrengthened beam with a vertical load of 43 kips. For a given section, this would be constant. At Section 4, the top (tension) strain is 358μ in./in. (10.38 ksi) and the bottom (compression) strain is 413μ in./in. (12.0 ksi). At Section 5 the top and bottom strains are 206 (6.0 ksi) μ in./in. and 278μ in./in. (8.1 ksi), respectively. The dashed line labeled no vertical is for the mockup with the amount of post-compression indicated, and no vertical load. This corresponds to an upward deflection of the mockup. In each figure, this line indicates a tensile force and positive moment are acting on the section. As expected, the tension strains increased with the amount of post- compression applied. Also on each figure is a line representing strains due to ST2.1 and a vertical load of 43 kips. These lines are the strengthened beam strains. By comparing the strengthened and

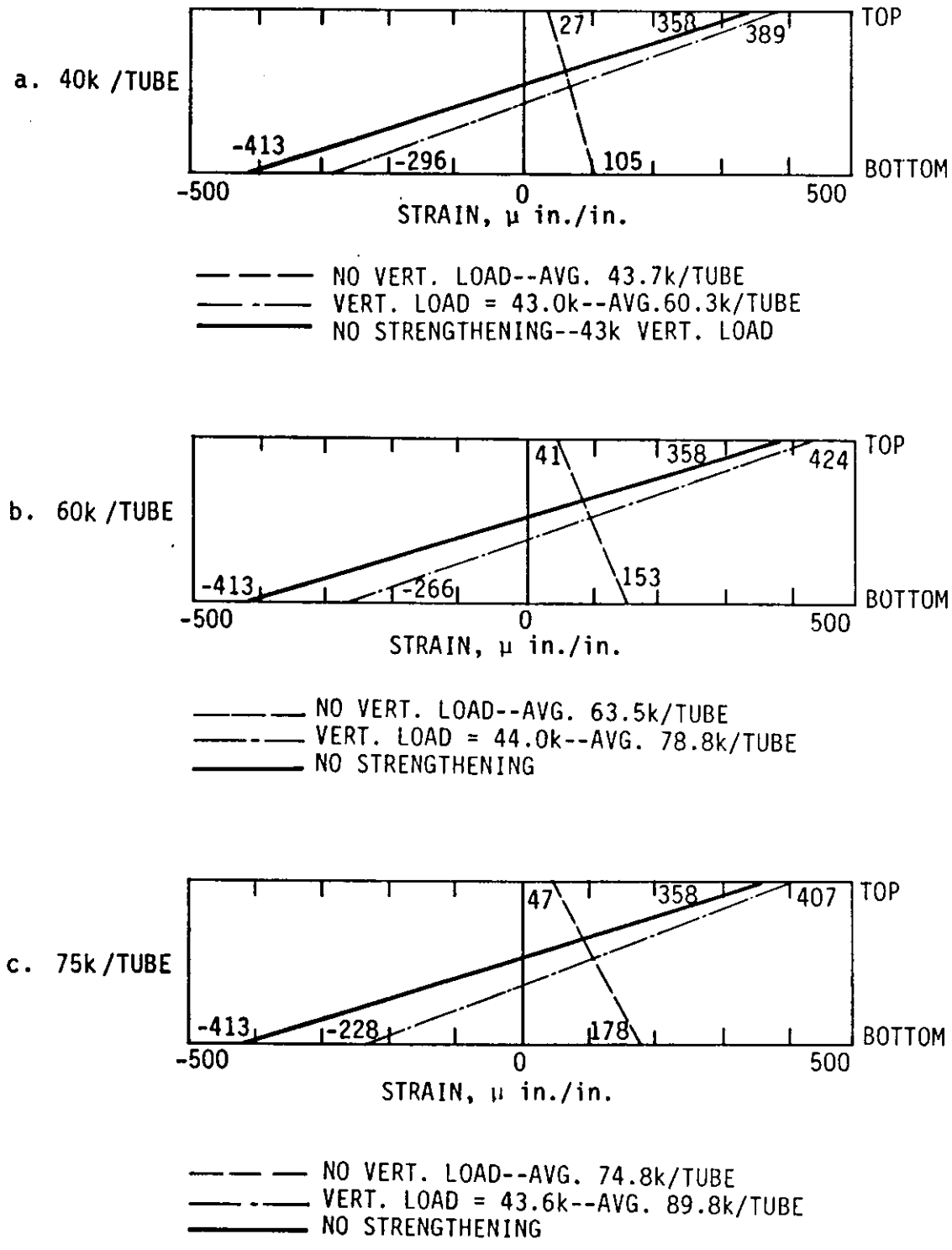

Fig. 4.5. Strains at Sections 4 and 5 for full-scale mockup with ST2.1 in place

d. 40k /TUBE

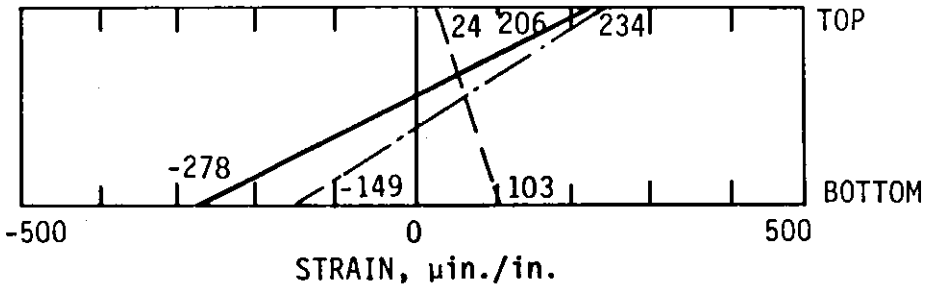

——— NO VERT. LOAD--AVG. 43.7k/TUBE
——·—— VERT. LOAD = 43.0k--AVG. 60.3k/TUBE
——————— NO STRENGTHENING

e. 60k /TUBE

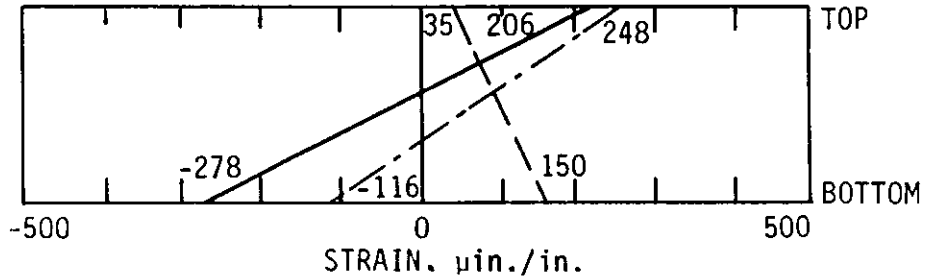

— — — NO VERT. LOAD--AVG. 63.5k/TUBE
— ·— VERT. LOAD = 44.0k--AVG. 78.8k/TUBE
——————— NO STRENGTHENING

f. 75k /TUBE

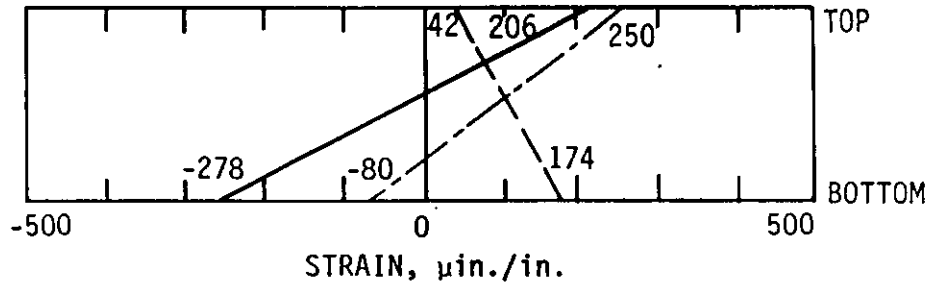

— — — NO VERT. LOAD--AVG. 74.8k/TUBE
——·—— VERT. LOAD = 43.6k--AVG. 89.8k/TUBE
——————— NO STRENGTHENING

Fig. 4.5. Continued

unstrengthened beam results, one can determine the change in strain due to ST2.1. The strain diagrams for each magnitude of compressive load at Section 5 are similar to those at Section 4.

Each diagram indicates that the effect of ST2.1 on the mockup was to decrease the bottom flange compression strains and increase the top flange tension strains. At Section 4 with 60 kips per tube post-compression (Fig. 4.5b), the compressive strains were reduced from 413μ in./in. to 266μ in./in. (4.3 ksi reduction); however, the tensile strains increased from 358μ in./in. to 424μ in./in. (1.9 ksi increase). These changes were approximately equal to the strains created by post-compression alone. They correspond to an 18% increase in top flange tension and a 36% decrease in bottom flange compression.

Figure 4.4b illustrates the increase in post-compression force due to vertical load. The tube compression increased approximately 0.4 kips per kip of vertical load. Bending of the compression tubes was also examined. Prior to installation of the independent lateral restraints (see Section 2.3.3), considerable bending occurred in the compression tubes. The change in lateral restraints significantly reduced the bending in the tubes. To further reduce the bending, small shims were fit between the ends of the tubes and the brackets. The shims evenly distributed the loading on the tubes and reduced bending due to small misalignments in the ends of the tubes and the bearing surface on the brackets.

4.4. Effects of ST2.2 and ST2.3 on Mockup

In this section the effects of ST2.2 and ST2.3 when applied to the mockup will be presented. As previously noted, essentially the only difference between ST2.2 and ST2.3 (see Figs. 2.9 and 2.10) is that ST2.2 applies upward force to the lower surface of the upper flange, while ST2.3 applies upward force to the lower surface of the lower flange. Figure 4.6 shows the effect of ST2.2 and ST2.3 acting on the mockup without a vertical load. The figure illustrates that ST2.3 created a larger upward deflection than ST2.2. At 100-kips tension per tendon the deflections for ST2.2 and ST2.3 were 0.147 in. and 0.219 in., respectively. Because the experimental results were not linear and somewhat irregular near the origin of the graph, there apparently were some minor seating effects at low loads. The large irregularities in the deflections for ST2.2 at loads above 50 kips are most likely due to movement of the pin bearing as the truss was loaded.

The solid lines on the graph are the deflection obtained from the finite-element model with either ST2.2 or ST2.3. The line fell between the experimental deflections for the two strengthening techniques.

ST2.2 and ST2.3 should have caused near identical deflections on the mockup. The finite-element model, however, does not consider local effects at the point of contact between the lower surface of the deck and beam flange and the strengthening truss (ST2.2). Apparently, these effects are a major source of the difference between theoretical and experimental values.

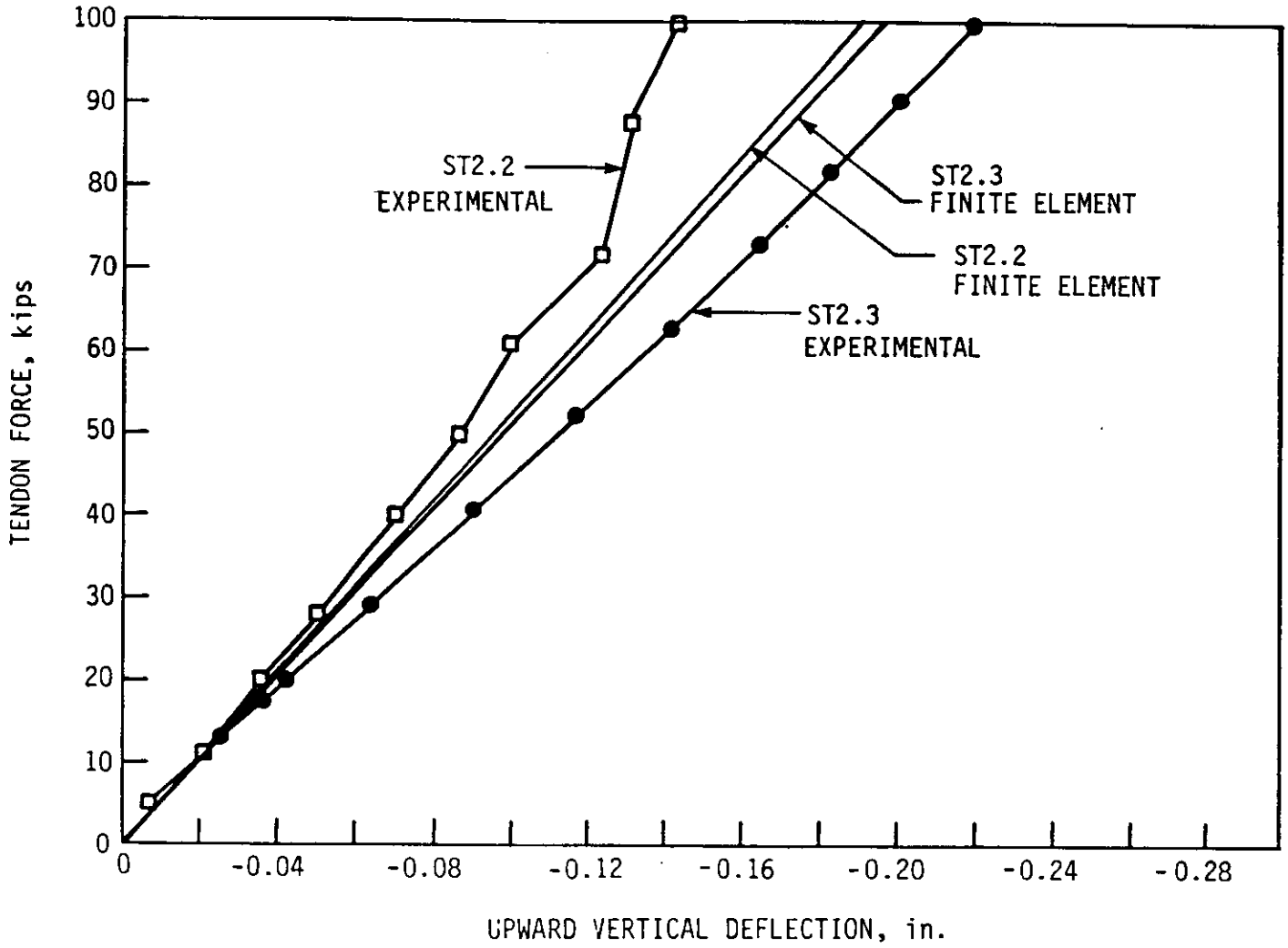

Fig. 4.6. Tendon load vs. deflection for ST2.2 and ST2.3

Figures 4.7a and b illustrate the effects of vertical loading on the mockup when ST2.2 and ST2.3, respectively, were attached to the mockup. The graphs plot vertical load versus deflection for three truss loads. Deflections for an unstrengthened mockup are also shown. The graphs display information similar to that found for ST2.1 in Fig. 4.4a. The deflection of the mockup remained linear after strengthening was applied. Again this indicated that the deflection was being reduced by the amount of initial deflection caused by strengthening. Since the initial deflections for the mockup with ST2.2 were less than those for the mockup with ST2.3, the final reduction in deflection was also less for ST2.2 than for ST2.3. For a load of 100 kips per tendon, the deflection of the mockup with ST2.2 was reduced from 0.735 in. to 0.359 in. (36%), while the deflection of the mockup with ST2.3 was reduced from 0.735 in. to 0.533 in. (27%). Thus, it can be concluded that ST2.2 was more effective than ST2.3 in reducing the deflection of the mockup. For both ST2.2 and ST2.3 the strengthened beam curves paralleled the unstrengthened curves; thus, the truss strengthening did not add stiffness to the beam cross-section.

Figures 4.1c and d display the experimental and theoretical strains at Section 4 due to ST2.2 and ST2.3, respectively. For each diagram, one line and pair of data points corresponds to an initial 100 kips per tendon acting alone. A second set of data corresponds to 100 kips per tendon and a vertical load of 43 kips. The comparisons are similar to those for ST2.1. While the deck was in compression

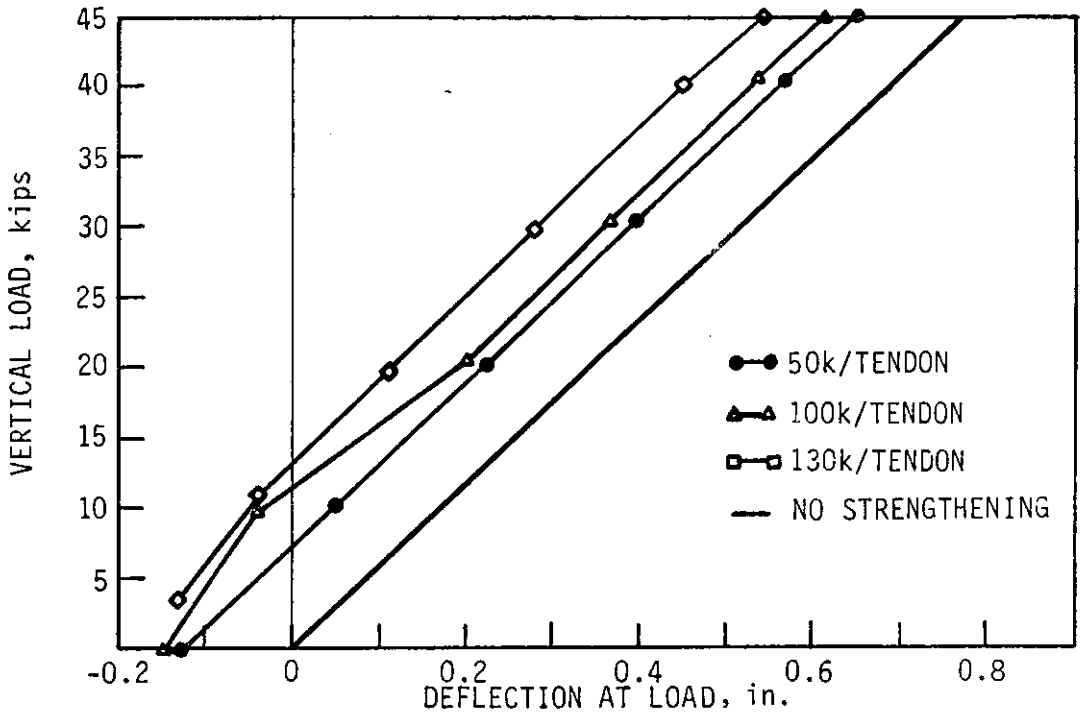

a. VERTICAL LOAD VS. DEFLECTION CURVES FOR ST2.2 SUBJECTED TO VARIOUS TENDON FORCES

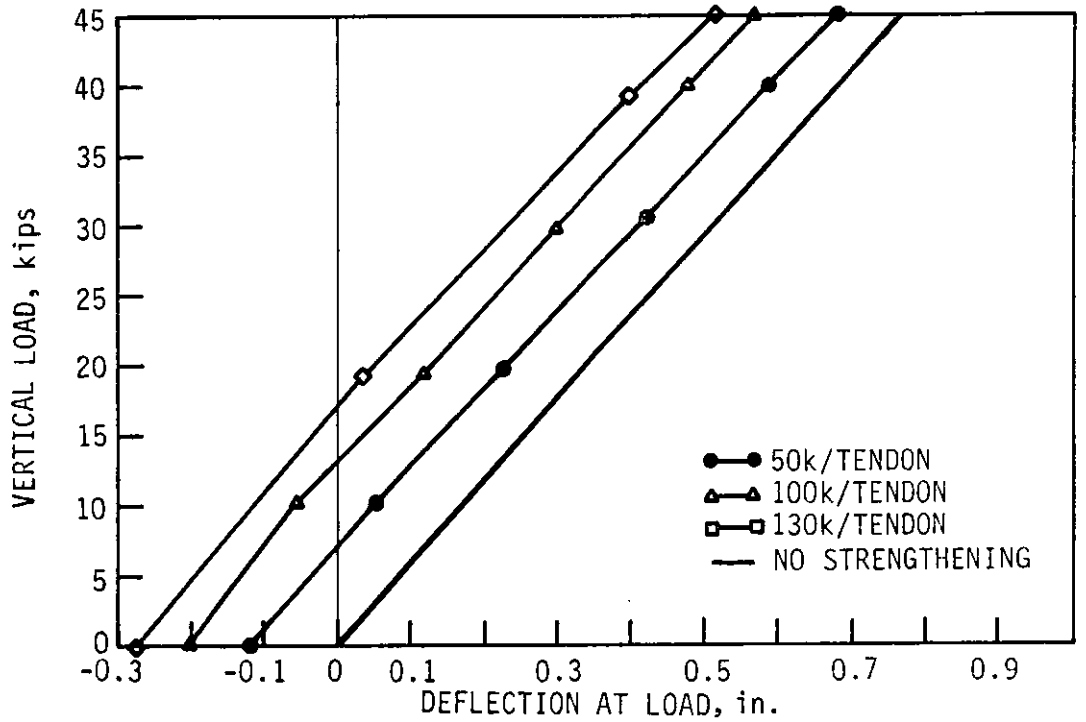

b. VERTICAL LOAD VS. DEFLECTION CURVES FOR ST2.3 SUBJECTED TO VARIOUS TENDON FORCES

Fig. 4.7. Response of ST2.2 and ST2.3 to vertical load

(positive moment bending), the theoretical model and the experimental mockup strains were in good agreement.

When the 43-kip load was applied, the deck went into tension (negative moment bending), and the finite-element model predicted a stiffer section than occurred experimentally. The experimental compression strains on the bottom flange during negative moment bending, however, were again close to the theoretical strains. Shown in Figs. 4.8 and 4.9 are the strain distributions for the mockup with ST2.2 and ST2.3, respectively. For each of the strengthening techniques, parts a, b, and c of the figures represent strains at Section 4 for tendon loads of 50, 100, and 130 kips per tendon. Parts d, e, and f of these figures correspond to strains at Section 5 for tendon loads of 50, 100, and 130 kips per tendon. The strain data within each diagram are illustrated as was done with ST2.1 (see Fig. 4.5). Data in these figures indicated that ST2.2 and ST2.3 were essentially causing only positive moment bending on the mockup. As one would expect, ST2.2 and ST2.3 acting alone resulted in compression strains in the top flange and tension strains in the bottom flange.

The positive moment bending increased as the force in the tendons increased. Comparing the strengthened and unstrengthened beam strains indicated that both techniques were very effective in reducing the strains in the loaded mockup. Since ST2.2 and ST2.3 caused pure positive moment bending in the mockup, both the top and bottom flange strains were reduced. At Section 4 with ST2.2, 100 kips per tendon and

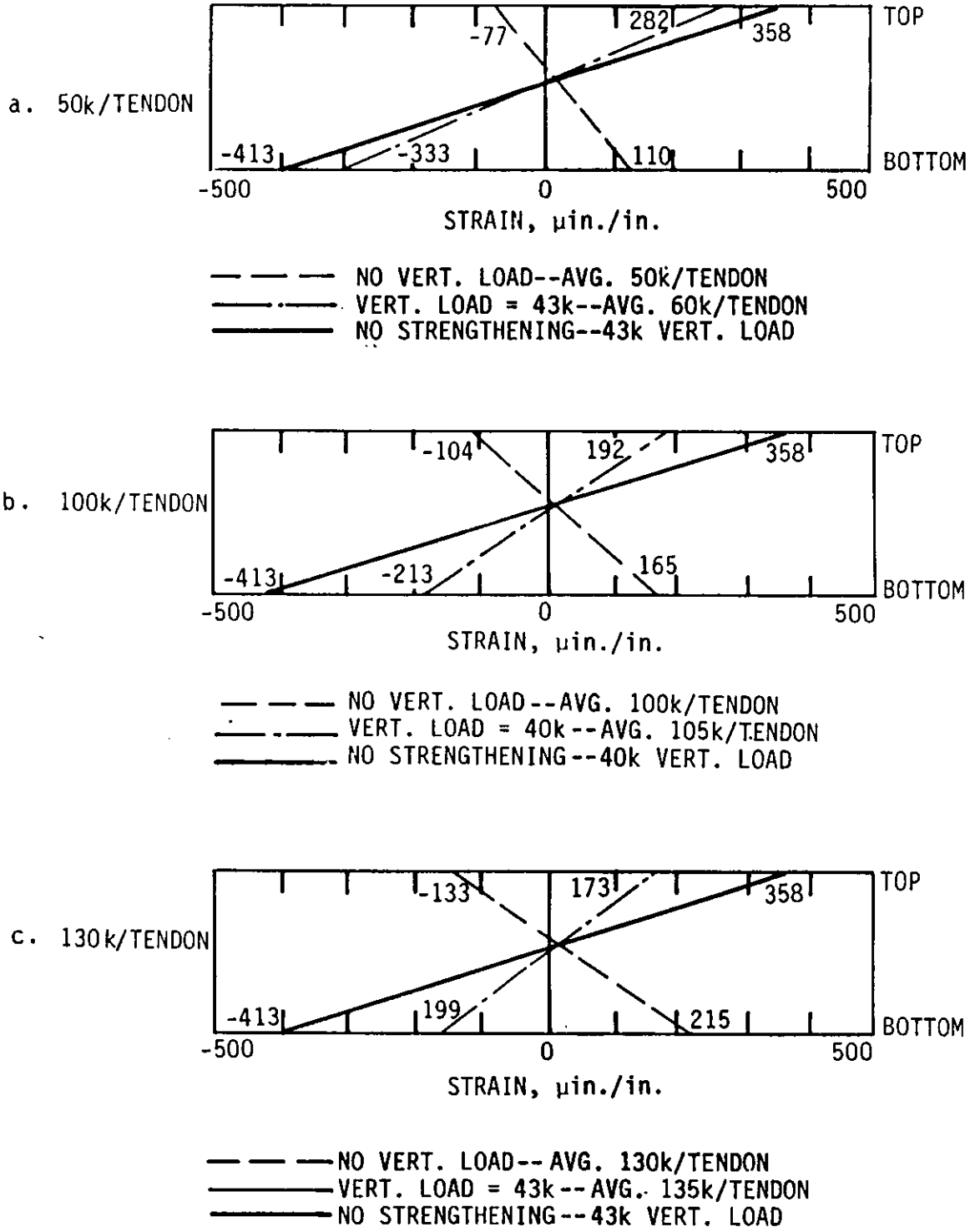

Fig. 4.8. Strains at Sections 4 and 5 for full-scale mockup with ST2.2 in place

d. 50k/TENDON

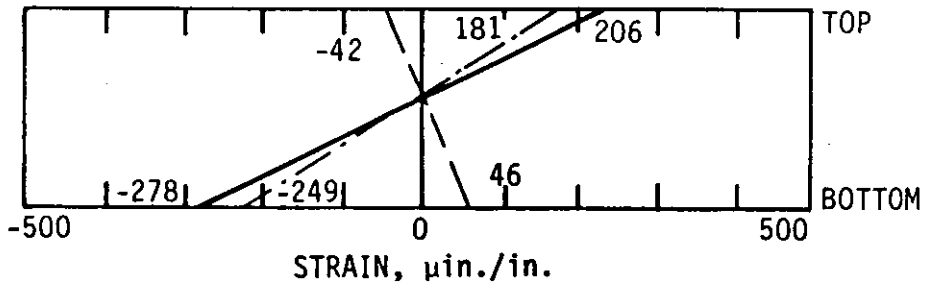

— — — NO VERT. LOAD -- AVG. 50k/TENDON
— · — VERT. LOAD = 40k -- AVG. 60k/TENDON
——— NO STRENGTHENING -- 40k VERT. LOAD

e. 100k/TENDON

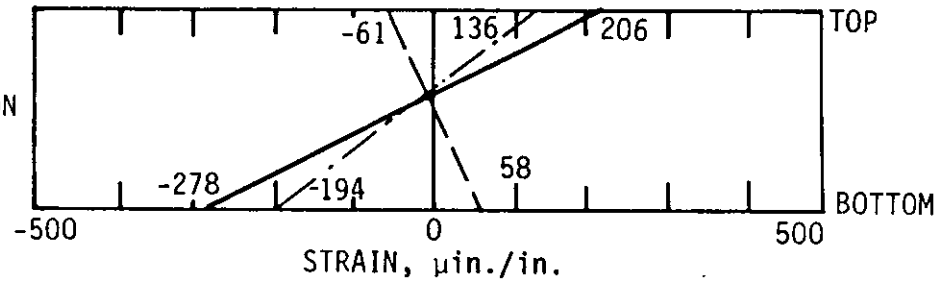

— — — NO VERT. LOAD -- AVG. 100k/TENDON
— · — VERT. LOAD = 40k -- AVG. 105k/TENDON
——— NO STRENGTHENING -- 40k VERT. LOAD

f. 130k/TENDON

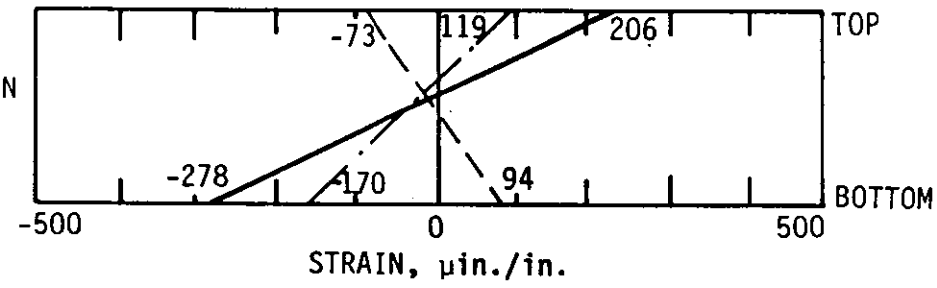

— — — NO VERT. LOAD -- AVG. 130k/TENDON
— · — VERT. LOAD = 40k -- AVG. 135k/TENDON
——— NO STRENGTHENING -- 40k VERT. LOAD

Fig. 4.8. Continued

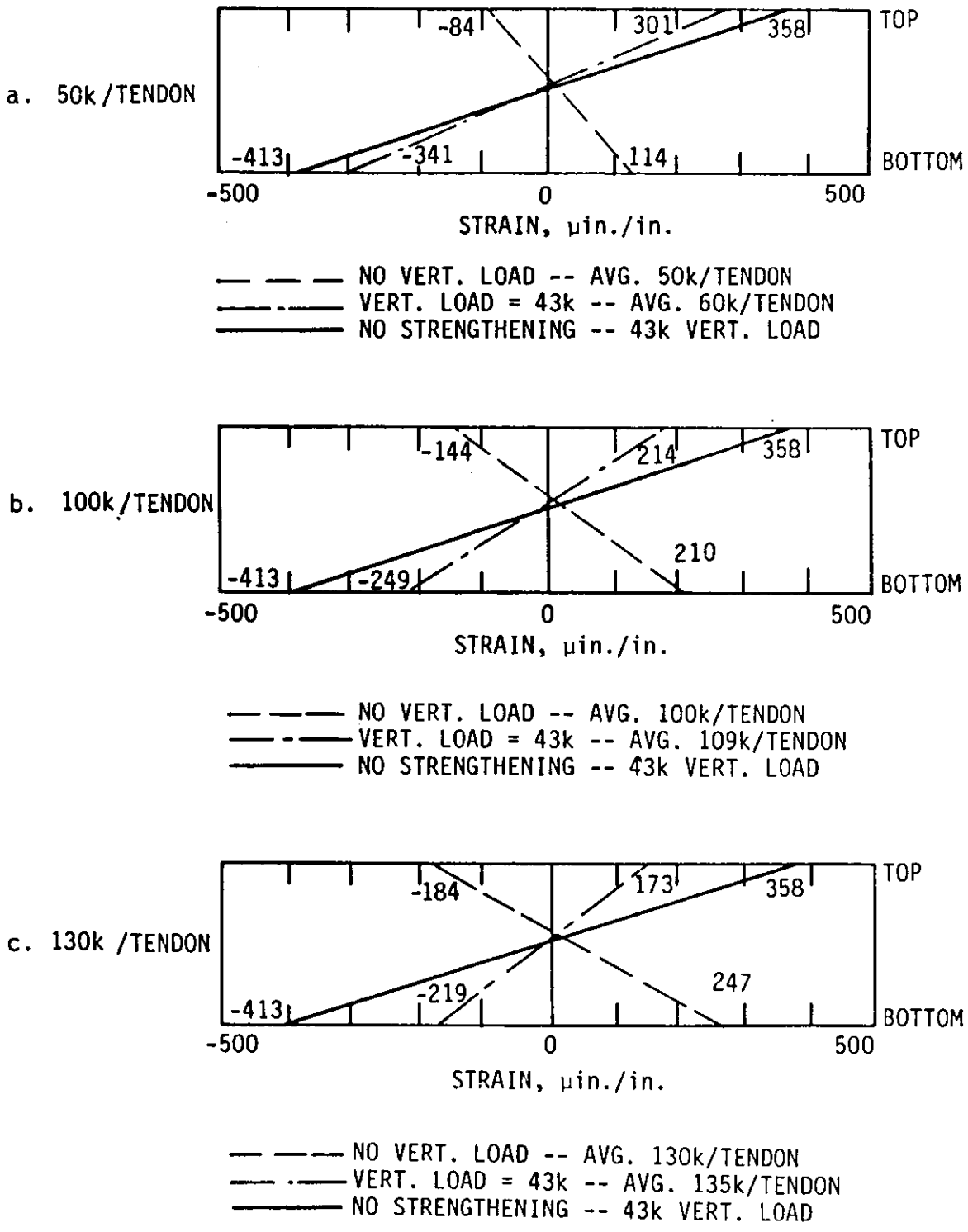

Fig. 4.9. Strains at Sections 4 and 5 for full-scale mockup with ST2.3 in place

d. 50k/TENDON

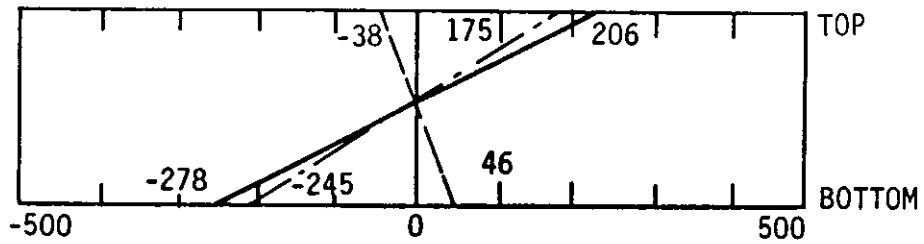

STRAIN, μ in./in.

— — — NO VERT. LOAD -- AVG. 50k/TENDON
— - — VERT. LOAD = 43K -- AVG. 60k/TENDON
——— NO STRENGTHENING -- 43k VERT. LOAD

e. 100k /TENDON

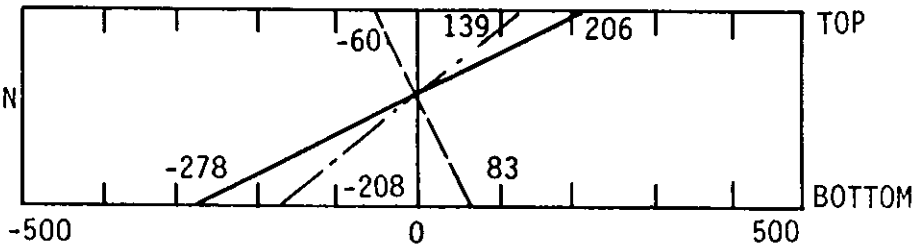

STRAIN, μ in./in.

— — — NO VERT. LOAD -- AVG. 104k/TENDON
— . — VERT. LOAD = 43k -- AVG. 109k/TENDON
——— NO STRENGTHENING -- 43k VERT. LOAD

f. 130k /TENDON

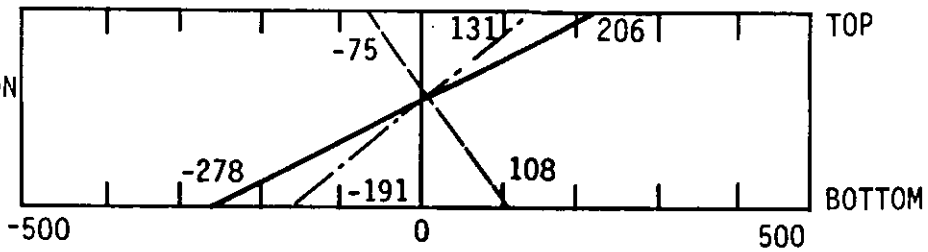

STRAIN, μ in./in.

— — — NO VERT. LOAD -- AVG. 130k/TENDON
— - — VERT. LOAD = 43k -- AVG. 135k/TENDON
——— NO STRENGTHENING -- 43k VERT. LOAD

Fig. 4.9. Continued

43 kips vertical load, (Fig. 4.8b), the top flange tension strain was reduced from 358μ in./in. to 192μ in./in. (4.8 ksi reduction). The bottom flange compression strain was reduced from -413μ in./in. to -213μ in./in. (5.8 ksi reduction). This represents a 46% stress reduction in the top flange and a 48% stress reduction in the bottom flange.

The strains for ST2.3 at the same section and loading (Fig. 4.9b) were reduced slightly less. The top flange tension strain was reduced from 358μ in./in. to 214μ in./in. (4.3 ksi reduction). The bottom flange strain was reduced from - 413μ in./in. to -249μ in./in. (4.8 ksi reduction). This represents a 40% stress reduction in both the top and bottom flange.

Figures 4.10 and 4.11 illustrate the behavior of ST2.2 and ST2.3 on the mockup. Figures 4.10a and b display the change in strut load due to an increasing vertical load for ST2.2 and ST2.3, respectively. On each graph, three lines appear, corresponding to the three magnitudes of tensile forces (50 k, 100k, and 130k) that were applied before the vertical loading was applied.

The lines on Figs. 4.10a and b are parallel, indicating that the increase in force in the struts due to vertical loading, remained essentially linear regardless of the initial force in the tendon. These results supported the deflection data, which indicated that the strengthening schemes did not add stiffness to the section. For ST2.2, the increase in strut load was approximately 0.25 kips per kip of

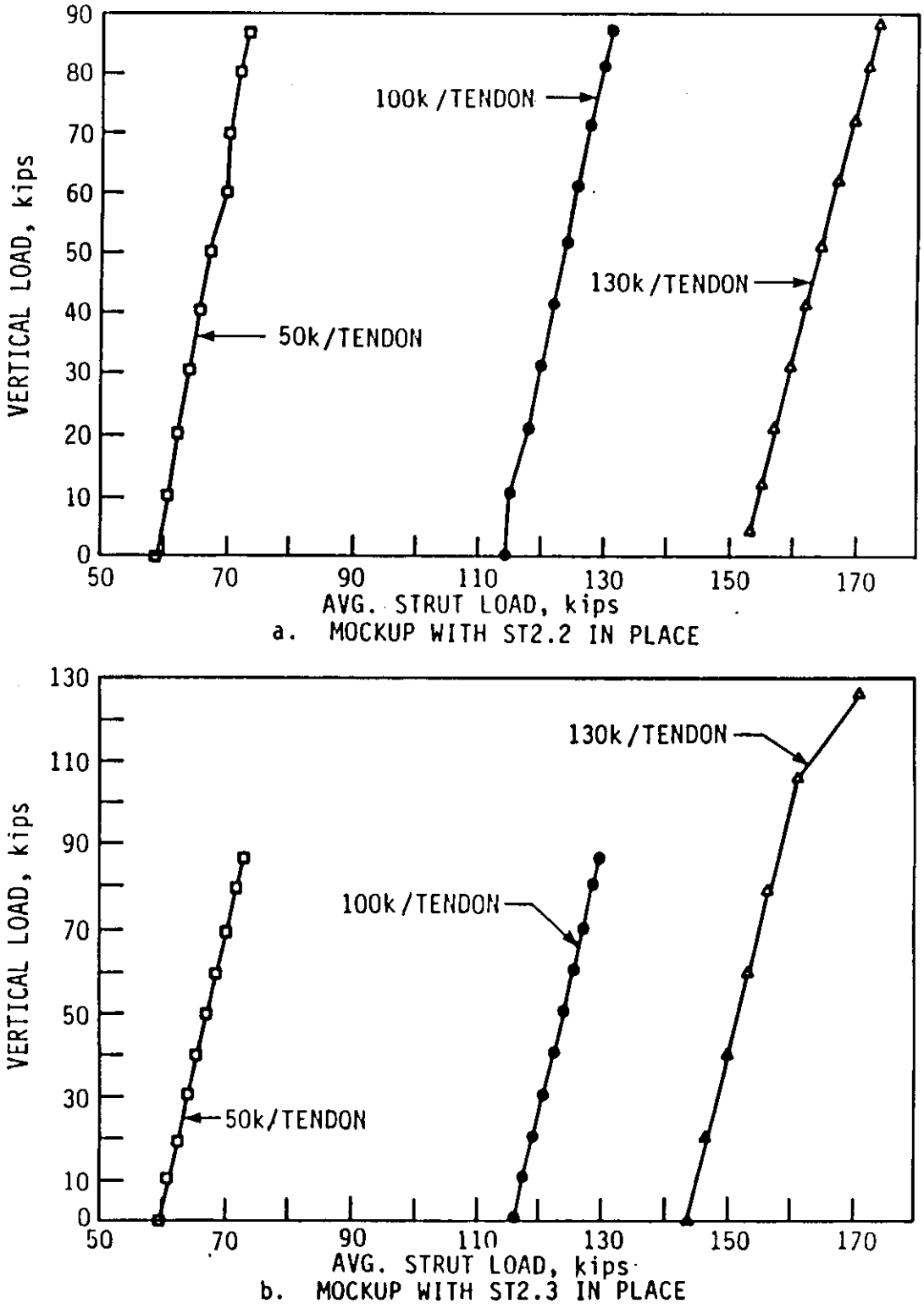

Fig. 4.10. Vertical load vs. average strut load for ST2.2 and ST2.3

vertical load. For ST2.3 the increase in strut load was approximately 0.20 kips per kip of vertical load. The results of tests on the mockup with ST2.2 and ST2.3 also showed that the loads in the four compression struts were within 4% of one another at all times. This indicated that the tendon was correctly distributing the force to the compression struts and that loading on the mockup was symmetric. Bending of the compression struts in ST2.2 and ST2.3 was not significant. The short length of the strut and the pin bracket were apparently effective in reducing bending.

Figure 4.11a illustrates the change in tendon force due to increasing vertical load. As previously noted, the initial tendon forces used in the testing of ST2.2 and ST2.3 were 50, 100, and 130 kips. As may be seen in Fig. 4.11a, the increase in tendon force for ST2.2 and ST2.3 as vertical loading was applied (or as the region was subjected to positive moment) was essentially the same, 0.15 kips per kip of applied vertical loading. For ST2.3 the force in the tie bars also increased as vertical loading was applied. This increase in force is illustrated in Fig. 4.11b. The tie bar forces are given for the initial tendon loads of 50, 100, and 130 kips per tendon. As noted for the increase in tendon forces, the lines for the increase in the bar forces were also parallel. This indicates that the increase in tie bar force remained essentially linear regardless of the initial force in the tie bar. For each initial tendon force, the increase in tie bar load was 0.018 kips per kips of vertical load.

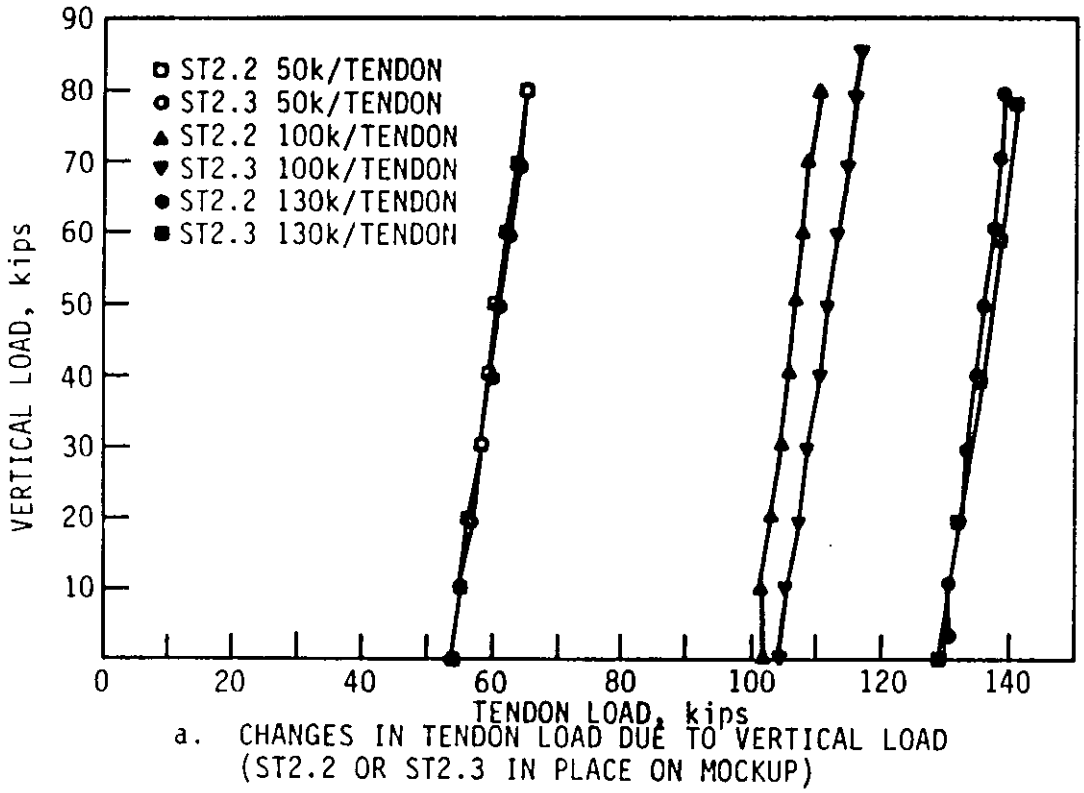

a. CHANGES IN TENDON LOAD DUE TO VERTICAL LOAD (ST2.2 OR ST2.3 IN PLACE ON MOCKUP)

Fig. 4.11. Response of tendons (ST2.2 and ST2.3) and ties (ST2.3) to vertical loading

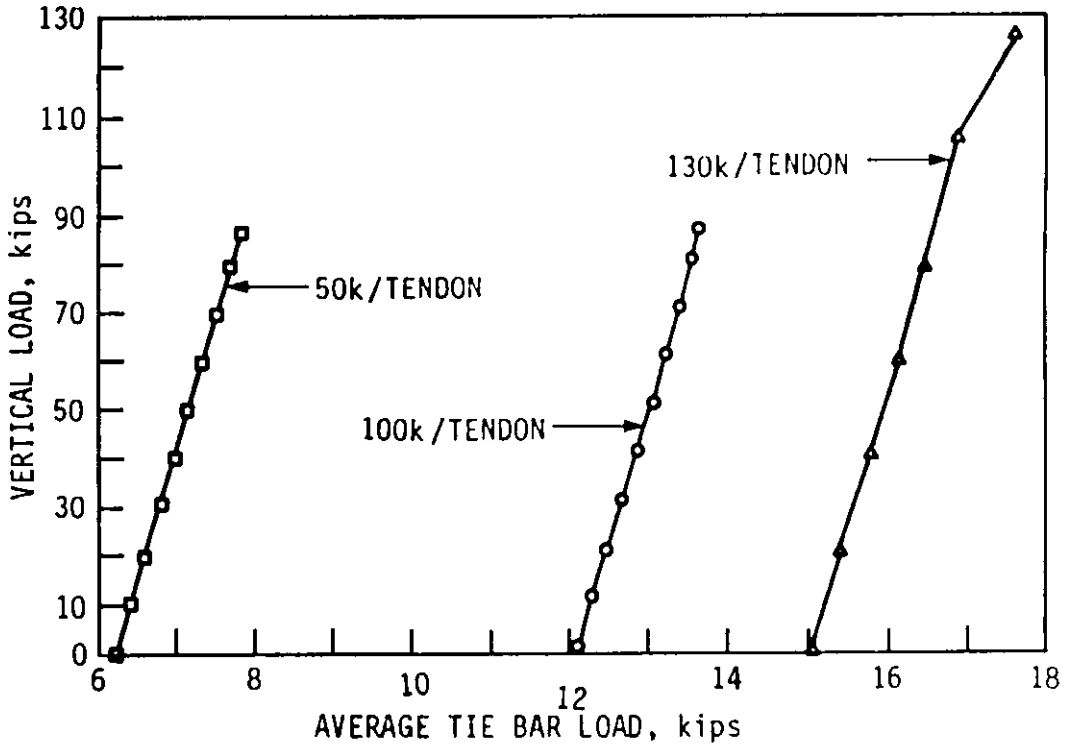

b. CHANGES IN TIE BAR LOAD DUE TO VERTICAL LOAD (ST2.3 IN PLACE ON MOCKUP)

Fig. 4.11. continued

The final test of the investigation involved the load testing to failure of the mockup with ST2.3 applied. Photographs of the failed mockup are shown in Fig. 4.12. The load deflection curve for this failure test is shown in Fig. 4.13. (In Fig. 4.7b, the same curve is shown for values of the vertical load from 0 to 45 kips.)

The deflection, which was essentially linear up to the previous load of 43 kips, maintained a smooth curve throughout the higher range of vertical loading. As previously noted, the hold-down force (see Fig. 3.1) was 75 kips. Since no additional deflection occurred when the applied vertical load reached 75 kips, and no uplift was observed at the hold-down, the actual hold-down force was obviously greater than 75 kips. For safety reasons, direct observation of the mockup was limited for vertical loads above 75 kips. Therefore, it was difficult to know exactly when failure began to occur. Yielding in the bottom flange at Section 4 first occurred at a vertical load of 105 kips. At a vertical load of 125 kips, the yield stress was exceeded at Sections 2, 4, and 6 (see Fig. 3.2). The buckling of the flange shown in Figs. 4.12b and c occurred exactly at Section 2 (see Fig. 3.2), 6 in. past the end of the cover plates. The bottom flange strain at Section 2 for the vertical load of 125 kips was 1446μ in./in. (41.9 ksi). At Section 4 the bottom and top flange strains were 1833μ in./in. (53.2 ksi) and 1389μ in./in. (40.3 ksi), respectively. When the vertical load was increased to 127 kips, the strains at Section 4

a. RESTRAINED END OF MOCKUP AT FAILURE

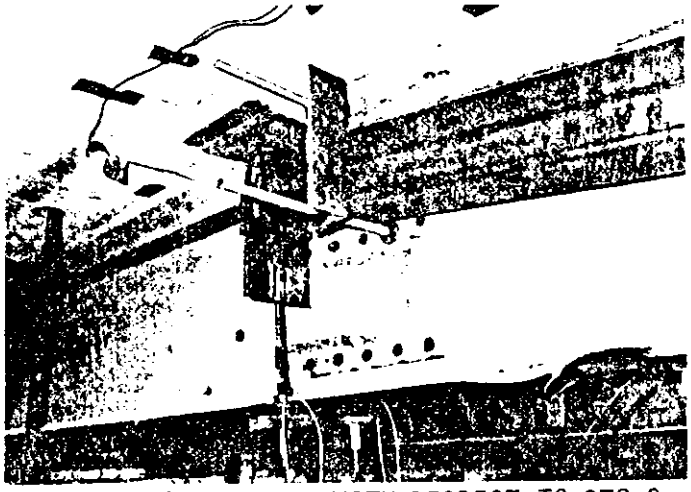

b. LOCATION OF FAILURE WITH RESPECT TO ST2.3

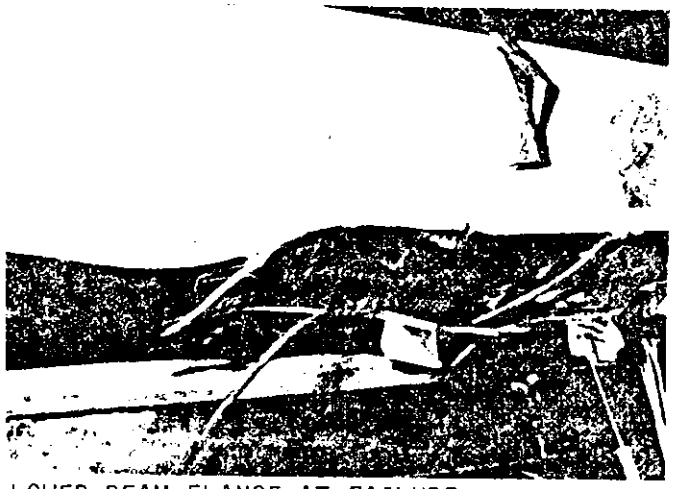

c. LOWER BEAM FLANGE AT FAILURE

Fig. 4.12. Photographs of mockup with ST2.3 tested to failure

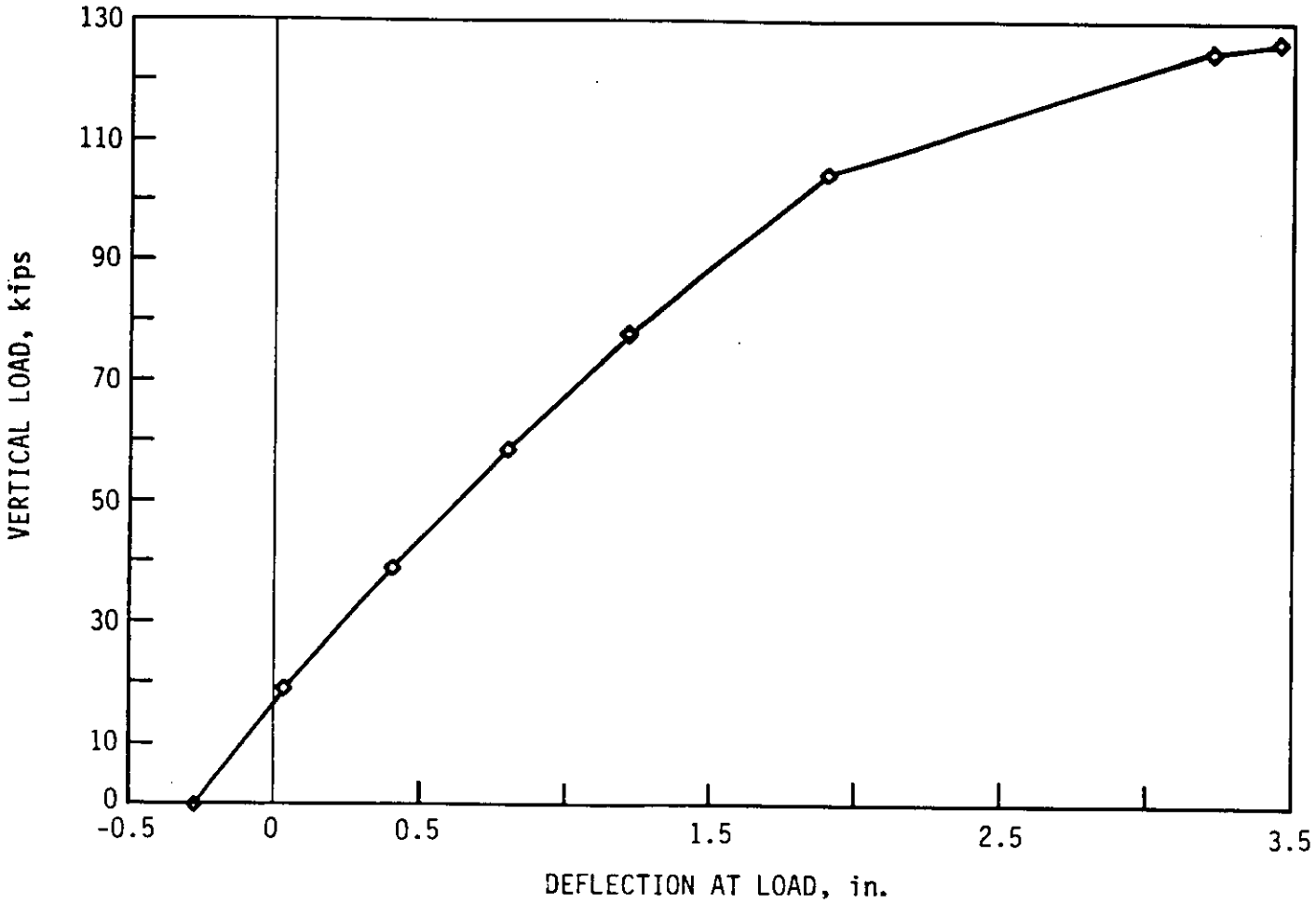

Fig. 4.13. Vertical-load deflection curve for mockup with ST2.3 in place tested to failure

increased. However, the strains at Section 2 decreased indicating that the failure occurred at approximately 125 k.

As expected, the test to failure established that the mockup would fail before the strengthening system. For the vertical load of 125 kips, yield stress was not exceeded at any point on the strengthening system. The final compression strut load was 170 kips per tube. This value was approximately 30% above the calculated AISC allowable load for this element assuming a uniform cross-section, pinned ends, and a length of 8 ft- 8 7/8 in. The force in the 1 1/4-in.-diameter tendons increased from 130 kips prior to vertical loading to 150 kips at 125 kips of vertical load. The 150-kips force in the tension tendon was 80% of ultimate strength of the tendons. The 5/8-in.-diameter tie bars reached 17.6 kips, which is approximately 40% of their ultimate capacity.

4.5. Finite-Element Analysis of One-Third Scale, Three-Span Continuous Composite Bridge

To investigate the effects of applying the superimposed truss to a three-span continuous composite bridge, a finite element analysis using ANSYS was performed. ANSYS is a large-scale, user-oriented, general purpose finite-element program for linear and nonlinear systems. Through the use of a finite-element analysis, the distribution effects of the superimposed truss, when used at some or all piers, could be examined.

The finite element model was adapted from a grillage model created to idealize a three span, one third scale model bridge in the ISU Structural Engineering Laboratory. The use of the grillage method to model bridges has been established and is documented in many references [7,13,14].

4.5.1. Grillage model

For the grillage model, all bridge components were modeled as three dimensional flexural elements. Each element was assigned appropriate values for flexure, torsion and shear. Bridge stringers and the concrete deck were modeled as composite members (longitudinally) with varying section properties, at interior vs. exterior stringers and coverplates in the negative moment region. Transversely the diaphragms and concrete deck were modeled as independent members. At locations without diaphragms, the concrete deck was modeled as independent (transverse) members. A drawing of the finite element grillage model without strengthening in place is shown in Fig. 4.14a.

Abutment and pier nodes shown in Fig. 4.14a provided appropriate boundary conditions for the model. These nodes and nodes corresponding to cover plate boundaries can be seen on either side of the pier support nodes on the model. Additional nodes were placed on stringers corresponding to the location of the applied vertical force from the superimposed truss at each pier.

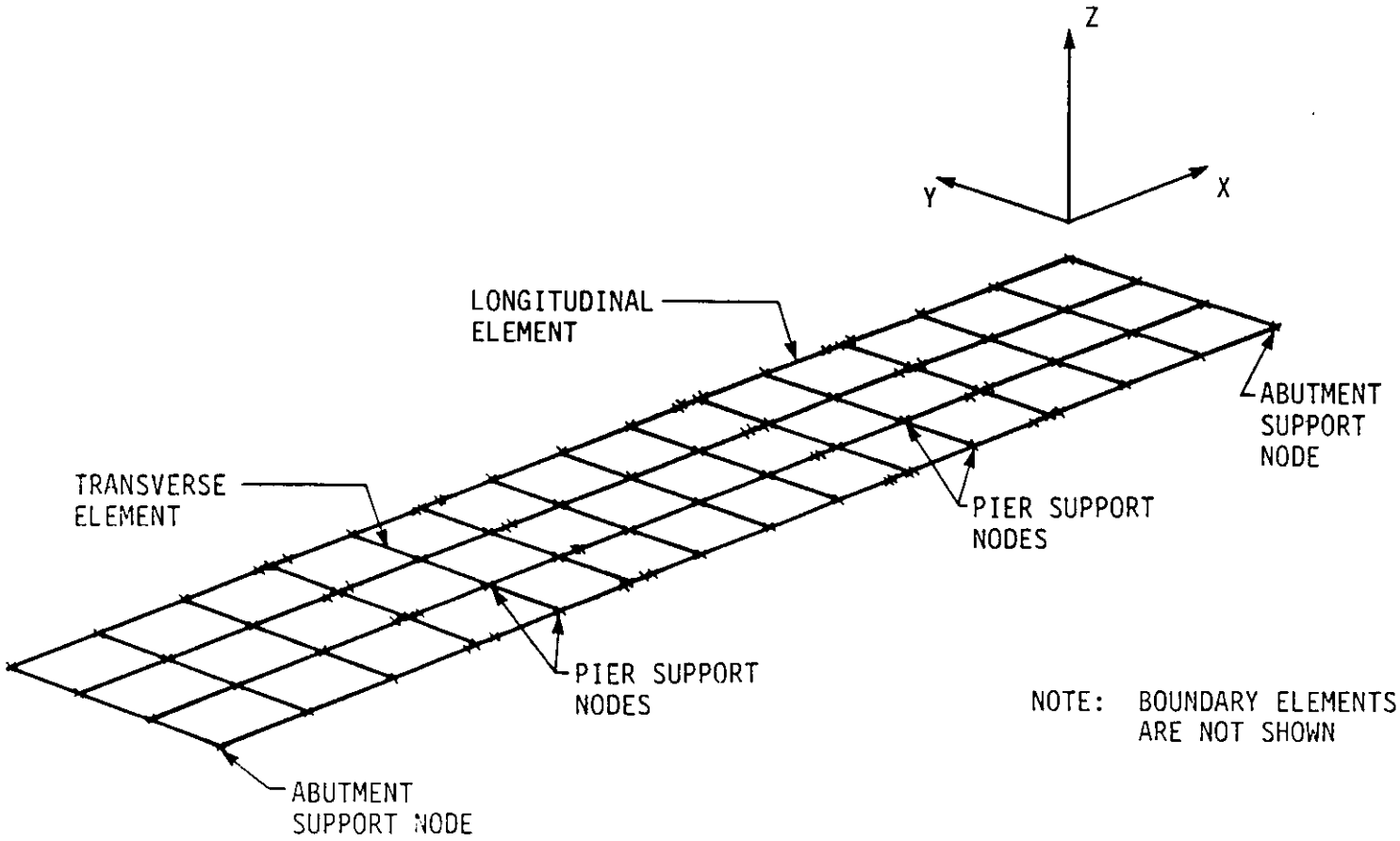

a. GRILLAGE MESH FOR LABORATORY MODEL BRIDGE

Fig. 4.14. ST2.2 or ST2.3 on three-span continuous bridge

4.5.2. ST2.2 (or ST2.3) on grillage model

In order to simulate the effect of the strengthening forces applied by the superimposed truss, vertical forces were placed on the bridge model at the appropriate nodes. Since minimal increase in stiffness was noted during the tests on the full scale mockup with either ST2.2 or ST2.3 in place, each could be modeled by simply including the resulting vertical forces on the stringers. The vertical forces simulated the effect of either ST2.2 or ST2.3 since the grillage model considered the steel beam and concrete deck as a single element.

The first step in evaluating the effect of the superimposed truss on the bridge was to apply strengthening at only one exterior stringer as shown in Fig. 4.14b (TC1). However, to evaluate the most effective use of superimposed trusses in strengthening a three-span bridge, three configurations were examined.

1. Trusses on exterior stringers (TC2)
2. Trusses on interior stringers (TC3)
3. Trusses on all stringers (TC4)

Schematics of the three configurations are shown in Figs. 4.14 c, d and e. Also, to examine the effect of different size trusses on the bridge, three lengths of trusses were tested on the grillage model. The first truss size examined matched the truss tested on the mockup. The truss length was 18 ft 2 in., thus vertical forces were applied at a 9 ft-1 in. on each side of the pier (see Figs. 2.9 and Figs. 4.14b). The second and third trusses tested were 20 ft and 22 ft long, thus the

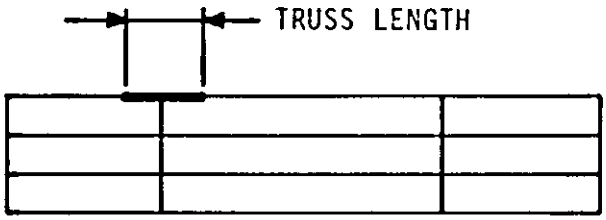

b. ONE SUPERIMPOSED TRUSS ON AN EXTERIOR STRINGER (TC1)

c. SUPERIMPOSED TRUSS ON ALL EXTERIOR STRINGERS (TC2)

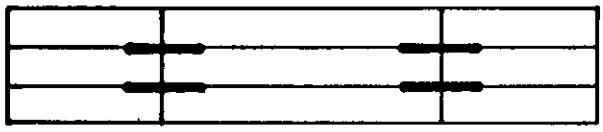

d. SUPERIMPOSED TRUSS ON ALL INTERIOR STRINGERS (TC3)

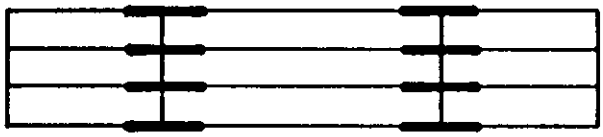

e. SUPERIMPOSED TRUSS ON ALL STRINGERS (TC4)

Fig. 4.14. continued

vertical forces were applied at 10 ft and 11 ft, respectively, on each side of the pier.

Distribution of the strengthening forces, both transverse and longitudinal, were determined by the use of moment fractions [8]. The moment fraction for a given stringer and section can be computed as indicated below for Stringer 1:

$$MF_1 = \frac{\Sigma S_1}{\Sigma \varepsilon S}$$

where

MF_1 = moment fraction for Stringer 1,

ε_1 = bottom flange strain in Stringer 1,

S_i = bottom flange relative section modulus for Stringer 1, and

$\Sigma \varepsilon S$ = sum of εS products for all stringers or sections.

4.5.3. Results of distribution

In the transverse direction, moment fractions were computed at three sections for each strengthening configuration; the center of the end span, the pier, and the midspan of the bridge. Longitudinally the moment fractions were computed for exterior and interior stringers at the center of the end-span, pier and bridge midspan. Since minimal change in moment fraction was found due to changing the length of the truss, the moment fractions shown in Figs. 4.15 through 4.21, represent all three truss lengths examined. Figures 4.15 and 4.16 illustrate the distribution of moment when only one exterior beam is strengthened (TC1). Figure 4.15 show the transverse distribution of moment at three

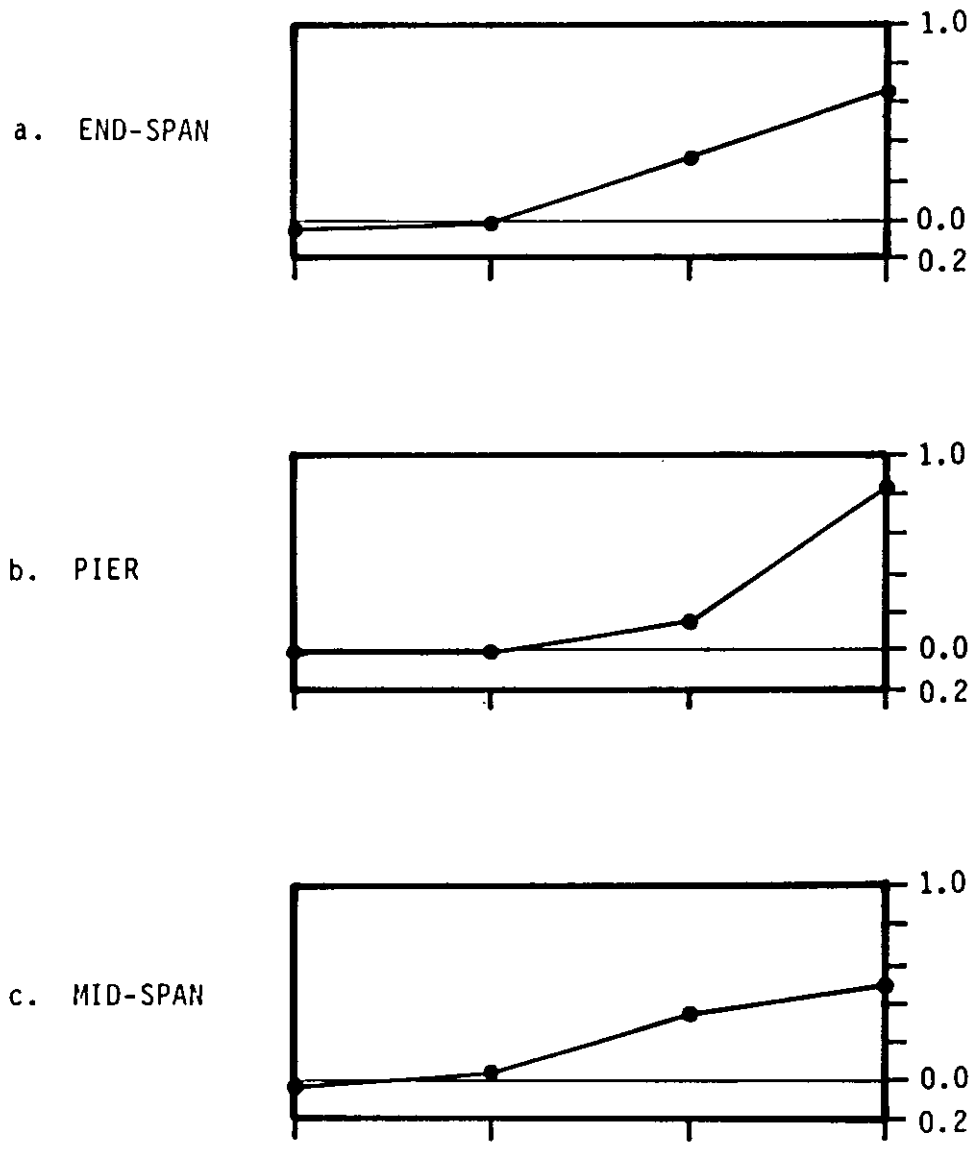

Fig. 4.15. Transverse moment fractions for one superimposed truss on an exterior stringer (TC1)

a. EXTERIOR STRINGER

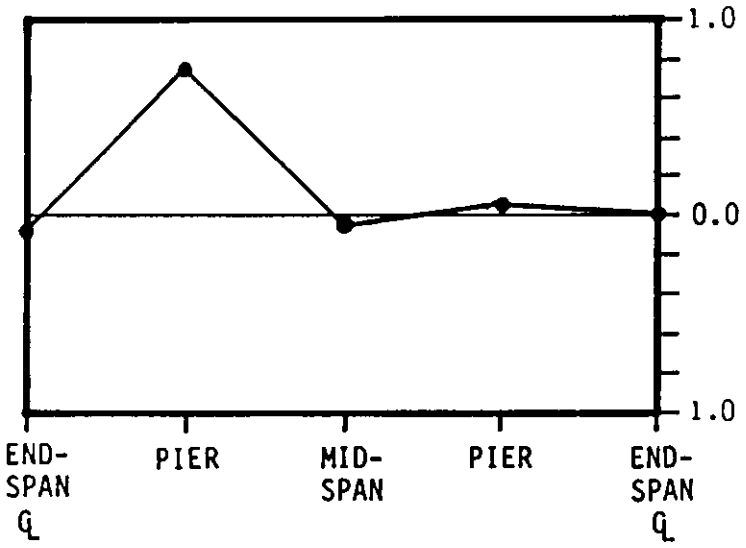

b. INTERIOR STRINGER

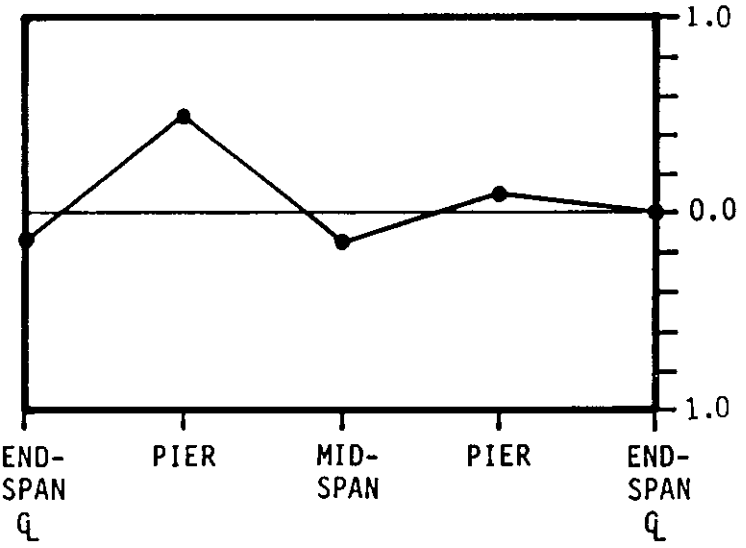

Fig. 4.16. Longitudinal moment fractions for one superimposed truss on an exterior stringer (TC1)

sections. At all three sections, the strengthening is seen to essentially effect only the beam being strengthened and the adjacent beam. However, a small negative effect can also be seen on the opposite exterior stringer. Fig. 4.16 gives the longitudinal distribution for the two beams affected by the strengthening. The largest portion of the moment fraction is in the exterior beam at the pier being strengthened and in the interior beam at the pier adjacent to the one being strengthened. The effect of the two beams farthest from strengthening, is essentially negligible as shown in Fig. 4.15. Figures 4.17 through 4.22 give the moment fractions for TC2, TC3 and TC4. The figures represent distributions for each of the three truss lengths examined.

Figures 4.17 and 4.18 illustrate the distribution of moment from strengthening only exterior stringers. At the end-span and pier approximately 40% of the moment stays in the exterior stringer and 10% is transferred to the interior stringers. At the bridge mid-span, however, the strengthening effect is essentially evenly distributed. In Fig. 4.18, a longitudinal distribution is shown for the same strengthening configuration. For the exterior stringers, the majority of the moment fraction is at the pier (near the point of strengthening). For the interior stringers, a larger portion of the moment has been distributed to the mid-span. Figures 4.19 and 4.20 display moment fractions for strengthening only interior stringers (TC3). As expected, the results are opposite to those for

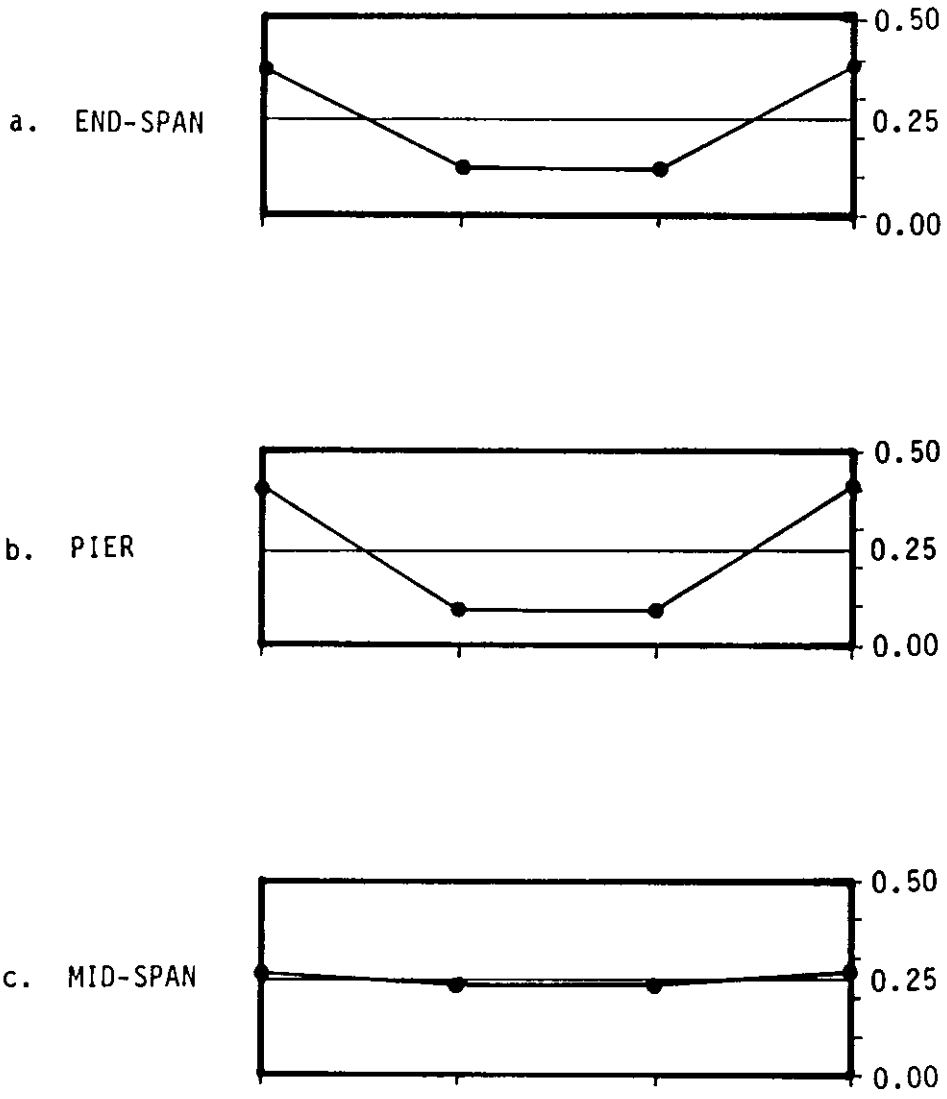

Fig. 4.17. Transverse moment fractions for all exterior stringers strengthened (TC2)

a. EXTERIOR STRINGER

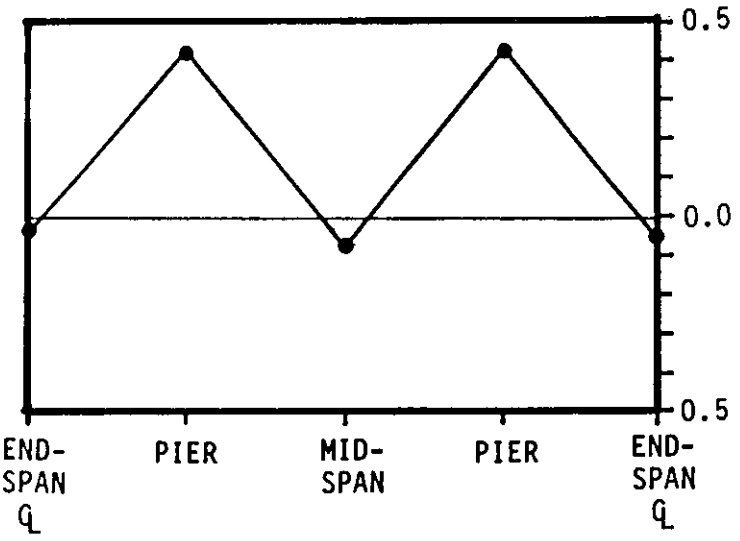

b. INTERIOR STRINGER

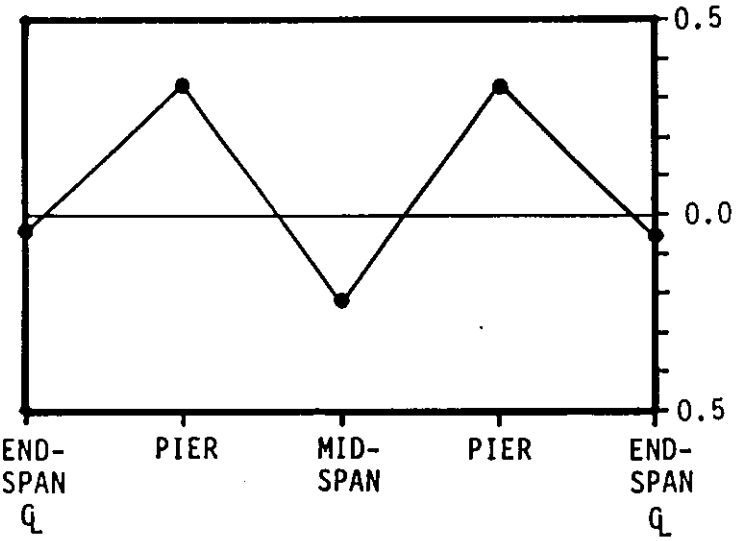

Fig. 4.18. Longitudinal moment fractions for all exterior stringers strengthened (TC2)

a. END-SPAN

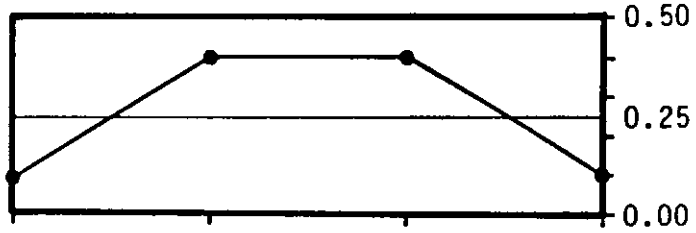

b. PIER

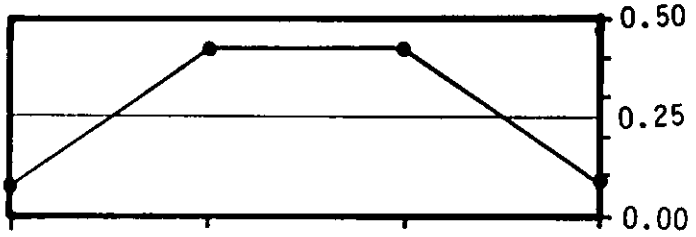

c. MID-SPAN

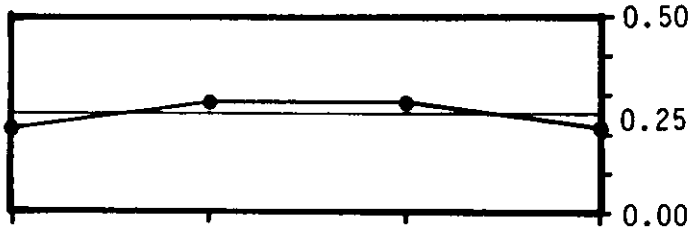

Fig. 4.19. Transverse moment fractions for all interior stringers strengthened (TC3)

a. EXTERIOR STRINGER

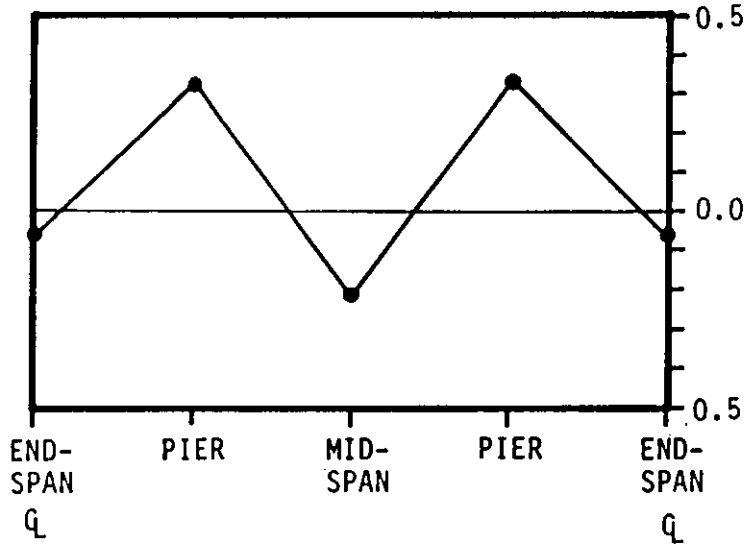

b. INTERIOR STRINGER

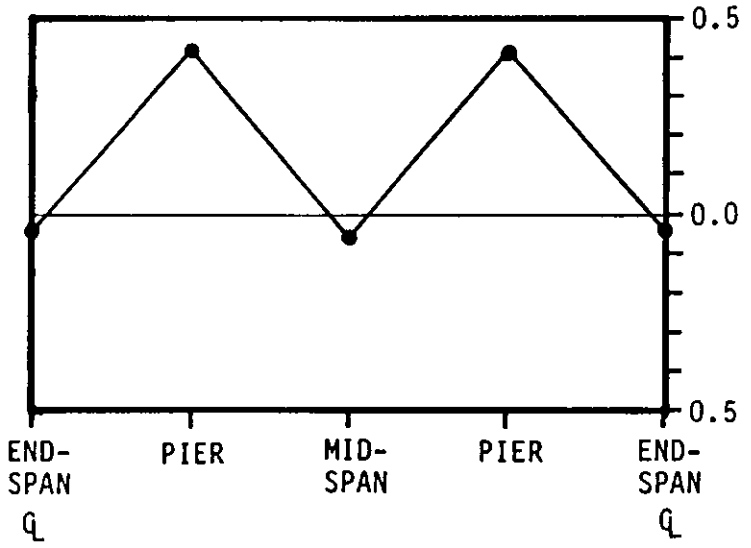

Fig. 4.20. Longitudinal moment fractions for all interior stringers strengthened (TC3)

a. TRANSVERSE

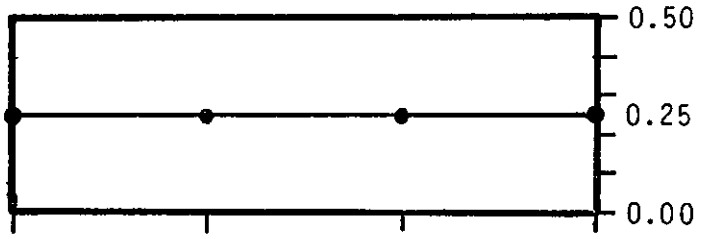

b. LONGITUDINAL

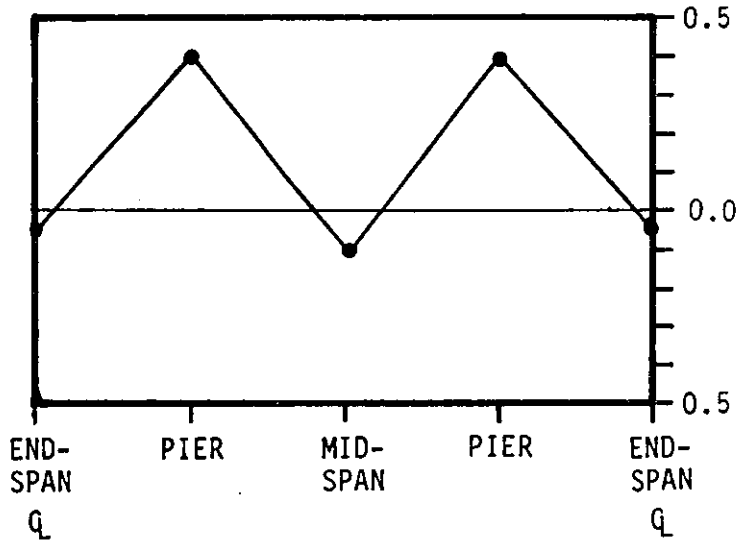

Fig. 4.21 Transverse and longitudinal moment fractions for all stringers strengthened (TC4)

strengthening only exterior stringers. The majority of moment is carried in the interior stringers transversely. Longitudinally, moments are more evenly distributed on the exterior stringers.

Strengthening all stringers (TC4) produces the moment fractions shown in Fig. 4.21. Since all sections were identical, only one transverse and one longitudinal distribution is shown. In the tranverse direction each stringer carried identical moment fractions of 25%. Therefore, Fig. 4.21a represents moment fractions at the center of the end span, pier and the mid-span of the bridge. Longitudinally the results are similar to the previous cases for stringers which were strengthened. Approximately 40% of the moment is at the piers, 10% at the mid-span and 5% at the end-spans.

The effect of changing the truss length (distance of vertical force from pier) did have a slight effect on the distribution of moment at a section. The effect differed for each strengthening configuration. For a stringer with superimposed truss forces acting, increasing the distance between the pier and vertical force increased the moment fraction distributed to the end and mid-span and decreased the moment fractions at the piers. For stringers without the superimposed truss forces acting, the moment fraction was decreased at all sections except the midspan of the bridge.

Table 4.1 gives the moment fractions for a distance between the pier and point of vertical loading of 9 ft-1 in. (mockup truss), 10 ft and 11 ft. Listed in the table are the moment fractions at the end-

Table 4.1. Change in moment fractions due to increasing length of superimposed truss

		Endspan	Pier	Midspan
Exterior Beams Strengthened				
Exterior	9'-1"	-0.043	0.428	-0.058
	10'-0"	-0.049	0.419	-0.066
	11'-0"	-0.057	0.405	-0.076
Interior	9'-1"	-0.052	0.341	-0.214
	10'-0"	-0.052	0.339	-0.218
	11'-0"	-0.052	0.336	-0.224
Interior Beams Strengthened				
Exterior	9'-1"	-0.056	0.332	-0.224
	10'-0"	-0.056	0.329	-0.228
	11'-0"	-0.056	0.327	-0.234
Interior	9'-1"	-0.040	0.432	-0.056
	10'-0"	-0.046	0.422	-0.066
	11'-0"	-0.053	0.410	-0.076
All Beams Strengthened				
Exterior	9'-1"	-0.045	0.411	-0.087
	10'-0"	-0.051	0.401	-0.097
	11'-0"	-0.056	0.389	-0.108
Interior	9'-1"	-0.042	0.414	-0.088
	10'-0"	-0.047	0.404	-0.088
	11'-0"	-0.052	0.393	-0.109

span, pier and mid-span for interior and exterior beams for each of the three strengthening schemes. The table indicates that very little change in distribution occurs due to increasing the truss length.

5. SUMMARY AND CONCLUSIONS

5.1. Summary

This report summarizes the research that has been completed in an investigation of the strengthening of continuous, composite bridges by two methods: post-compression of stringers and superimposed trusses within stringers. The research program included reviewing the literature, testing each strengthening scheme on a full-scale mockup of the negative moment region of a bridge stringer, conducting a finite-element analysis of the laboratory bridge beam mockup for each strengthening scheme, and conducting a finite-element analysis of a one-third scale three-span continuous model bridge strengthened with superimposed trusses.

The literature review involved a search of publications from both the United States and foreign countries. The superimposed truss was researched as an applied strengthening mechanism, which when added to the existing structure "doubled" the structure at some or all locations. Several reports of research involving applied strengthening mechanisms were examined. Post-compression was a relatively unexplored strengthening idea. The engineering literature contained only one example of the strengthening of an existing structure by attaching elements that were subsequently compressed.

The primary purpose of this study was to determine the feasibility of strengthening the negative moment region of continuous composite bridges by two new methods:

1. Post-compression of stringers
2. Superimposed truss within stringers.

Both strengthening schemes were designed to reverse the moments and resulting stresses from service loads.

As part of an earlier research project at ISU, which studied strengthening the negative moment region of continuous composite bridges, a full-size composite beam mockup was constructed in the Structural Engineering Laboratory. This full-scale mockup was used during this research project to test the post-compression strengthening scheme and the superimposed truss-strengthening scheme.

For the superimposed truss, researchers found that this may be accomplished by applying the vertical strengthening force to either the bottom of the bridge deck or the lower flange of the bridge beam. In either case the superimposed truss would cause only positive moment bending when applied. Post-compression is analogous to post-tensioning; however, along with positive moment bending, the post-compression strengthening scheme applies tension to the section rather than compression.

A series of tests were conducted on the full-scale mockup: first with the post-compression strengthening scheme in place, and then with the superimposed truss-strengthening scheme in place. Tests were also performed to establish the strength characteristics of the mockup without any of the strengthening schemes in place. These tests were

necessary for determining the amount that stresses and deflections were reduced by each strengthening scheme.

The post-compression strengthening scheme was effective in reducing the bottom flange beam stresses. The top flange beam stresses, however, were actually slightly increased, due to the tension applied to the section. At the design strengthening loads, the post-compression strengthening scheme increased the top flange beam stress 18% and decreased the bottom flange beam stress 36%.

The post-compression tubes and brackets used by the system performed well throughout testing. However, some modifications could be made in order to reduce the potential for bending in the post-compression tubes. Those modifications would consist of a redesigned end condition at the point where force is transferred between the compression tubes and brackets.

The superimposed truss-strengthening scheme was very effective in reducing both the top and bottom flange beam stresses since it applied only positive bending to the full-scale mockup. The superimposed truss (ST2.2), which applied the strengthening force to the bottom of the bridge deck, reduced the top and bottom flange beam stresses by 46% and 48%, respectively. The superimposed truss (ST2.3), which applied the strengthening force to the lower beam flange, reduced both the top and bottom flange beam stresses by 40%.

A test was also conducted on the full-scale mockup with the superimposed truss (ST2.3) in place, in which the system was tested to

failure. From that test, the performance of strengthening scheme at high stress levels was evaluated. The test confirmed that failure would occur in the full-scale bridge mockup before it would occur in the applied strengthening mechanism (the superimposed truss). Although both designs for the superimposed truss performed extremely well, a modification of the end condition for the superimposed truss, which bears against the bottom of the deck (ST2.2), should be considered.

In addition to the experimental laboratory work, finite-element analyses were performed on the full-scale bridge beam mockup with each of the three strengthening schemes applied. The deflections and strains for the finite-element analyses were in good agreement with the experimental results when the concrete deck was in compression. However, when the concrete deck was in tension, the results of the finite-element analyses did not compare well with the experimental values. This is most likely due to a decrease in the tensile capacity of the concrete deck on the laboratory mockup, resulting from its age, and cracks that developed in the concrete deck during previous strengthening tests.

Finite-element analyses were also performed on a one-third scale, continuous, composite, model bridge to determine the distribution effects of applying superimposed trusses in some or all negative regions. The results indicated that longitudinally approximately 40% of the strengthening moment stays at the pier in the stringer being

strengthened. Approximately 5 and 10% of the moment is transferred to the end and mid-spans, respectively. Transversely, between 10 and 20% of the moment is transferred from the strengthened to unstrengthened stringers. Of that moment, approximately 30% remains at the piers, 20% is carried by the mid-span and 5% by the end-span.

5.2. Conclusions

The following conclusions were developed as a result of this study.

(1) Post-compression strengthening (ST2.1), when applied to the negative moment region, caused positive moment and tension in the section. While there was a reduction in bottom flange beam stress, an undesirable increase in top flange beam and deck stress also resulted.

(2) Superimposed truss strengthening (ST2.2, ST2.3), when applied to the negative moment region, caused only positive moment in the section. Stress reduction in both the top and bottom beam flanges was significant.

(3) For the superimposed truss, applying the vertical strengthening force to the lower surface of the top beam flange (ST2.2) was more effective than applying it to the lower surface of the bottom beam flange (ST2.3). The difference found in this study, however, was small.

(4) None of the strengthening schemes (ST2.1, ST2.2, or ST2.3) caused a significant increase in stiffness of the mockup.

Similarly, no overall change in behavior of the mockup was found due to their application.

(5) The superimposed truss-strengthening scheme (ST2.2) has the greatest potential for field application. Fabrication, installation, and maintenance considerations as well as strengthening performance make it the best choice for actual bridge strengthening.

(6) The choice of a strengthening scheme using ST2.2 or ST2.3 should be based on the required strengthening of the bridge being examined.

(7) Changing the length of the superimposed truss does not significantly effect the distribution of moments in the bridge.

6. RECOMMENDED FURTHER RESEARCH

On the basis of the literature review, mockup testing, and finite-element analysis, it would be logical to continue this strengthening research as follows:

(1) Strengthening composite bridges of the type investigated in this study with a superimposed truss is feasible; the next logical step is to design and implement superimposed truss strengthening on an actual bridge. The strengthening for the bridge should be initially tested and then monitored for a period of several years to ensure that no unforeseen problems develop.

(2) If one assumes that the implementation phase of the strengthening is successful, there will be a need for a design procedure for strengthening continuous, composite bridges that is similar to the procedures presented in the manual [8] provided to the Iowa DOT for strengthening simple-span composite bridges using post-tensioning.

(3) The feasibility of using a post-compression strengthening system similar to ST2.1 in conjunction with post-tensioning should be investigated. If used simultaneously at a critical section, the undesirable axial effects associated with individual use would be minimized, and the desirable positive moment effect could be magnified.

7. REFERENCES

1. Bathe, K. J., E. L. Wilson, and F. E. Peterson, SAP IV, *A Structural Analysis Program for Static and Dynamic Response of Linear Systems*, Berkeley: College of Engineering, University of California, 1974.

2. Dunker, K. F., F. W. Klaiber, B. L. Beck, and W. W. Sanders, Jr., "Strengthening of Existing Single-Span Steel Beam and Concrete Deck Bridges, Final Report-Part II," ERI Project 1536, ISU-ERI-Ames-85231, Ames: Engineering Research Institute, Iowa State University.

3. Dunker, K. F., F. W. Klaiber, F. W. Daoud, W. E. Wiley, and W. W. Sanders, Jr., "Strengthening of Existing Continuous Composite Bridges, Final Report," ERI Project 1846, ISU-ERI-Ames-88007, Ames: Engineering Research Institute, Iowa State University, 1987.

4. Dunker, K. F., F. W. Klaiber, and W. W. Sanders, Jr., "Design Manual for Strengthening Single-Span Composite Bridges by Post-Tensioning, Final Report-Part III," ERI Project 1536, ISU-ERI-Ames-85229, Ames: Engineering Research Institute, Iowa State University, 1985.

5. Dunker, K. F., "Strengthening of Simple Span Composite Bridges by Post-Tensioning," Ph.D. Dissertation, Iowa State University, Ames, Iowa, 1985.

6. Ferjencik, P., and M. Tochacek, *Die Vorspannung im Stahlbau* (Prestressing in Steel Structures) (in German). Berlin: Wilhelm Ernest & Sohn, 1975.

7. Hambly, E. C., and Pennells, E., "Grillage Analysis Applied to Cellular Bridge Decks," *The Structural Engineer*, 2:67-275, 1975.

8. Jaeger, L. G., and Bahkt, Baidar, "The Grillage Analogy in Bridge Analysis," *Canadian Journal of Civil Engineering*, 9:224-235, 1982.

9. Kandall, C., "Increasing the Load-Carrying Capacity of Existing Steel Structures," *Civil Engineering*, 38(10):48-51, October 1968.

10. Kim, J. B., R. J. Brungraber, and J. M. Yadlosky, "Truss Bridge Rehabilitation Using Steel Arches," *Journal of Structural Engineering*, 110(7):1588-1597, July 1984.

11. Klaiber, F. W., D. J. Dedic, K. F. Dunker, and W. W. Sanders, Jr., "Strengthening of Existing Single Span Steel Beam and Concrete Deck Bridges (Phase I)," ERI Project 1536, ISU-ERI-Ames-83185, Ames: Engineering Research Institute, Iowa State University, 1983.

12. Klaiber, F. W., K. F. Dunker, T. J. Wipf, and W. W. Sanders, Jr., "Methods of Strengthening Existing Highway Bridges," National Cooperative Highway Research Program Report 293, Transportation Research Board, 1987.

13. Klaiber, F. W., K. F. Dunker, and W. W. Sanders, Jr., "Feasibility Study of Strengthening Existing Single Span Steel Beam Concrete Deck Bridges, Final Report," ERI Project 1460, ISU-Ames-81251, Ames: Engineering Research Institute, Iowa State University, 1981.

14. Klaiber, F. W., T. J. Wipf, K. F. Dunker, R. B. Abu-Kishk, and S. M. Planck, "Alternate Methods of Bridge Strengthening", ISU-ERI-Ames-89262, Ames: Engineering Research Institute, Iowa State University, 1989.

15. Mueller, T., "Umbau der Strassenbruecke ueber die Aare in Aarwangen," (Alteration of the Highway Bridge over the Aare River in Aarwangen) (in German), *Schweizerische Bauzeitung*, 87(11):199-203, March 13, 1969.

16. Reiffenstuhl, H., "Eine Bruecke mit Druckspannbewehrung-Konstruktion, Berechnung, Baudurchfuehrung, Messungen," (A Bridge with Compression-Stressed Reinforcing-System, Computation, Construction, Field Measurements) (in German), *Beton-und Stahlbetonbau*, 77(11):273-278, November 1982.

17. Reiffenstuhl, H., "Das Vorspannen von Bewehrung auf Druck: Grundsaetzliches and Anwendungsmoeglichkeiten," (Prestressing of Reinforcing in Compression: Fundamentals and Application Possibilities) (in German) *Beton-und Stahlbetonbau*, 77(3):69-73, March 1982.

18. Reiffenstuhl, H., "Verstaerkung eines Sporthallendaches mit Druckspannbewehrung" (Strengthening of an Athletic Building Roof with Compression Stressed Reinforcement), *Beton-und Stahlbetonbau*, 78(6):149-154, June 1983 (German).

19. Wiley, W. E., "Post-tensioning of Composite T-Beams Subjected to Negative Moment," M.S. Thesis, Iowa State University, Ames, Iowa, 1988.

8. ACKNOWLEDGMENTS

I would like to express my thanks to Dr. F. Wayne Klaiber and Dr. Kenneth F. Dunker for serving as my co-major professors and for their guidance throughout my research. I would also like to thank Dr. Frederick M. Graham for serving on my graduate committee.

Appreciation is also given to Douglas Wood, Research Associate, for his assistance during the laboratory phase of this project. Ivan Alexander, ERI's machinest, also deserves acknowledgment for the fabrication work he performed.

I would like to thank graduate student William E. Wiley and undergraduates Darin N. Johnson, Deborah M. McAuley and Elizabeth A. Johnson for their contributions to this project.

Special appreciation must also be given to graduate student Rula B. Abu-Kishk for her support and encouragement. Thank you Rula.

I would like to thank my parents, Sam and Nora, for their continuous support and confidence in me. Mom, you were my biggest source of encouragement. Dad, you've supported everything I've done, but more important, thank you for the distractions.

I would like to dedicate this work to the memory of my uncle, John B. Jones III. You taught me so much. Your pride as an engineer, and unending sense of humor, I will always carry with me.